eNeuro

Research Article: Confirmation | Cognition and Behavior

Intrinsic excitability in layer IV-VI anterior insula to basolateral amygdala projection neurons correlates with the confidence of taste valence encoding

https://doi.org/10.1523/ENEURO.0302-22.2022

Cite as: eNeuro 2022; 10.1523/ENEURO.0302-22.2022

Received: 24 July 2022
Revised: 1 September 2022
Accepted: 11 September 2022

Intrinsic excitability in layer IV-VI anterior insula to basolateral amygdala projection neurons correlates with the confidence of taste valence encoding

Sailendrakumar Kolatt Chandran[1, *], Adonis Yiannakas[1, 3, *], Haneen Kayyal[1], Randa Salalha[1], Federica Cruciani[1], Liron Mizrahi[1], Mohammad Khamaisy[1], Shani Stern[1], Kobi Rosenblum[1,2]

[1]Sagol Department of Neurobiology, University of Haifa, Mount Carmel, Haifa, Israel

[2]Center for Gene Manipulation in the Brain, University of Haifa, Mount Carmel, Haifa, Israel

[3]Institute of Biochemistry and Molecular Medicine, University of Bern, Bern, Switzerland

*Authors contributed equally to this work

Author contributions

SKC and AY led the project. AY, SKC and KR designed the research. KR supervised the research. SKC, AY, HK, and MK performed the research. SKC, AY, LM, RS, FC, and SS analyzed the data. AY, SKC and KR drafted the paper. All authors reviewed and contributed to the manuscript.

Correspondence

Prof. Kobi Rosenblum, Ph.D.

Sagol Department of Neurobiology

University of Haifa

Haifa, 3498838, Israel

kobir@psy.haifa.ac.il

Dr. Adonis Yiannakas, Ph.D.

Institute of Biochemistry and Molecular Medicine

University of Bern,

Bern, 3012, Switzerland

adonis.yiannakas@gmail.com

Dr. Sailendrakumar Kolatt Chandran, Ph.D.

Sagol Department of Neurobiology

University of Haifa

Haifa, 3498838, Israel

sailendrakumarkc@gmail.com

Word Count

Abstract: 208

Significance statement: 120

Introduction: 801

Materials and methods: 2715

Results: 3993

Discussion: 1874

Number of Figures: 5

Number of tables: 5

Number of multimedia: 7

Data availability

All data generated or analyzed during this study are included in the manuscript and supporting files. Source data files have been provided for all figures.

Acknowledgments

The authors would like to thank all current members of the Rosenblum labs for their help and support, to the veterinary team headed by Barak Carmi and Corina Dollingher and technical team headed by Yair Bellehsen. Graphical illustrations were created using BioRender.com.

Conflict of interest statement

Authors report no conflict of interest.

Funding

This research was supported by a grant from the Israel Science Foundation (ISF); ISF 946/17 and ISF 258/20 to KR.

Abstract

Avoiding potentially harmful, and consuming safe food is crucial for the survival of living organisms. However, the perceived valence of sensory information can change following conflicting experiences. Pleasurability and aversiveness are two crucial parameters defining the perceived valence of a taste and can be impacted by novelty. Importantly, the ability of a given taste to serve as the conditioned stimulus (CS) in conditioned taste aversion (CTA), is dependent on its valence. Activity in anterior insula (aIC) layer IV-VI pyramidal neurons projecting to the basolateral amygdala (BLA) is correlated with, and necessary for CTA learning and retrieval, as well as the expression of neophobia towards novel tastants, but not learning taste familiarity. Yet, the cellular mechanisms underlying the updating of taste valence representation in this specific pathway are poorly understood. Here, using retrograde viral tracing and whole -cell patch-clamp electrophysiology in trained mice, we demonstrate that the intrinsic properties of deep-lying layer IV-VI, but not superficial layer I-III aIC-BLA neurons, are differentially modulated by both novelty and valence, reflecting the subjective predictability of taste valence arising from prior experience. These correlative changes in the profile of intrinsic properties of LIV-VI aIC-BLA neurons were detectable following both simple taste experiences, as well as following memory retrieval, extinction learning and reinstatement.

Significance statement

Learning to form aversive or safe taste memories is dependent on genetic predisposition as well as previous experiences. In mice, anterior insula neurons projecting to the basolateral amygdala (aIC-BLA) are indispensable for learning and retrieving learned taste aversion. Kolatt Chandran et al. demonstrate that the intrinsic properties of aIC-BLA neurons, represent the certainty of taste valence prediction, but not percept. Predictive valence-specific changes are reflected through excitability, being low when taste outcome is highly predictive (i.e., following aversive taste memory retrieval or unreinforced familiarization), and high when taste valence is uncertain (i.e., following novelty or aversive taste memory extinction). In addition, the results propose a neuronal mechanism underlying the long delay between taste and visceral discomfort in conditioned taste aversion.

Introduction

In the natural setting, animals approach novel taste stimuli tentatively, as to closely examine them according to a genetic plan, as well as in relation to associated visceral consequences (Schier and Spector, 2019). Bitter and sour tastes are innately aversive, acting as warning signals for the presence of toxins (Bachmanov et al., 1996). Conversely, neophobia to innately appetitive sweet and moderately salty tastants dissipates over time (Lin et al., 2012). Importantly, animals can learn to avoid innately appetitive tastants (e.g., saccharin-, or NaCl-water – the conditioned stimulus, CS), through conditioned taste aversion - CTA (Garcia et al., 1955; Nachman and Ashe, 1973). This single-trial associative learning paradigm results in robust aversion following the pairing of the CS with a malaise-inducing agent (the unconditioned stimulus, US), such as LiCl (Bures et al., 1998). CTA memories are robust, but can be extinguished through unreinforced CS re-exposures, and subsequently reinstated through US re-exposure (Schachtman et al., 1985; Mickley et al., 2004). Unlike other forms of classical conditioning, the inter-stimulus interval (ISI) between taste experience (CS) and visceral outcome (US), extends to several hours (Adaikkan and Rosenblum, 2015). How CTA learning enables this long-trace associative process, within timeframes that deviate from classical Hebbian plasticity mechanisms is currently unknown (Chinnakkaruppan et al., 2014; Adaikkan and Rosenblum, 2015).

The primary taste cortex - the anterior insula (aIC), along with the basolateral amygdala (BLA), govern the encoding and retrieval of taste information (Piette et al., 2012; Bales et al., 2015). Gustatory processing in IC neurons encompasses thalamocortical and corticocortical inputs that relay taste-, as well as palatability-related inputs from the BLA, that reflect the emotional valence associated with taste stimuli (Stone et al., 2020). Neuronal taste responses at the IC and BLA are plastic and spatially dispersed, using temporal information to encode multiple types of information

relating to stimulus identity and palatability (Grossman et al., 2008; Sadacca et al., 2012; Arieli et al., 2020; Vincis et al., 2020). Both synaptic plasticity and neuronal intrinsic properties are proposed to serve as cellular mechanisms underlying learning and memory (Citri and Malenka, 2008; Sehgal et al., 2013). CTA learning promotes LTP induction in the BLA-IC pathway (Jones et al., 1999; Juárez-Muñoz et al., 2017), and strengthens cell-type specific functional connectivity along the projection (Haley et al., 2016). Intrinsic excitability is the tendency of neurons to fire action potentials when exposed to inputs, reflecting changes in the suit and properties of specific ion channels (Disterhoft et al., 2004; Song and Moyer, 2018). Even though independent mechanisms are involved, recent evidence indicates learning and memory necessitates the that coupling of intrinsic and synaptic plasticity (Turrigiano, 2011; Greenhill et al., 2015; Wu et al., 2021).

The IC is an integration hub tuned for the encoding of both exteroceptive as interoceptive information (Gogolla et al., 2014; Haley and Maffei, 2018; Livneh et al., 2020; Koren et al., 2021). By virtue of its extensive network of connectivity, this elongated cortical structure has been shown to integrate sensory, emotional, motivational, and cognitive brain centers through distinct mechanisms. For example, deletions of either *Fos* or *Stk11* in BLA-aIC neurons, alter intrinsic properties at the aIC, and impair CTA acquisition (Levitan et al., 2020). Furthermore, approach behaviors in social decision-making are modulated by subjective and sex-specific affective states that regulate cell-type-specific changes in intrinsic properties at IC projections to the nucleus accumbens (Rogers-Carter et al., 2018, 2019; Rieger et al., 2022). The posterior IC (pIC) integrates visceral-sensory signals of current physiological states with hypothalamus-gated amygdala anticipatory inputs relating to food or water ingestion, to predict future physiological states (Livneh et al., 2017, 2020). Conversely, aversive visceral stimuli such as LiCl, activate

CaMKII neurons projecting to the lateral hypothalamus in right-, but not the left IC, whose optogenetic activation or inhibition can bidirectionally regulate food consumption (Wu et al., 2020). We have previously shown that the aIC-BLA projection is necessary and sufficient for CTA acquisition and retrieval (Lavi et al., 2018; Kayyal et al., 2019), while CTA retrieval requires activation of the projection concomitant with parvalbumin (PV) interneurons (Yiannakas et al., 2021). Moreover, artificial activation of aIC-BLA projecting neurons is sufficient to induce CTA for appetitive taste (Kayyal et al., 2019). Here, using retrograde viral tracing, behavioral analysis, and whole-cell patch-clamp slice electrophysiology, we assessed two hypotheses: (1) That the intrinsic properties of the aIC-BLA projection change as a function of certainty of taste valence prediction, but not percept; and (2) that predictive valence-specific changes in intrinsic properties would be reflected through excitability, being low when taste outcome is highly predictive (i.e., following CTA retrieval or unreinforced familiarization), and high when taste valence is uncertain (i.e., following novelty or extinction). Our data demonstrate for the first time that the intrinsic properties of LIV-VI aIC-BLA neurons are differentially regulated by innate and learned drives, reflecting the confidence of currently perceived taste valence.

Materials and methods

Animals

Animals used were 8–12-week-old C57BL/6j (WT) adult male mice. Mice were kept in the local animal resource unit at the University of Haifa on a 12-hour dark/light cycle. Water and chow pellets were available ad libitum, while ambient temperature was tightly regulated. All procedures conducted were approved by the University of Haifa Animal Care and Use Committee (Ethics

License 554/18), as prescribed by the Israeli National Law for the Protection of Animals – Experiments with Animals (1994).

Animal surgery and viral injections

Following surgery and stereotactic injection of viral vectors, behavioral paradigms were performed, as previously described (Yiannakas et al., 2021). Briefly, mice were treated with norocarp (0.5mg/kg), before being anesthetized (M3000 NBT Israel/Scivena Scientific) and transferred to a Model 963 Kopf® stereotactic device. Upon confirming the lack of pain responses, the skull was surgically exposed and drilled to bilaterally inject 0.25µl of ssAAV_retro2-hSyn1-chi-mCherry-WPRE-SV40p(A) (physical titer 8.7 x 10E12 vg/ml), at the BLA (AP -1.58; ML ± 3.375; DV - 4.80). Viral delivery was performed using a Hamilton micro-syringe (0.1uL/minute), while the sculp was cleaned and closed using Vetbond®. Animals were then administered with 0.5mg/kg norocarp and 0.5mg/kg of Baytril (enrofloxacin), and then transferred to a clean and heat-adjusted enclosure for 2 hours. Upon inspection, mice were returned to fresh cages along with similarly treated cage-mates. Weight-adjusted doses of the Norocarp and Baytril were administered for an additional 3 days. All AAV constructs used in this study were obtained from the Viral Vector Facility of the University of Zurich (http://www.vvf.uzh.ch/).

Electrophysiological studies of the influence of innate taste identity, novelty, and valence on aIC-BLA excitability

WT mice treated with viral constructs labeling aIC-BLA projecting neurons were used for electrophysiological studies. Upon recovery, mice were randomly assigned into treatment groups

(Figure 1). Following 24hrs of water deprivation, animals were water restricted for 3 days, receiving water in pipettes ad libitum for 20 minutes/day (Kayyal et al., 2019; Yiannakas et al., 2021). This regime has been extensively used by our lab as it allows rodents to reliably learn to drink from water pipettes with minimal weight loss. Mean total drinking was recorded on the 3rd day of water restriction. Novel taste consumption groups were presented with 1.0mL of either 0.5% saccharin (*Saccharin 1x*), or Quinine 0.014% (*Quinine 1x*). One hour following the final taste presentation, animals were subjected to patch-clamp electrophysiology (Kayyal et al., 2021; Yiannakas et al., 2021). The *Water* group underwent the same behavioral procedure without novel taste presentations were sacrificed for electrophysiological investigations one hour following water presentation. To dissociate between taste identity and familiarity-related changes in electrophysiological properties, a cohort of mice treated to label the aIC-BLA projection were similarly water deprived following familiarization with saccharin (*Saccharin 5x*). Following the initial water restriction, *Saccharin 5x* animals were allowed access to 0.5% saccharin, in 20minute sessions for 4 days. On the fifth day, mice were provided with 1.0ml of the tastant, 1 hour prior to sacrifice for electrophysiological recordings. Additionally, WT animals injected with the same viral vector, were allowed a month to recover, following which they were sacrificed for electrophysiological investigations without any behavioral manipulation (*Cage Controls*).

Electrophysiological studies of the influence of learned aversive taste memory retrieval on aIC-BLA excitability

WT mice were treated with viral constructs labelling aIC-BLA projecting neurons to assess the electrophysiological properties of the projection during aversive or appetitive taste memory retrieval. Upon recovery, mice in CTA retrieval group were trained in CTA for saccharin (LiCl

208 0.14M, 1.5% body weight), while the appetitive saccharin retrieval group (*Saccharin 2x*) received
209 a matching body weight adjusted injection of saline (Yiannakas et al., 2021). Three days following
210 conditioning, both groups underwent a memory retrieval task, receiving 1.0mL of the conditioned
211 tastant 1 hour prior to sacrifice (Figures 2, 4). Brain tissue was extracted and prepared for
212 electrophysiological recording, as above.

213

214 ## Electrophysiological studies of the influence of learned aversive taste memory extinction
215 ## and reinstatement on aIC-BLA excitability

216 Electrophysiological studies of CTA extinction and reinstatement were conducted in a cohort of
217 WT male mice (Yiannakas et al., 2021). Following surgery, recovery and water restriction, animals
218 were randomly assigned to the extinction and reinstatement groups (Figures 3-4). The aversion
219 index for the extinction and reinstatement groups were calculated by the formula.

220 Aversion index= $\left[\frac{Volume\ of\ water}{volume\ of\ (water+tastant)}\right]$*100.

221 Adult male mice used to study extinction and reinstatement were trained in CTA for saccharin
222 following extinction, the reinstatement group received an identical intraperitoneal dose to the
223 original unconditioned stimulus (LiCl 0.14M, 1.5% body weight), 24 hours prior to retrieval.
224 Conversely, the extinction group received a similarly weight-adjusted dose of saline. During the
225 final retrieval session, both groups of mice were allowed access to 1.0mL of the CS, 1 hour prior
226 to sacrifice under deep anesthesia and slice preparation for electrophysiology.

227

Electrophysiology tissue preparation

The slice electrophysiology and recording parameters were used as described previously (Kayyal et al., 2021; Yiannakas et al., 2021). Briefly, mice were deeply anesthetized using isoflurane, while brains were extracted following decapitation. Three-hundred um thick coronal brain slices were obtained with a Campden-1000® Vibratome. Slices were cut in ice-cold sucrose-based cutting solution containing the following (in mM): 110 sucrose, 60 NaCl, 3 KCl, 1.25 NaH2PO4, 28 NaHCO3, 0.5 CaCl2, 7 MgCl2, 5 D-glucose, and 0.6 ascorbate. The slices were allowed to recover for 30 min at 37°C in artificial CSF (ACSF) containing the following (in mM): 125 NaCl, 2.5 KCl, 1.25 NaH2PO4, 25 NaHCO3, 25 D-glucose, 2 CaCl2, and 1 MgCl2. Slices were then kept for an additional 30 min in ACSF at room temperature until electrophysiological recording. The solutions were constantly gassed with carbogen (95% O2, 5% CO2).

Intracellular whole-cell recording

After the recovery period, slices were placed in the recording chamber and maintained at 32-34°C with continuous perfusion of carbogenated ACSF (2 ml/min). Brain slices containing the anterior insular cortices were illuminated with infrared light and pyramidal cells were visualized under a differential interference contrast microscope with 10X or 40X water-immersion objectives mounted on a fixed-stage microscope (BX51-WI; Olympus®). The image was displayed on a video monitor using a charge-coupled device (CCD) camera (QImaging®, Canada). Insula to BLA projection cells infected with AAV were identified by visualizing $mCherry^{+}$ cells. Recordings were amplified by Multiclamp™ Axopatch™ 200B amplifiers and digitized with Digidata® 1440 (Molecular Devices®). The recording electrode was pulled from a borosilicate glass pipette (3–5 M) using an electrode puller (P-1000; Sutter Instruments®) and filled with a K-gluconate-based

internal solution containing the following (in mM): 130 K-gluconate, 5 KCl, 10 HEPES, 2.5 MgCl2, 0.6 EGTA, 4 Mg-ATP, 0.4 Na3GTP and 10 phosphocreatine (Na salt). The osmolarity was 290 mOsm, and pH was 7.3. The recording glass pipettes were patched onto the soma region of $mCherry^{+}$ pyramidal neurons and neighboring non fluorescent pyramidal neurons.

The recordings were made from the soma of insula pyramidal cells, particularly from layer 2/3 and Layer 5/6. Liquid junction potential (10 mV) was not corrected online. All current clamp recordings were low pass filtered at 10 kHz and sampled at 50 kHz. Pipette capacitance and series resistance were compensated and only cells with series resistance smaller than 20 MΩ were included in the dataset. Data quantification was done with Clampfit (Molecular Devices, Sunnyvale, CA) and subsequently analyzed using GraphPad Prism®. The method for measuring active intrinsic properties was based on a modified version of previous protocols (Kaphzan et al., 2013; Chakraborty et al., 2017; Sharma et al., 2018).

Recording parameters

Resting membrane potential (RMP) was measured 10 sec after the beginning of whole-cell recording (rupture of the membrane under the recording pipette). The dependence of firing rate on the injected current was obtained by injection of current steps (of 500ms duration from 0 to 400 pA in 50 pA increments). Input resistance was calculated from the voltage response to a hyperpolarizing current pulse (-150 pA). SAG ratio was calculated from voltage response -150 pA. The SAG ratio during the hyperpolarizing steps was calculated as $[(1-\Delta V_{SS}/\Delta V_{max}) \times 100\%]$ as previously reported by (Song, Ehlers, & Moyer, 2015). The membrane time constant was determined using a single exponential fit in the first 100ms of the raising phase of cell response to a 1 second, -150 pA hyperpolarization step.

For measurements of a single action potential (AP), after initial assessment of the current required to induce an AP at 15ms from the start of the current injection with large steps (50 pA), a series of brief depolarizing currents were injected for 10ms in steps of 10 pA increments. The first AP that appeared on the 5ms time point was analyzed. A curve of dV/dt was created for that trace and the 30 V/s point in the rising slope of the AP was considered as threshold (Chakraborty et al., 2017). AP amplitude was measured from the equipotential point of the threshold to the spike peak, whereas AP duration was measured at the point of half-amplitude of the spike. The medium after-hyperpolarization (mAHP) was measured using prolonged (3 seconds), high-amplitude (3 nA) somatic current injections to initiate time-locked AP trains of 50 Hz frequency and duration (10 – 50 Hz, 1 or 3 s) in pyramidal cells. These AP trains generated prolonged (20 s) AHPs, the amplitudes and integrals of which increased with the number of APs in the spike train. AHP was measured from the equipotential point of the threshold to the anti-peak of the same spike (Gulledge et al., 2013). Fast (fAHP), and slow AHP (sAHP) measurements were identified as previously described (Andrade et al., 2012; Song and Moyer, 2018). Series resistance, Rin, and membrane capacitance were monitored during the entire experiment. Changes of at least 30% in these parameters were criteria for exclusion of data.

Classification of Burst and Regular spiking neurons

At the end of recordings, neurons were classified as either burst (BS) or regular spiking (RS) as reported previously (Kim et al., 2015; Song et al., 2015). Briefly, neurons that fired two or more action potentials (doublets or triplets) potential towards a depolarizing current step above the spike threshold current were defined as burst spiking (BS). Regular spiking (RS) neurons on the other hand, were defined as neurons that fired single action potential in response to a depolarizing current step above spike threshold (Extended Figure 1-2A).

297

298 Statistical analysis of individual intrinsic properties across treatments

299 Group size was based on previously published results using similar methods (Gould et al., 2021;
300 Kayyal et al., 2021), as well as through conducting power analysis calculations, in order to obtain
301 power ≥ 0.8 with alpha=0.05 (https://www.stat.ubc.ca/~rollin/stats/ssize/n2.html). Individual
302 intrinsic properties of aIC-BLA projecting neurons in the respective treatment groups (Figures 1-
303 4) were analyzed using appropriate statistical tests (One-way or Two-way ANOVA, GraphPad
304 Prism®), as defined in the Table 5: Statistics table. Two-way repeated measurements of analysis
305 of variance (RM-ANOVA) followed by Sidak's (for two groups) or Tukey's (for more than two
306 groups) post-hoc multiple comparison test was performed for firing properties. The intrinsic
307 properties were determined with Two-tailed unpaired t-tests, and One-way ANOVA followed by
308 Tukey's or Dunn's multiple comparisons test were used. For all tests, $*p < 0.05$ was considered
309 significant. D'Agostino & Pearson test used for the identifying the normal distribution of the data.
310 Multiple comparisons were corrected post hoc with Tukey's for One-way/ Two-way ANOVA and
311 Dunn's for Kruskal-Wallis test.

312 Following spike-sorting, the ratio of BS:RS aIC-BLA projecting neurons in the sampled population
313 was compared across our treatments (Mann-Whitney test, GraphPad Prism®). Similarly,
314 individual intrinsic properties in BS and RS aIC-BLA projecting neurons were analyzed following
315 spike-sorting (One-way or Two-way ANOVA, GraphPad Prism®). All data reported as mean ±
316 standard error (SEM).

317

Immunohistochemistry

From each electrophysiological recording, three 300µm-thick mouse brain slices were obtained starting from Bregma coordinates 1.78, 1.54 and 1.18, respectively. Slices were washed with PBS and fixed using 4% paraformaldehyde in PBS at 4^0C for 24 hours. Slices were then transferred to 30% sucrose/PBS solution for 48 hours and mounted on glass slides using Vectashield® mounting medium with DAPI (H-1200). Slides were then visualized using a vertical light microscope at 10x and 20x magnification (Olympus CellSens Dimension®). Images were processed using Image-Pro Plus® V-7 (Media Cybernetics). The localization of labelled mCherry+ neurons in the agranular aIC - where recordings were obtained from, was quantified manually across three Bregma-matched slices, for each animal. Quantification was done using randomly assigned IDs for individual animals, regardless of treatment. Representative images were additionally processed using the Olympus CellSens 2-D deconvolution® function.

Principal component analysis (PCA) of the profile of intrinsic properties across treatment groups

Principal component analysis (PCA) of the standardized intrinsic properties of the LIV-VI aIC-BLA (Figure 5; Extended Figure 5-1) was performed using the correlation matrix on GraphPad Prism9, MATLAB R2020b, and IBM SPSS Statistics 27. The covariance matrix was used for each PCA was performed in six behavioral groups, the low memory prediction (Saccharin 1x, n=20; Saccharin 2x, n=20, and Extinction, n=14), and the high memory prediction (Saccharin 5x, n=18; CTA retrieval, n=27, and Reinstatement, n=15), RS vs. BS neurons. A total of 114 neurons (BS vs. RS) across all intrinsic properties and excitability changes (50–400 pA) (Extended Figure 5-1A), and later all intrinsic properties with only 350 pA (highest excitability differences between

341 treatment groups; Extended Figure 5-1, B). PCA was conducted on 63 burst spiking neurons using
342 12 variables: 350 (pA), RMP (mV), mAHP (mV), sAHP (mV), fAHP (mV), IR (MΩ), Sag Ratio,
343 Time constants (ms), AP amplitude (mV), AP Halfwidth (ms), AP threshold (mV), Rheobase (pA),
344 (Figure 5 A &B). The adequacy of the sample was evaluated using the Bartlett's test and the Kaiser-
345 Meyer-Olkin (KMO) measure was applied. The degrees of freedom (df) were calculated using the
346 following formula:

347 $$df = \#variables - 1.$$

348 The number of principal components was chosen according to the percentage of variance explained
349 (>75%). The parallel analysis evaluated the optimal number of components and selected 3 PCs,
350 explaining 62.47% of the variance. Oblique factor rotation (par) of the first three PCA components,
351 using a standard 'rotatefactors' routine from MATLAB Statistics Toolbox. This approach
352 maximizes the varimax criterion using an orthogonal rotation. To optimize variance, oblique factor
353 rotation (paramax) was used, and the threshold chosen to define a variable as a significant
354 contributor was a variance ≥ 0.7 given the small sample size. The correlation matrix was adequate
355 as the null hypothesis of all zero correlation was rejected [χ_{66}^2=387.444, p<0.001], and KMO
356 exceeded 0.5 (KMO=0.580).
357 To calculate the proportion of the variance of each variable that the principal components can
358 explain, communalities were calculated and ranged from 0.426 to 0.897 (extended Figure 5-1, A-
359 C). The communalities scores were calculated using the following formula: $= \frac{\sum_{i=1}^{m} \lambda}{\#variables * \lambda}$; where
360 *m* is the number of selected PCs. The threshold chosen was Comm ≥ 60%.
361 Due to the imbalance in sample sizes between groups, the PCA space is biased in favor of the
362 group with bigger sample size. The BS neurons in the six behavioral groups previously mentioned
363 were resampled to ensure that sample sizes were balanced across groups datasets (Figure 5, A&B).

Particularly, we reduced the number of Saccharin 1X and 2X observations by using random sampling ("randn" function in MATLAB); for Saccharin 1x, we chose 10 of the 17 total elements, and for Saccharin 2x, we selected 10 of the 13 total elements.

K-means clustering

Unbiased clustering analysis based on the K-means algorithm was conducted to search for an optimal division of samples into a pre-determined number of clusters within an unlabeled multidimensional data set (MacQueen, 1967). In the present study we chose K-means clustering methods to cluster the similar groups into a high and low predictive valance outcome following the memory, based on their intrinsic properties. As a popular method for a cluster analysis, K-means clustering aims to partition n observations into k –clusters in which each observation belongs to the cluster with the nearest mean, serving as a prototype of a cluster. In this classification a set of clustering results with different number of clusters can be calculated by setting a different k. The final step is to determine the optimal dimension which gives the best classification. To assess the distribution of bursting neurons in multidimensional space, we performed a k-means cluster analysis in MATLAB for the principal components (k = 2 clusters, maximum iterations was 100 with random starting locations, squared Euclidean distance metric used), which explained 62.47% of the variance in intrinsic properties (Figure 5; extended Figure 5-1 and 5-2).

Results

To prove or refute our hypotheses, we conducted a series of electrophysiological recordings in slice preparation from the mouse aIC, in which we labelled aIC-BLA projecting neurons using retrograde adeno-associated viral tracing – retro AAV (see Methods). Electrophysiological

387 recordings were obtained from the aIC-BLA projecting neurons in LI-III (Table 2) and LIV-VI
388 (Table 1), following novel appetitive or aversive taste stimuli (Figure 1), following appetitive or
389 aversive taste memory retrieval (Figure 2), as well as following extinction and reinstatement
390 (Figures 3-4). We focused on deep-lying LIV-VI aIC-BLA projecting neurons (Table 1), as
391 intrinsic properties in superficial LI-III aIC-BLA projecting neurons were unaffected by taste
392 identity, familiarity, or valence (Table 2). We measured action potential (AP) firing frequency in
393 response to incrementally increasing depolarizing current injections, as well as 11 distinct of
394 intrinsic properties (Tables 1-4 and Table 5: Statistics Table): resting membrane potential (RMP);
395 slow, medium and fast after-hyperpolarization (sAHP, mAHP, fAHP); input resistance (IR), SAG
396 ratio; the amplitude, half-width and threshold for APs; the time taken for a change in potential to
397 reach 63% of its final value (membrane time constant - τ), as well as the minimum current
398 necessary for AP generation (Rheobase). Statistical analysis was conducted using repeated
399 measures one- or two-way ANOVA (see Table 5: Statistics table).

400

401 ## When taste is both appetitive and novel, excitability in LIV-VI aIC-BLA projection neurons
402 ## is increased

403 To delineate the mechanisms through which novelty is encoded on the LIV/VI aIC-BLA
404 projection, we labeled the projection (see methods), and compared the intrinsic properties across
405 neutral, innately aversive, and innately appetitive taste stimuli. Following surgery recovery mice
406 were randomly assigned to the following behavioral groups: Water (Control for procedure, Water;
407 n=6 animals, 23 cells), 0.5 % Saccharin for the first (Novel innate appetitive, Saccharin 1x; n=5
408 animals, 20 cells), or fifth time (Familiar appetitive, Saccharin 5x; n=6 animals, 18 cells), 0.04%
409 Quinine (Novel aversive, Quinine 1x; n=4 animals, 19 cells), or cage controls that did not undergo

410 water-restriction (Base-line control, Cage control; n=4 animals, 19 cells). This approach allowed
411 us to examine excitability changes that relate to the innate aversive/appetitive nature and
412 novelty/familiarity associated with tastants, while accounting for the effects of acute drinking, as
413 well as the water restriction regime itself. Guided by evidence regarding the induction of plasticity
414 cascades, the expression of immediate early genes, as well as the timeframes involved in LTP and
415 LTD in IC neurons (Rosenblum et al., 1997; Hanamori et al., 1998; Jones et al., 1999; Escobar and
416 Bermúdez-Rattoni, 2000), the five treatment groups were sacrificed 1 hour following taste
417 consumption. Even though changes in activity can be observed within seconds to minutes,
418 depending on their novelty, salience and valence (Barot et al., 2008; Lavi et al., 2018; Wu et al.,
419 2020), sensory experiences can modulate the function of IC neurons for hours (Juárez-Muñoz et
420 al., 2017; Rodríguez-Durán et al., 2017; Haley et al., 2020; Kayyal et al., 2021; Yiannakas et al.,
421 2021).We had previously identified a CaMKII-dependent short-term memory trace at the IC that
422 last for the first 3 hours following taste experiences, regardless of their valence (Adaikkan and
423 Rosenblum, 2015). To address whether similar time-dependency of the physiological correlations
424 engaged by the IC during novel taste learning, a 6th group was sacrificed 4 hours following novel
425 saccharin exposure (Figure 1 – Saccharin 1x (4hrs)).

426 Daily water intake prior to the final taste exposure and was not different among the five groups
427 that underwent water restriction (Figure 1B, One-way ANOVA, $p=0.4424$, $F=0.9766$, R squared
428 $=0.1634$). However, excitability in response to incremental depolarizing currents was significantly
429 different between the six groups (Figure 1D – Two-way ANOVA, $p<0.0001$, $F(8,880)=1269$).
430 Exposure to saccharin for the first time (i.e., novel appetitive), at the 1-hour time-point, resulted
431 in enhanced excitability on the aIC-BLA projection compared to all other groups (Figure 1D, see
432 Table 1). Conversely, fAHP (Figure 1H; One-way ANOVA, $p<0.0001$, $F=8.380$, R squared

433 =0.2758) in the Quinine 1x group was increased compared to all other groups, in contrast to
434 Saccharin 1x where it was most decreased (see Table 1). In fact, fAHP in the Saccharin groups
435 recorded at 1hr ($p<0.0001$, $z=5.150$) or 4hours ($p=0.0099$, $z=3.406$) following novel taste
436 consumption was decreased compared to innately aversive Quinine 1x (Figure 1H). Even though
437 fAHP in the Saccharin 1x group was decreased compared to both the Cage control ($p=0.0136$, z
438 =3.318) and Water ($p=0.0177$, $z=3.243$) groups, this was not the case for the Saccharin 1x (4hr)
439 group ($p>0.9999$ for both – see Table 1). Importantly, fAHP (Figure 1H) was nearly identical in
440 treatment groups where the tastant could be deemed as highly familiar and safe, such as the Cage
441 control group (that did not undergo water restriction), as well as animals in the Water or Saccharin
442 5x groups (that had undergone water restriction).

443 Significant differences in terms of τ (Figure 1J; One-way ANOVA, $p<0.0001$, $F(5, 110)$;R
444 squared, 0.2169), were observed between the Cage control and Saccharin 1x (4hrs) groups
445 ($p=0.0003$, $q=6.326$), Water vs. Saccharin 1x (4hr) ($p=0.0488$, $q=4.115$), Saccharin 1x and
446 Saccharin 1x (4hrs) groups ($p=0.0002$, $q=6.521$), and Saccharin 5x vs. Saccharin 1x (4hr), $p=$
447 (0.0081, $q=4.975$, $df=110$). On the other hand, significant differences in AP half-width (Figure
448 1I; Kruskal-Wallis test; $p=0.0125$, Kruskal-Wallis statistic=14.54) were only observed between
449 the Saccharin 1x (4hrs) compared to Saccharin 1x ($p=0.0065$, $z=3.519$) groups (see Table 1).

450 These results demonstrate that in the context of taste novelty, innately appetitive saccharin drove
451 increases in excitability and decreases in fAHP of LIV-VI aIC-BLA projecting neurons, compared
452 to innately aversive quinine (Figure 1D, H). Compared to the Cage control and Water groups,
453 fAHP on the projection was significantly enhanced by innately aversive quinine and was decreased
454 by innately appetitive novel saccharin (Figure 1H). However, the effect of appetitive taste novelty
455 on firing frequency was time-dependent, as it was observed at 1hr, but not 4hrs following novel

456 taste exposure (Figure 1D). Furthermore, following familiarity acquisition for saccharin
457 (Saccharin 5x), excitability was decreased compared to Saccharin 1x, matching the Cage control,
458 Water, and Quinine 1x groups (Figure 1D). This led us to consider whether increased excitability
459 is not related to taste identity or palatability (Wang et al., 2018), but the perceived salience of taste
460 experiences, which encompasses both novelty and valence (Ventura et al., 2007; Kargl et al.,
461 2020). Previous studies have suggested that the induction of plasticity signaling cascades and IEGs
462 in pyramidal neurons of the aIC (commonly used as surrogates for changes in excitability), is a
463 crucial step for the association of taste and visceral information during CTA learning (Adaikkan
464 and Rosenblum, 2015; Soto et al., 2017; Wu et al., 2020). Activation of the aIC-BLA projection
465 is indeed necessary for the expression of neophobia towards saccharin (Kayyal et al., 2021), as
466 well as for CTA learning and retrieval (Kayyal et al., 2019). Yet, its chemogenetic inhibition does
467 not affect the attenuation of neophobia, nor the expression of aversion towards innately aversive
468 quinine (Kayyal et al., 2019). Furthermore, aversive taste memory retrieval necessitates increases
469 in pre-synaptic inhibitory input on the projection (Yiannakas et al., 2021). Bearing this in mind,
470 we hypothesized that increases in excitability on the projection could be indicative of a labile state
471 of the taste trace at the aIC, which manifests when taste cues are not (yet) highly predictive of the
472 visceral outcome of the sensory experience (Bekisz et al., 2010; Galliano et al., 2021). In such a
473 scenario, taste memory retrieval following strong single-trial aversive learning would be expected
474 to result in decreased excitability compared to control animals. To assess this hypothesis, we next
475 examined intrinsic excitability in mice retrieving an appetitive (Saccharin 2x, CTA retrieval
476 control) or learned aversive memory (CTA retrieval) for saccharin.

477

Learned aversive taste memory retrieval decreases the excitability of LIV-VI aIC-BLA projecting neurons

Following recovery from rAAV injection, mice in the CTA retrieval group underwent water restriction and CTA conditioning for 0.5% saccharin (see Methods, Figure 2A). Electrophysiological recordings were obtained from aIC-BLA neurons 3 days later, 1 hour following retrieval (n=8 animals, 27 cells). Mice in the Saccharin 2x group on the other hand, were familiarized with saccharin without conditioning, and recordings were obtained within the same period, following retrieval (n=5 animals, 20 cells). Through this approach we aimed to examine the hypothesis that like innately aversive and highly familiar appetitive responses (Figure 1), learned aversive taste memory retrieval would be correlated with suppression of the intrinsic excitability on the projection.

As expected, CTA retrieval mice, exhibited decreased consumption of the conditioned tastant compared to control animals that were only familiarized with saccharin (Figure 2B, Mann-Whitney test, $p=0.0085$; Sum of ranks: 52.50, 38.50; Mann-Whitney $U=2.500$). Intrinsic excitability in LIV-VI aIC-BLA projecting neurons was increased in response to depolarizing current injections (Figure 2D; $p<0.0001$, $F(8, 360)=483.3$), and was significantly different between the two treatments ($p=0.0014$, $F(1, 45)=11.60$). Excitability was enhanced in the Saccharin 2x group compared to CTA retrieval, while a significant interaction was identified between the treatment and current injection factors ($p<0.0001$, $F(8, 360)=9.398$). Fast AHP (fAHP) on LIV-VI aIC-BLA projecting neurons tended to be increased in the CTA retrieval group (see Table 1), however differences compared to Saccharin 2x failed to reach significance (Unpaired t-test; $p=0.0527$, $t=1.990$, $df=45$). Conversely, AP amplitude in the Saccharin 2x group was significantly decreased compared to CTA retrieval (Figure 2G; Unpaired t-test; $p=0.0002$, $t=3.983$, $df=45$). In addition,

the CTA retrieval group exhibited significantly decreased IR (Figure 2H; Unpaired t-test; p=0.0036, t=3.072, df=45) and significantly enhanced SAG ratio (Figure 2I; Unpaired t-test; p=0.0037, t=3.060, df=45), compared to Saccharin 2x. In accord with our hypothesis, excitability on LIV-VI aIC-BLA projecting neurons was decreased by aversive taste memory retrieval. We have previously shown that compared to CTA retrieval and reinstatement, appetitive memory retrieval and extinction were associated with (a) an enhancement of IEG induction (c-fos and Npas4) at the aIC, and (b) decreased frequency of pre-synaptic inhibition on the aIC-BLA (Yiannakas et al., 2021). In accord, other published work investigating the induction of IEG in the rodent IC, found that consistent with a reduction in spiking activity (Grossman et al., 2008), the induction of c-fos in IC neurons was decreased by aversive taste memory retrieval (Haley et al., 2020). Earlier studies have also reported increases in c-fos following the extinction of cyclosporine A-induced CTA (Hadamitzky et al., 2015). We thus hypothesized that if excitability in these cells serves as key node for a change in valence prediction, extinction - which constitutes a form of appetitive re-learning, would be associated with enhanced excitability compared to CTA retrieval and reinstatement (Berman, 2003; Suzuki et al., 2004; Morrison et al., 2016; Slouzkey and Maroun, 2016). In addition, through these extinction and reinstatement studies, we were able to examine the real-life relevance of these changes on intrinsic excitability, in a context where behavioral performance reflects the balance between contrasting memories and the availability of retrieval cues (Figure 3).

The predictability of the valence arising from taste experiences determines the profile of intrinsic properties of LIV-VI aIC-BLA projecting neurons

Using similar approaches, electrophysiological recordings were obtained from LIV-VI aIC-BLA

524 projecting neurons from mice having undergone unreinforced CTA extinction (Extinction; n=5, 14
525 cells), or US-mediated CTA reinstatement (Reinstatement; n=3 animals, 15 cells). Behaviorally,
526 the two groups of animals were similar in terms of their aversion profile over 9 unreinforced
527 extinction sessions (Figure 3B; 2-way ANOVA; Extinction: $p<0.0001$, $F(8, 54) = 13.44$;
528 Treatment: $p=0.0681$, $F(1, 54) = 3.466$; Interaction: $p=0.9697$, $F(8, 54) = 0.2803$). As expected,
529 saccharin consumption during the test day in the Reinstatement group was decreased compared to
530 Extinction (Figure 3C; Mann-Whitney test; $p=0.0179$; Sum or ranks: 30, 6; Mann-Whitney $U=0$).
531 Consistent with our findings in Figure 2, aversive taste memory retrieval in the Reinstatement
532 group was associated with decreased excitability compared to the Extinction group (Figure 3E; 2-
533 way ANOVA, Current injection: $p<0.0001$, $F(8, 216) = 370.1$; Treatment: $p=0.0297$, $F(1, 27)$
534 $= 5.291$; Interaction: $p<0.0001$, $F(8, 216) = 10.30$). CTA Reinstatement was also associated with
535 increases in the AP threshold (Figure 3F; Unpaired t-test: $p=0.0076$, $t = 2.887$, $df=27$) and τ (Figure
536 3G; Unpaired t-test: $p=0.0153$, $t=2.589$, $df=27$) compared to Extinction.

537 Unlike animals that underwent familiarization with the tastant without conditioning (Figure 1),
538 excitability on the projection in the Extinction group was not decreased by familiarization (Figure
539 3). Conversely, even though the intrinsic mechanisms employed would appear to differ, aversive
540 taste memory retrieval regardless of prior experience, was associated with baseline excitability of
541 the aIC-BLA projection (Figure 3). Our findings in this section (Figure 3), revealed that during
542 taste memory retrieval, excitability on the projection is not solely dependent on the relevant
543 novelty or appetitive nature of tastants, and does not subserve the persistence of CTA memories
544 (Figure 2). Instead, excitability on the aIC-BLA projection is indeed shaped by prior experience
545 but is best predicted by the probability for further aversive (re)learning.

546 Next, to distinguish between intrinsic properties changes that reproducibly reflect taste identity,

familiarity, and valence over the course of time and experience, we compared the profile of intrinsic properties across pairs of behavioral groups in which the currently perceived novelty, as well as innate or learned valence associated with taste was notably different. Through this comparison we were led to conclude that excitability on aIC-BLA projecting neurons is driven by taste stimuli of positive valence, however this effect is dependent on subjective experience and the possibility for further associative learning (Figure 4A). Excitability on aIC-BLA projecting neurons in the treatment groups where the tastant was perceived as appetitive (Saccharin 1x, Saccharin 2x and Extinction), was closely matched, and was significantly enhanced compared to the innately or learned aversive (Quinine 1x, CTA retrieval and Reinstatement) groups (Figure 4A; Two-way ANOVA; Current injection: $p<0.0001$, $F(5, 872) = 1218$; Treatment: $p=0.0014$, $F(5, 109) = 4.281$; Interaction: $p<0.0001$, $F(40, 872) = 4.978$). As previously identified in Figure 1H, fAHP reflected the innate aversive nature of the tastant, being increased in the Quinine 1x group compared to all other groups (Figure 4B; One-way ANOVA; $F = 10.65$, $p<0.0001$, R squared $= 0.3283$, see Table 1). Significant differences in IR (Figure 4C; One-way ANOVA; $F = 2.775$, $p=0.0213$, R squared $= 0.1129$) and SAG ratio (Figure 4D; One-way ANOVA; $F = 2.610$, $p=0.0286$, R squared $= 0.1069$) were only observed between the CTA retrieval and Saccharin 2x groups. AP amplitude (Figure 4E; One-way ANOVA, $p=0.0054$, $F=3.526$, R squared $= 0.1392$) in the Saccharin 2x group was decreased compared to both CTA retrieval ($p=0.0129$, $q=4.768$, $df=109$) and Quinine 1x ($p=0.0087$, $q=4.944$, $df=109$). Conversely, the Extinction and Reinstatement groups, where familiarity with the tastant was the highest, exhibited increased AP half-width compared to all other groups (Figure 4F; One-way ANOVA, Kruskal-Wallis test; $p=0.0002$; Kruskal-Wallis statistic, 24.03). Significant differences in terms of τ (Figure 4G; One-way ANOVA, $p=0.0047$, $F = 3.606$) were only observed in comparing the Saccharin 1x and

570 Reinstatement groups (p=0.0022, q=5.525, df=109). Hence, neuronal excitability is indeed a
571 feature associated with predictive power to modulate taste valence, however it does not fully reflect
572 the breadth of intrinsic property changes among the different behavioral groups.

573

574 ## The predictability of taste valence intrinsic is primarily reflected on the excitability of burst
575 ## spiking, but not regular spiking LIV-VI aIC-BLA projecting neurons

576 Our initial analysis of individual intrinsic properties (Figures 1-3) highlighted that excitability is
577 enhanced following appetitive experiences in which the internal representation is still labile and is
578 associated with the possibility for further aversive learning (novelty or extinction). Conversely,
579 following extensive familiarization, aversive conditioning, or reinstatement, whereby taste
580 exposure leads to memory retrieval of specific valence, excitability on LIV-VI aIC-BLA projecting
581 neurons was similar to baseline (Figures 1 and 4). While the precise mechanism through which
582 sensory input is encoded at the cortex (and other key regions), is still a matter of ongoing research,
583 studies indicate that bursting in cortical layer V pyramidal neurons can encode oscillating currents
584 into a pattern that can be reliably transmitted to distant post-synaptic terminals (Kepecs and
585 Lisman, 2003; Samengo et al., 2013; Zeldenrust et al., 2018). Spike burst is defined as the
586 occurrence of three or more spikes from a single neurons with <8ms intervals (Ranck, 1973;
587 Connors et al., 1982). In brain slices from naïve mice, half of the neurons of a given structure
588 exhibit burst firing, while the distribution of burst spiking (BS) to regular spiking (RS) neurons,
589 changes along the anterior-posterior axis of the subiculum (Staff et al., 2000; Jarsky et al., 2008).
590 Importantly, the two cell types fine-tune the output of brain structures by virtue of differences in
591 synaptic plasticity, as well as intrinsic excitability mechanisms (Graves et al., 2012; Song et al.,
592 2012). Furthermore, there are changes in the ratio of BS:RS neurons in individual brain structures,

593 as well as differences in the recruitment of signaling events, ion channels and metabotropic
594 receptors among the two cell types (Wozny et al., 2008; Shor et al., 2009). Correspondingly,
595 complex region and task-specific rules govern the molecular and electrophysiological mechanisms
596 through which information encoding and retrieval takes place in the two cell types (Dunn et al.,
597 2018; Dunn and Kaczorowski, 2019). Little is currently known regarding the influence of cell
598 identity in the repertoire of plasticity mechanisms employed by the IC to facilitate taste-guided
599 behaviors (Maffei et al., 2012; Haley and Maffei, 2018).

600 Our post-hoc spike sorting analysis allowed us to distinguish between BS and RS LIV-VI aIC-
601 BLA projecting neurons, and thus their relative contribution to behaviorally driven changes in the
602 suit of intrinsic properties (Extended Figures 1-3, 2-1 and 3-1). Through this comparison, we
603 uncovered that Saccharin 1x differed to other groups in terms of excitability and fAHP in BS LIV-
604 VI aIC-BLA neurons (Extended Figure 1-3), while no such changes were observed in RS neurons
605 (see Summary of RS intrinsic properties table no.4). Similarly, excitability in the Saccharin 2x
606 group was significantly enhanced compared to CTA retrieval in BS-, but not in RS LIV-VI aIC-
607 BLA neurons (Extended Figure 2-1A, F). Significant differences in IR, SAG ratio and AP
608 amplitude between CTA retrieval and Saccharin 2x were primarily driven by BS LIV-VI aIC-BLA
609 neurons (Extended Figure 2-1B-D, G-I). Conversely, significant differences in AP half-width
610 between the aversive and appetitive memory retrieval groups were only observed in RS neurons
611 (Extended Figure 2-1J). Correspondingly, excitability in the Extinction group was enhanced
612 compared to Reinstatement in BS-, and not RS LIV-VI aIC-BLA neurons (Extended Figure 3-1A,
613 H). Indeed, excitability on BS LIV-VI aIC-BLA neurons following extinction and reinstatement,
614 reflected the subjective predictability of taste memory retrieval, being high following extinction
615 compared to reinstatement (Extended Figure 3-1). However, this effect was mediated through

616 alternative mechanisms compared to single-trial learning and memory retrieval (Extended Figure
617 1-3, 2-1, 3-1). Significant differences between the Extinction and Reinstatement groups, were
618 observed in terms of the sAHP, AP threshold, SAG ratio and τ in BS but not in RS LIV-VI aIC-
619 BLA neurons (Extended Figure 3-1B-F).

620 Encouraged by these findings, we focused on the Saccharin 1x, Saccharin 2x, Saccharin 5x, CTA
621 Retrieval, Extinction and Reinstatement groups, as to isolate the contribution of BS LIV-VI aIC-
622 BLA neurons in encoding the subjective predictability of taste experience during taste learning,
623 re-learning, and memory retrieval (Figure 5). Consistent with studies in the hippocampus (Graves
624 et al., 2016), we found that the percentage of BS LIV-VI aIC-BLA projecting neurons in the
625 sampled population was highest in the context of novel taste learning (Extended Figure 1-2B:
626 Saccharin 1x, 85%), and subsided following progressive familiarization (Extended Figure 1-2B;
627 Saccharin 2x, 65%, Mann-Whitney test: p=0.0562; Sum of ranks: 303.5, 161.5; Mann-Whitney U
628 =70.50; Saccharin 5x, 55.56%, Mann-Whitney test: p=0.0034; Sum of ranks: 291, 87; Mann-
629 Whitney U =32;). Interestingly, animals retrieving CTA, exhibited the lowest proportion of BS
630 neurons among the six treatments (Extended Figure 1-2B; CTA retrieval, 44.44% BS), and
631 significant differences were observed compared to control animals (Extended Figure 1-2B;
632 Saccharin 2x, 65% BS; Mann-Whitney test: p=0.0102; Sum of ranks: 257, 208; Mann-Whitney U
633 =55). Thus, the ratio of BS:RS LIV-VI aIC-BLA projecting neurons was plastic in relation to
634 experience and was highest in response to appetitive novelty – in accord with studies investigating
635 the intrinsic excitability of subiculum output neurons in relation to contextual novelty and valence
636 encoding (Dunn et al., 2018). Indeed, the ratio of BS:RS LIV-VI aIC-BLA neurons was
637 progressively decreased by familiarity acquisition (Saccharin 1x> 2x> 5x), as well as following
638 aversive taste memory recall (CTA retrieval), compared to both appetitive learning (Extended

Figure 1-2B; Saccharin 1x, Mann-Whitney test: $p<0.0001$; Sum of ranks: 407, 188; Mann-Whitney U =35) and re-learning (Extended Figure 1-2B; Extinction, Mann-Whitney test: $p=0.0007$; Sum of ranks: 182, 224; Mann-Whitney U =29). However, our comparison failed to account for the influence of complex experiences over time, as differences between Extinction and Reinstatement failed to reach significance (Extended Figure 1-2B; Mann-Whitney test: $p=0.3870$, Sum of ranks: 133.5, 97.50, Mann-Whitney U =42.50), while perplexingly, the ratio of BS:RS aIC-BLA neurons in these groups was differentially increased compared to Saccharin 5x (Extended Figure 1-2B; Extinction, Mann-Whitney test: $p=0.0300$; Sum of ranks: 81, 150; Mann-Whitney U =26; Reinstatement, Mann-Whitney test: $p=0.3498$; Sum of ranks: 90, 120; Mann-Whitney U =35;), but not Saccharin 2x (Extended Figure 1-2B; Extinction, Mann-Whitney test: $p=0.2397$; Sum of ranks: 143.5, 156.5; Mann-Whitney U =52.50; Reinstatement, Mann-Whitney test: $p>0.9999$; Sum of ranks: 153.50, 122.5; Mann-Whitney U =62.50). No further statistical analysis were performed in intrinsic properties of aIC-BLA regular spiking neurons representing (Figure 1 and Figure 3), because of the small sample size.

Changes in the intrinsic properties of neuronal ensembles have recently been suggested to contribute to homeostatic mechanisms integrating both cellular and synaptic information (Wu et al., 2021). In our current study, we randomly sampled from neuroanatomically defined LIV-VI aIC-BLA projecting neurons, and even following spike sorting (Extended Figures 1-2), the probability of recording from engram cells (10% of neurons within a region) would be extremely low (Tonegawa et al., 2015). Importantly, the correlative nature does not exclude the possibility that these changes are the consequence of representational drift (Driscoll et al., 2017). We thus set out to examine the hypothesis that applying linear dimension reduction method on the complement of intrinsic properties recorded in BS LIV-VI aIC-BLA neurons would allow us to distinguish

662 between taste experiences that differ in terms of their perceived predictability (or the associated
663 probability for further aversive learning).

664

665 ## Principal component analysis of the profile of intrinsic properties in BS LIV-VI aIC-BLA
666 ## projecting neurons separates treatment groups in relation to the perceived predictability of
667 ## taste valence for saccharin

668 We assigned six of our treatment groups into highly predictive scenarios (Saccharin 5x, CTA
669 retrieval and Reinstatement), and low predictive scenarios (Saccharin 1x, Saccharin 2x,
670 Extinction). We used parallel analysis to select the components across the complement of intrinsic
671 properties in each treatment group, with the first three principal components (PC1-3) explaining
672 30.84%, 17.88%, and 13.75% of the total variance, respectively, and 62.47% of the variance,
673 collectively (Extended Figure 5-2). PC1 (Figure 5B, Extended Figure 5-2) was characterized by
674 strong negative loadings for Rheobase (-0.88304), sAHP (-0.85985) and mAHP (-0.82421), while
675 a positive correlation was identified for IR (0.694764). The direction of PC2 (Figure 5B, Extended
676 Figure 5-2) was positively correlated with fAHP (0.682681) and AP halfwidth (0.614103) and was
677 negatively correlated with Excitability at 350pA (-0.69587). PC3 (Figure 5B, Extended Figure 5-
678 2) positively correlated with SAG ratio (0.889949) and RMP (0.682681), whereas a significant
679 negative correlation with mAHP (-0.6095) was also identified. Unlike aversive or appetitive taste
680 memory retrieval (i.e., highly predictive), appetitive novelty or extinction learning (i.e., low
681 predictive), was associated with increased input resistance, faster action potential generation and
682 decreased afterhyperpolarization on BS aIC-BLA neurons (Figure 5). Importantly, PCA of the
683 intrinsic properties of LIV-VI aIC-BLA projecting neurons regardless of cell type (BS and RS
684 together, Extended Figure 5-1), failed to segregate the two groups of treatments. This cell-type

specific profile of intrinsic properties could provide the framework through which BS LIV-VI aIC-BLA projecting neurons are able to inspect the gastrointestinal consequences associated with tastants over prolonged timescales, when these consequences are not accurately predicted by sensory experience or memory retrieval alone (Adaikkan and Rosenblum, 2015; Lavi et al., 2018; Kayyal et al., 2019).

Discussion

Learning and memory are subserved by plasticity in both synapse strength and neuronal intrinsic properties (Citri and Malenka, 2008; Sehgal et al., 2013). While Hebbian rules can explain associative learning paradigms where seconds separate the CS and US (Krabbe et al., 2018), additional cellular-level mechanisms are needed to explain how learning operates in paradigms where the time between CS and US extends to hours (Adaikkan and Rosenblum, 2015; Wu et al., 2021). In this study, we demonstrate that following taste experiences, taste percept and prior experience are integrated in the intrinsic properties of the aIC in a time-dependent and cell-type specific manner. We further show that regardless of the identity or prior history associated with taste, the intrinsic properties of BS LIV-VI aIC-BLA projecting neurons encodes the perceived confidence of taste valence attribution.

We focused on the aIC-BLA projection; a circuit causally involved in the acquisition and retrieval of CTA memories (Kayyal et al., 2019, 2021). We examined the hypothesis that excitability in aIC-BLA neurons can serve as a taste valence updating mechanism enabling the prolonged ISI between CS and US in CTA learning (Adaikkan and Rosenblum, 2015), and/or contributes to anticipatory

706 valence attribution (Barrett and Simmons, 2015). Our basic proposition diverged from Hebb's fa-
707 mous postulate that cells with increased excitability over hours can potentially wire together with
708 cells conveying incoming modified valence information (Hebb, 1961).

709 The confidence with which taste valence is encoded is the product of the subjectively perceived-
710 (a) appetitive or aversive nature of tastants and (b) novelty or familiarity associated with tastants
711 (Russell, 1980; Kahnt and Tobler, 2017). We first examined each axis separately and later in tan-
712 dem as to better simulate real-life scenarios. We measured the intrinsic properties of aIC-BLA
713 neurons 1 hour following taste experience – a previously established suitable time point (Jones et
714 al., 1999; Haley et al., 2020).

715 To dissociate novelty-related changes from those involving hydration, taste identity and familiar-
716 ity; we compared the intrinsic properties of aIC-BLA neurons following Water – a neutral and
717 familiar tastant, Saccharin – an innately appetitive tastant, in the context of novelty (1x) or famil-
718 iarity (5x), and Quinine – an innately aversive novel tastant (Figure 1). Excitability was high fol-
719 lowing novel saccharin exposure, but not in response to Quinine (Figure 1D). Indeed, concerted
720 activity at the aIC and BLA encodes the presence, identity, and palatability of taste experiences
721 within the 2 seconds preceding swallowing (Katz et al., 2001; Grossman et al., 2008; Fontanini et
722 al., 2009). Palatability can be enhanced as a function of experience (Austen et al., 2016), but can
723 also be decreased by sensory satiety and alliesthenia (Rolls et al., 1981; Yeomans, 1998; Siemian
724 et al., 2021). However, excitability on the projection was enhanced in response to novelty and was
725 decreased following familiarization (Figure 1). Further inconsistent with palatability encoding;
726 changes in excitability captured 1 hour following novel saccharin exposure subsided 4 hours later
727 (Figure 1), while excitability remained plastic even following longer periods of water restriction,
728 that could be considered monotonous (Figure 5). Deciphering whether and how aIC-BLA neurons

729 contribute to palatability processing would require *in vivo* recordings to capture taste-evoked
730 changes, within timescales that are beyond the scope and means of our current study (Vincis and
731 Fontanini, 2016).

732 The correlation identified between excitability and innate current taste valence, encouraged us to
733 examine the predictability of future outcomes following aversive taste memory retrieval. Bearing
734 in mind our previous findings using transcription-dependent activity markers at the aIC (Yiannakas
735 et al., 2021), we hypothesized that aversive taste memory retrieval (CTA retrieval or Reinstate-
736 ment), would be associated with decreased excitability compared to stimulus- and familiarity-
737 matched controls (Saccharin 2x and Extinction). Indeed, excitability on aIC-BLA projecting neu-
738 rons following CTA retrieval was decreased compared to Saccharin 2x (Figure 2B), while Rein-
739 statement, was also associated with decreased excitability compared to Extinction (Figure 3E).
740 Hence, regardless of the complexity of taste memory retrieval, excitability in aIC-BLA neurons
741 was best predicted by the subjective predictability of taste valence - increasing in response to in-
742 nately appetitive taste experiences in which the perceived possibility for avoidance learning was
743 high/taste valence predictability was low (Figure 4). Conversely, when the subjective confidence
744 with which taste valence was predicted was high, excitability on the projection remained un-
745 changed (Figures 1, 4).
746 Innately and learned aversive tastants were both associated with decreased excitability on aIC-
747 BLA projecting neurons compared to appetitive controls, however these effects were mediated
748 through alternative mechanisms (Figures 2-4). Quinine increased fAHP on the projection com-
749 pared to saccharin, regardless of familiarity or perceived valence (Figures 1 and 4). Post-spike
750 after-hyperpolarization (AHP) has a key function in transducing the summed result of processed
751 synaptic input, directly impacting neuronal excitability in relation to both learning and aging (Oh

and Disterhoft, 2020). In pyramidal cells of the hippocampus and cortex, differences in fAHP are mediated by the Ca^{2+}- and voltage-dependent BK currents that promote repolarization at the beginning APs trains (Shao et al., 1999). Interestingly, studies in the prefrontal cortex (PFC), have shown that fear conditioning decreases excitability, whereas extinction training enhances excitability and decreases medium- and slow AHP (Santini et al., 2008; Maglio et al., 2021). Chronic ethanol consumption has shown to suppress excitability and to increase AHP in IC neurons (Luo et al., 2021). Conversely, oxytocin-dependent signaling has been shown to promote social affective behaviors, via increases in excitability and decreases in sAHP in IC neurons (Rogers-Carter et al., 2018). Further studies would be necessary to fully address this, but our findings could indicate that enhanced fAHP is induced by innately aversive tastants or quinine specifically.

Unlike Quinine, CTA memory retrieval, was associated with increased AP amplitude and SAG ratio, as well as decreased IR in BS LIV-VI aIC-BLA projecting neurons, compared to control animals (Figure 2, Extended Figure 2-1). On the other hand, the decreased excitability in the Reinstatement group compared to Extinction was characterized by decreased AP threshold, increased τ, and decreased sAHP (Figures 3, 4, Extended Figure 3-1). The hyperpolarization-activated, cyclic nucleotide-gated current (I_h) regulates membrane depolarization following hyperpolarization (Hogan and Poroli, 2008; Shah, 2014). The opening of HCN channels generates an inward current, that modulates AHP, RMP and IR in cortical pyramidal and PV interneurons (Yang et al., 2018). However, conductance through I_h channels, regulates synaptic integration at the soma of pyramidal neurons, by suppressing excitability, decreasing IR, and increasing τ (Hogan and Poroli, 2008). Evidence indicates that this dichotomous impact of HCN channels on neuronal excitability, is mediated by A-type K channels at the dendrites (Mishra and Narayanan, 2015), and M-type channels at the soma (Hu et al., 2007). Notably, AP half-width was significantly increased in the Extinction

and Reinstatement groups that had undergone extinction training, compared to all other saccharin-treated groups (Figure 4F). Mechanistically, this effect could reflect changes in the distribution and/or the properties of voltage- or calcium-gated ion channels (Faber and Sah, 2002; Grubb and Burrone, 2010; Kuba et al., 2010). Such broadening of spike width has also been reported in infralimbic PFC neurons projecting to the amygdala in response to extinction training (Senn et al., 2014). PV-dependent restriction of excitability and burst firing, is instrumental in experience-dependent plasticity in the amygdala (Morrison et al., 2016), the hippocampus (Donato et al., 2013; Xia et al., 2017) and visual cortex (Yazaki-Sugiyama et al., 2009; Kuhlman et al., 2013). Conversely, in the striatum, PV interneurons restrict bursting, calcium influx, and synaptic plasticity to appropriate temporal windows that facilitate learning, but not retrieval (Owen et al., 2018). Elegant recent studies report that rapid eye movement sleep is associated with a PV-dependent somatodendritic decoupling in pyramidal neurons of the PFC (Aime et al., 2022). At the IC, the maturation of GABAergic PV circuits is key for multisensory integration and pruning of cross-modal input to coordinate the detection of relevant information (Gogolla et al., 2014). Activation of IC PV disrupts the expression of taste-guided goal-directed behavior (Vincis et al., 2020), and enhances taste-guided aversive responses (Yiannakas et al., 2021). Our findings could be indicative of a prediction-dependent decoupling mechanism at the IC, whereby the restriction of bursting activity in LIV-VI aIC-BLA neurons impinges on innate drives towards the tastant and further learning, depending on prior experience.

We further probed our results and hypotheses using PCA and attempted to segregate behaviors based on the perceived ability of the CS to predict the consequences of sensory experience, and the probability for further learning (Figure 5). We focused on BS LIV-VI aIC-BLA projecting neurons since bursting has been implicated in coincidence detection by deep-layer neurons

798 (Boudewijns et al., 2013; Shai et al., 2015), as well as the encoding of novelty and valence relating
799 to different modalities (Song et al., 2015; Dunn et al., 2018; Yousuf et al., 2019). Our PCA of
800 intrinsic properties in BS LVI-VI aIC-BLA projecting neurons demonstrated that distinct plasticity
801 rules are at play depending on the balance between the probability for associative learning and the
802 certainty with which taste predicts the valence of experience during retrieval (Extended Figure 5-
803 1, 2). We propose that increased excitability and reduced fAHP on BS LIV-VI aIC-BLA projecting
804 neurons might represent a transient neuronal state in the absence of adequate predictive cues for
805 the outcome of taste experiences (Adaikkan and Rosenblum, 2015).

806 The IC has long been considered crucial for interoception, which is increasingly understood to be
807 supported by distinct direct or indirect functional bidirectional connectivity. Indeed, interoceptive
808 inputs relating to the processing, or anticipation of physiological states of hydration and satiety
809 manifest at the pIC (Livneh et al., 2017, 2020; Livneh and Andermann, 2021). However, this is
810 rarely the case when it comes to physiological hydration or satiety inputs and the aIC, that has is
811 primarily involved in interoceptive processes in the context food poisoning or CTA (Chen et al.,
812 2020; Wu et al., 2020). As other studies currently in press demonstrate, hydration correlates and
813 requires decreased activity in aIC-BLA and increases in pIC-BLA CB1 receptor-expressing neu-
814 rons (Zhao et al., 2022). In fact, and in further accord with our previous findings (Lavi et al., 2018;
815 Kayyal et al., 2019), optogenetic activation of the aIC-BLA projection was found to be anxiogenic,
816 while physiological conditions that are associated with negative valence and anxiety were encoded
817 by changes in activity on the projection (Nicolas et al., 2022). Under uncertain conditions that are
818 associated with greater potential significance, recruitment of the aIC is thought to contribute to
819 attention, effort, and accurate processing (Lovero et al., 2009), as to identify better response op-

820 tions (Preuschoff et al., 2008). In agreement with earlier computational models of the cortical con-
821 nectivity (Mumford, 1991, 1992), recent work indicates that the aIC facilitates prediction-related
822 encoding driven by hedonics, rather than homeostatic needs (Darevsky et al., 2019; Price et al.,
823 2019; Darevsky and Hopf, 2020). Our results, propose a cellular framework for such an emotional
824 predictive function at the aIC. Indeed, sex can be an important biological variable when examining
825 brain circuits in relation to behavior (Rogers-Carter et al., 2018). Even though we cannot exclude
826 the possibility of sex-specific differences, in previous studies where we manipulated activity at the
827 IC in a cell-type specific manner, we found no differences between male and female mice (Kayyal
828 et al., 2019; Yiannakas et al., 2021). Future studies will further explore whether and how the inter-
829 play between such distinct mechanisms at the aIC, enables its complex role in learning, memory,
830 and decision-making.

831

832 References

833 Adaikkan C, Rosenblum K (2015) A molecular mechanism underlying gustatory memory trace
834 for an association in the insular cortex. Elife 4:1–15.

835 Aime M, Calcini N, Borsa M, Campelo T, Rusterholz T, Sattin A, Fellin T, Adamantidis A (2022)
836 Paradoxical somatodendritic decoupling supports cortical plasticity during REM sleep.
837 Available at: https://www.science.org.

838 Andrade R, Foehring RC, Tzingounis A v. (2012) The calcium-activated slow AHP: Cutting
839 through the Gordian Knot. Front Cell Neurosci:1–38.

840 Arieli E, Gerbi R, Shein-Idelson M, Moran A (2020) Temporally-precise basolateral amygdala
841 activation is required for the formation of taste memories in gustatory cortex. Journal of
842 Physiology 598.

843 Austen JM, Strickland JA, Sanderson DJ (2016) Memory-dependent effects on palatability in
844 mice. Physiol Behav 167.

845 Bachmanov AA, Reed DR, Tordoff MG, Price RA, Beauchamp GK (1996) Intake of ethanol,
846 sodium chloride, sucrose, citric acid, and quinine hydrochloride solutions by mice: A

847 genetic analysis. Behav Genet 26:563–573.

848 Bales MB, Schier LA, Blonde GD, Spector AC (2015) Extensive gustatory cortex lesions
849 significantly impair taste sensitivity to KCl and quinine but not to sucrose in rats. PLoS One
850 10:1–25.

851 Barot SK, Kyono Y, Clark EW, Bernstein IL (2008) Visualizing stimulus convergence in
852 amygdala neurons during associative learning. Proceedings of the National Academy of
853 Sciences 105:20959–20963.

854 Barrett LF, Simmons WK (2015) Interoceptive predictions in the brain. Nat Rev Neurosci
855 16:419–429.

856 Bekisz M, Garkun Y, Wabno J, Hess G, Wrobel A, Kossut M (2010) Increased excitability of
857 cortical neurons induced by associative learning: An ex vivo study. European Journal of
858 Neuroscience 32:1715–1725.

859 Berman DE (2003) Modulation of taste-induced Elk-1 activation by identified neurotransmitter
860 systems in the insular cortex of the behaving rat. Neurobiol Learn Mem 79:122–126.

861 Boudewijns ZSRM, Groen MR, Lodder B, Mcmaster MTB, Kalogreades L, Haan R De,
862 Narayanan RT, Meredith RM, Mansvelder HD, de Kock CPJ (2013) Layer-specific high-
863 frequency spiking in the prefrontal cortex of awake rats. Front Cell Neurosci.

864 Bures J, Bermudez-Rattoni F, Yamamoto T (1998) The CTA paradigm. In: Conditioned Taste
865 Aversion, memory of a special kind.

866 Chakraborty D, Fedorova O v., Bagrov AY, Kaphzan H (2017) Selective ligands for Na+/K+-
867 ATPase α isoforms differentially and cooperatively regulate excitability of pyramidal
868 neurons in distinct brain regions. Neuropharmacology 117:338–351.

869 Chen K, Kogan J, Fontanini A (2020) Spatially distributed representation of taste quality in the
870 gustatory insular cortex of awake behaving mice. Current Biology:1–10.

871 Chinnakkaruppan A, Wintzer ME, McHugh TJ, Rosenblum K (2014) Differential Contribution
872 of Hippocampal Subfields to Components of Associative Taste Learning. Journal of
873 Neuroscience.

874 Citri A, Malenka RC (2008) Synaptic plasticity: Multiple forms, functions, and mechanisms.
875 Neuropsychopharmacology 33:18–41.

876 Connors BW, Gutnick MJ, Prince DA (1982) Electrophysiological properties of neocortical
877 neurons in vitro. J Neurophysiol 48:1302–1320.

878 Darevsky D, Gill TM, Vitale KR, Hu B, Wegner SA, Hopf FW (2019) Drinking despite
879 adversity: behavioral evidence for a head down and push strategy of conflict-resistant
880 alcohol drinking in rats. Addiction Biology 24:426–437.

881 Darevsky D, Hopf FW (2020) Behavioral indicators of succeeding and failing under higher-
882 challenge compulsion-like alcohol drinking in rat. Behavioural Brain Research 393.

883 Disterhoft JF, Wu WW, Ohno M (2004) Biophysical alterations of hippocampal pyramidal
884 neurons in learning, ageing and Alzheimer's disease. Ageing Res Rev 3:383–406.

885 Donato F, Rompani SB, Caroni P (2013) Parvalbumin-expressing basket-cell network plasticity
886 induced by experience regulates adult learning. Nature.

887 Dunn AR, Kaczorowski CC (2019) Regulation of intrinsic excitability: Roles for learning and
888 memory, aging and Alzheimer's disease, and genetic diversity. Neurobiol Learn Mem 164.

889 Dunn AR, Neuner SM, Ding S, Hope KA, O'Connell KMS, Kaczorowski CC (2018) Cell-type-
890 specific changes in intrinsic excitability in the subiculum following learning and exposure
891 to novel environmental contexts. eNeuro 5:18.2018.

892 Escobar ML, Bermúdez-Rattoni F (2000) Long-term potentiation in the insular cortex enhances
893 conditioned taste aversion retention. Brain Res 852:208–212.

894 Faber ESL, Sah P (2002) Physiological role of calcium-activated potassium currents in the rat
895 lateral amygdala. Journal of Neuroscience 22.

896 Fontanini A, Grossman SE, Figueroa JA, Katz DB (2009) Distinct Subtypes of Basolateral
897 Amygdala Taste Neurons Reflect Palatability and Reward. Journal of Neuroscience
898 29:2486–2495.

899 Galliano E, Hahn C, Browne LP, Villamayor PR, Tufo C, Crespo A, Grubb MS (2021) Brief
900 sensory deprivation triggers cell type-specific structural and functional plasticity in
901 olfactory bulb neurons. Journal of Neuroscience 41:2135–2151.

902 Garcia J, Kimeldorf DJ, Koelling RA (1955) Conditioned aversion to saccharin resulting from
903 exposure to gamma radiation. Science 122:157–158.

904 Gogolla N, Takesian AE, Feng G, Fagiolini M, Hensch TK (2014) Sensory integration in mouse
905 insular cortex reflects GABA circuit maturation. Neuron 83:894–905.

906 Gould NL, Kolatt Chandran S, Kayyal H, Edry E, Rosenblum K (2021) Somatostatin
907 Interneurons of the Insula Mediate QR2 Dependent Novel Taste Memory Enhancement.
908 eNeuro:ENEURO.0152-21.2021 Available at:
909 https://www.eneuro.org/content/early/2021/09/13/ENEURO.0152-21.2021 [Accessed
910 September 14, 2021].

911 Graves AR, Moore SJ, Bloss EB, Mensh BD, Kath WL, Spruston N (2012) Hippocampal
912 Pyramidal Neurons Comprise Two Distinct Cell Types that Are Countermodulated by
913 Metabotropic Receptors. Neuron 76:776–789.

914 Graves AR, Moore SJ, Spruston N, Tryba AK, Kaczorowski CC (2016) Brain-derived
915 neurotrophic factor differentially modulates excitability of two classes of hippocampal
916 output neurons. J Neurophysiol 116:466–471.

917 Greenhill SD, Ranson A, Fox K (2015) Hebbian and Homeostatic Plasticity Mechanisms in
918 Regular Spiking and Intrinsic Bursting Cells of Cortical Layer 5. Neuron 88:539–552.

919 Grossman SE, Fontanini A, Wieskopf JS, Katz DB (2008) Learning-related plasticity of temporal
920 coding in simultaneously recorded amygdala-cortical ensembles. Journal of Neuroscience
921 28:2864–2873.

922 Grubb MS, Burrone J (2010) Activity-dependent relocation of the axon initial segment fine-tunes
923 neuronal excitability. Nature 465.

924 Hadamitzky M, Bösche K, Engler A, Schedlowski M, Engler H (2015) Extinction of conditioned
925 taste aversion is related to the aversion strength and associated with c-fos expression in the
926 insular cortex. Neuroscience 303:34–41.

927 Haley MS, Bruno S, Fontanini A, Maffei A (2020) LTD at amygdalocortical synapses as a novel
928 mechanism for hedonic learning. Elife.

929 Haley MS, Fontanini A, Maffei A (2016) Laminar- and Target-Specific Amygdalar Inputs in Rat
930 Primary Gustatory Cortex. The Journal of Neuroscience 36:2623–2637.

931 Haley MS, Maffei A (2018) Versatility and Flexibility of Cortical Circuits. Neuroscientist.

932 Hanamori T, Kunitake T, Kato K, Kannan H (1998) Responses of neurons in the insular cortex to
933 gustatory, visceral, and nociceptive stimuli in rats. J Neurophysiol 79:2535–2545 Available
934 at: http://www.ncbi.nlm.nih.gov/pubmed/9582226.

935 Hebb DO (1961) Distinctive features of learning in the higher animal. Brain mechanisms and
936 learning: A Symposium:37–46.

937 Hogan QH, Poroli M (2008) Hyperpolarization-activated current (Ih) contributes to excitability
938 of primary sensory neurons in rats. Brain Res 1207:102–110.

939 Hu H, Vervaeke K, Storm JF (2007) M-channels (Kv7/KCNQ channels) that regulate synaptic
940 integration, excitability, and spike pattern of CA1 pyramidal cells are located in the
941 perisomatic region. Journal of Neuroscience 27.

942 Jarsky T, Mady R, Kennedy B, Spruston N (2008) Distribution of bursting neurons in the CA1
943 region and the subiculum of the rat hippocampus. Journal of Comparative Neurology 506.

944 Jones MW, French PJ, Bliss T V., Rosenblum K (1999) Molecular mechanisms of long-term
945 potentiation in the insular cortex in vivo. J Neurosci 19:RC36–RC36.

946 Juárez-Muñoz Y, Ramos-Languren LE, Escobar ML (2017) CaMKII Requirement for in Vivo
947 Insular Cortex LTP Maintenance and CTA Memory Persistence. Front Pharmacol.

948 Kahnt T, Tobler PN (2017) Reward, value, and salience. In: Decision Neuroscience: An
949 Integrative Perspective, pp 109–120.

950 Kaphzan H, Buffington SA, Ramaraj AB, Lingrel JB, Rasband MN, Santini E, Klann E (2013)
951 Genetic reduction of the α1 Subunit of Na/K-ATPase corrects multiple hippocampal
952 phenotypes in angelman syndrome. Cell Rep.

953 Kargl D, Kaczanowska J, Ulonska S, Groessl F, Piszczek L, Lazovic J, Buehler K, Haubensak W

(2020) The amygdala instructs insular feedback for affective learning. Elife 9:1–36.

Katz DB, Simon SA, Nicolelis MA (2001) Dynamic and multimodal responses of gustatory cortical neurons in awake rats. J Neurosci.

Kayyal H, Kolatt Chandran S, Yiannakas A, Gould N, Khamaisy M, Rosenblum K (2021) Insula to mPFC reciprocal connectivity differentially underlies novel taste neophobic response and learning. Elife 10 Available at: http://www.ncbi.nlm.nih.gov/pubmed/34219650.

Kayyal H, Yiannakas A, Kolatt Chandran S, Khamaisy M, Sharma V, Rosenblum K, Kayyal H, Chandran SK, Khamaisy M, Sharma V, Rosenblum K (2019) Activity of Insula to Basolateral Amygdala Projecting Neurons is Necessary and Sufficient for Taste Valence Representation. The Journal of Neuroscience.

Kepecs A, Lisman J (2003) Information encoding and computation with spikes and bursts. In: Network: Computation in Neural Systems.

Kim EJ, Juavinett AL, Kyubwa EM, Jacobs MW, Callaway EM (2015) Three Types of Cortical Layer 5 Neurons That Differ in Brain-wide Connectivity and Function. Neuron 88:1253–1267.

Koren T, Yifa R, Amer M, Krot M, Boshnak N, Ben-Shaanan TL, Azulay-Debby H, Zalayat I, Avishai E, Hajjo H, Schiller M, Haykin H, Korin B, Farfara D, Hakim F, Kobiler O, Rosenblum K, Rolls A (2021) Insular cortex neurons encode and retrieve specific immune responses. Cell 184.

Krabbe S, Gründemann J, Lüthi A (2018) Amygdala Inhibitory Circuits Regulate Associative Fear Conditioning. Biol Psychiatry 83:800–809.

Kuba H, Oichi Y, Ohmori H (2010) Presynaptic activity regulates Na+ channel distribution at the axon initial segment. Nature 465.

Kuhlman SJ, Olivas ND, Tring E, Ikrar T, Xu X, Trachtenberg JT (2013) A disinhibitory microcircuit initiates critical-period plasticity in the visual cortex. Nature 501:543–546 Available at: http://www.ncbi.nlm.nih.gov/pubmed/23975100%0Ahttp://www.pubmedcentral.nih.gov/articlerender.fcgi?artid=PMC3962838.

Lavi K, Jacobson GA, Rosenblum K, Lüthi A (2018) Encoding of Conditioned Taste Aversion in Cortico-Amygdala Circuits. Cell Rep 24:278–283.

Levitan D, Liu C, Yang T, Shima Y, Lin JY, Wachutka J, Marrero Y, Ghoddousi RAM, Beltrame E da V, Richter TA, Katz DB, Nelson SB (2020) Deletion of stk11 and fos in mouse bla projection neurons alters intrinsic excitability and impairs formation of long-term aversive memory. Elife 9:1–29.

Lin JY, Amodeo LR, Arthurs J, Reilly S (2012) Taste neophobia and palatability: The pleasure of drinking. Physiol Behav 106:515–519.

990 Livneh Y, Andermann ML (2021) Cellular activity in insular cortex across seconds to hours:
991 Sensations and predictions of bodily states. Neuron:S0896-6273(21)00653-X.

992 Livneh Y, Ramesh RN, Burgess CR, Levandowski KM, Madara JC, Fenselau H, Goldey GJ,
993 Diaz VE, Jikomes N, Resch JM, Lowell BB, Andermann ML (2017) Homeostatic circuits
994 selectively gate food cue responses in insular cortex. Nature 546:611–616 Available at:
995 http://dx.doi.org/10.1038/nature22375.

996 Livneh Y, Sugden AU, Madara JC, Essner RA, Flores VI, Sugden LA, Resch JM, Lowell BB,
997 Andermann ML (2020) Estimation of Current and Future Physiological States in Insular
998 Cortex. Neuron 105:1094-1111.e10.

999 Lovero KL, Simmons AN, Aron JL, Paulus MP (2009) Anterior insular cortex anticipates
1000 impending stimulus significance. Neuroimage 45:976–983.

1001 Luo YX, Galaj E, Ma YY (2021) Differential alterations of insular cortex excitability after
1002 adolescent or adult chronic intermittent ethanol administration in male rats. J Neurosci Res
1003 99.

1004 MacQueen J (1967) Some methods for classification and analysis of multivariate observations.
1005 In: Proceedings of the fifth Berkeley Symposium on Mathematical Statistics and
1006 Probability.

1007 Maffei A, Haley M, Fontanini A (2012) Neural processing of gustatory information in insular
1008 circuits. Curr Opin Neurobiol.

1009 Maglio LE, Noriega-Prieto JA, Maroto IB, Martin-Cortecero J, Muñoz-Callejas A, Callejo-
1010 Móstoles M, de Sevilla DF (2021) Igf-1 facilitates extinction of conditioned fear. Elife 10.

1011 Mickley GA, Kenmuir CL, McMullen CA, Snyder A, Yocom AM, Likins-Fowler D, Valentine
1012 EL, Weber B, Biada JM (2004) Long-term age-dependent behavioral changes following a
1013 single episode of fetal N-methyl-D-Aspartate (NMDA) receptor blockade. BMC Pharmacol
1014 4:1–16.

1015 Mishra P, Narayanan R (2015) High-conductance states and A-type K+channels are potential
1016 regulators of the conductance-current balance triggered by HCN channels. J Neurophysiol
1017 113.

1018 Morrison DJ, Rashid AJ, Yiu AP, Yan C, Frankland PW, Josselyn SA (2016) Parvalbumin
1019 interneurons constrain the size of the lateral amygdala engram. Neurobiol Learn Mem
1020 135:91–99 Available at: http://dx.doi.org/10.1016/j.nlm.2016.07.007.

1021 Mumford D (1991) On the computational architecture of the neocortex - I. The role of the
1022 thalamo-cortical loop. Biol Cybern 65:135–145.

1023 Mumford D (1992) On the computational architecture of the neocortex - II The role of cortico-
1024 cortical loops. Biol Cybern 66:241–251.

1025 Nachman M, Ashe JH (1973) Learned taste aversions in rats as a function of dosage,

concentration, and route of administration of LiCl. Physiol Behav 10:73–78.

Nicolas C, Ju A, Wu W, Eldirdiri H, Delcasso S, Jacky D, Supiot L, Fomari C, Verite A, Masson M, Rodriguez-Rozada S, Wiegert SJ, Beyeler A (2022) Linking emotional valence and anxiety in a mouse insula-amygdala circuit. Res Sq Available at: https://www.researchsquare.com/article/rs-964107/v1 [Accessed August 28, 2022].

Oh MM, Disterhoft JF (2020) Learning and aging affect neuronal excitability and learning. Neurobiol Learn Mem 167.

Owen SF, Berke JD, Kreitzer AC (2018) Fast-Spiking Interneurons Supply Feedforward Control of Bursting, Calcium, and Plasticity for Efficient Learning. Cell 172.

Piette CE, Baez-Santiago MA, Reid EE, Katz DB, Moran A (2012) Inactivation of basolateral amygdala specifically eliminates palatability-related information in cortical sensory responses. Journal of Neuroscience 32:9981–9991.

Preuschoff K, Quartz SR, Bossaerts P (2008) Human insula activation reflects risk prediction errors as well as risk. Journal of Neuroscience 28:2745–2752.

Price AE, Stutz SJ, Hommel JD, Anastasio NC, Cunningham KA (2019) Anterior insula activity regulates the associated behaviors of high fat food binge intake and cue reactivity in male rats. Appetite 133:231–239.

Ranck JB (1973) Studies on single neurons in dorsal hippocampal formation and septum in unrestrained rats. Part I. Behavioral correlates and firing repertoires. Exp Neurol 41:462–531.

Rieger NS, Varela JA, Ng AJ, Granata L, Djerdjaj A, Brenhouse HC, Christianson JP (2022) Insular cortex corticotropin-releasing factor integrates stress signaling with social affective behavior. Neuropsychopharmacology.

Rodríguez-Durán LF, Martínez-Moreno A, Escobar ML, Rodriguez-Duran LF, Martinez-Moreno A, Escobar ML (2017) Bidirectional modulation of taste aversion extinction by insular cortex LTP and LTD. Neurobiol Learn Mem 142:85–90.

Rogers-Carter MM, Djerdjaj A, Gribbons KB, Varela JA, Christianson JP (2019) Insular cortex projections to nucleus accumbens core mediate social approach to stressed juvenile rats. Journal of Neuroscience 39:8717–8729.

Rogers-Carter MM, Varela JA, Gribbons KB, Pierce AF, McGoey MT, Ritchey M, Christianson JP (2018) Insular cortex mediates approach and avoidance responses to social affective stimuli. Nat Neurosci 21:404–414 Available at: http://dx.doi.org/10.1038/s41593-018-0071-y.

Rolls BJ, Rolls ET, Rowe EA, Sweeney K (1981) Sensory specific satiety in man. Physiol Behav 27.

Rosenblum K, Berman DE, Hazvi S, Lamprecht R, Dudai Y (1997) NMDA receptor and the

1062 tyrosine phosphorylation of its 2B subunit in taste learning in the rat insular cortex. Journal
1063 of Neuroscience 17:5129–5135.

1064 Russell JA (1980) A circumplex model of affect. J Pers Soc Psychol 39:1161–1178.

1065 Sadacca BF, Rothwax JT, Katz DB (2012) Sodium concentration coding gives way to evaluative
1066 coding in cortex and amygdala. Journal of Neuroscience 32.

1067 Samengo I, Mato G, Elijah DH, Schreiber S, Montemurro MA (2013) Linking dynamical and
1068 functional properties of intrinsically bursting neurons. J Comput Neurosci 35.

1069 Santini E, Quirk GJ, Porter JT (2008) Fear conditioning and extinction differentially modify the
1070 intrinsic excitability of infralimbic neurons. Journal of Neuroscience 28:4028–4036.

1071 Schachtman TR, Brown AM, Miller RR (1985) Reinstatement-induced recovery of a taste-LiCl
1072 association following extinction. Anim Learn Behav 13:223–227.

1073 Schier LA, Spector AC (2019) The functional and neurobiological properties of bad taste.
1074 Physiol Rev.

1075 Sehgal M, Song C, Ehlers VL, Moyer JR (2013) Learning to learn - Intrinsic plasticity as a
1076 metaplasticity mechanism for memory formation. Neurobiol Learn Mem 105:186–199.

1077 Senn V, Wolff SBE, Herry C, Grenier F, Ehrlich I, Gründemann J, Fadok JP, Müller C, Letzkus
1078 JJ, Lüthi A (2014) Long-range connectivity defines behavioral specificity of amygdala
1079 neurons. Neuron 81:428–437.

1080 Shah MM (2014) Cortical HCN channels: function, trafficking and plasticity. J Physiol
1081 592:2711–2719.

1082 Shai AS, Anastassiou CA, Larkum ME, Koch C (2015) Physiology of Layer 5 Pyramidal
1083 Neurons in Mouse Primary Visual Cortex: Coincidence Detection through Bursting. PLoS
1084 Comput Biol 11.

1085 Shao LR, Halvorsrud R, Borg-Graham L, Storm JF (1999) The role of BK-type Ca2+-dependent
1086 K+ channels in spike broadening during repetitive firing in rat hippocampal pyramidal cells.
1087 Journal of Physiology 521:135–146.

1088 Sharma V, Ounallah-Saad H, Chakraborty D, Hleihil M, Sood R, Barrera I, Edry E, Kolatt
1089 Chandran S, ben Tabou de Leon S, Kaphzan H, Rosenblum K (2018) Local Inhibition of
1090 PERK Enhances Memory and Reverses Age-Related Deterioration of Cognitive and
1091 Neuronal Properties. The Journal of Neuroscience.

1092 Shor OL, Fidzinski P, Behr J (2009) Muscarinic acetylcholine receptors and voltage-gated
1093 calcium channels contribute to bidirectional synaptic plasticity at CA1-subiculum synapses.
1094 Neurosci Lett 449.

1095 Siemian JN, Arenivar MA, Sarsfield S, Aponte Y (2021) Hypothalamic control of interoceptive
1096 hunger. Current Biology 31.

1097 Slouzkey I, Maroun M (2016) PI3-kinase cascade has a differential role in acquisition and
1098 extinction of conditioned fear memory in juvenile and adult rats. Learning and Memory
1099 23:723–731.

1100 Song C, Detert JA, Sehgal M, Moyer JR (2012) Trace fear conditioning enhances synaptic and
1101 intrinsic plasticity in rat hippocampus. J Neurophysiol 107:3397–3408.

1102 Song C, Ehlers VL, Moyer JR (2015) Trace fear conditioning differentially modulates intrinsic
1103 excitability of medial prefrontal cortex–basolateral complex of amygdala projection neurons
1104 in infralimbic and prelimbic cortices. Journal of Neuroscience 35:13511–13524.

1105 Song C, Moyer JR (2018) Layer- and subregion-specific differences in the neurophysiological
1106 properties of rat medial prefrontal cortex pyramidal neurons. J Neurophysiol.

1107 Soto A, Gasalla P, Begega A, López M (2017) c-Fos activity in the insular cortex, nucleus
1108 accumbens and basolateral amygdala following the intraperitoneal injection of saccharin
1109 and lithium chloride. Neurosci Lett.

1110 Staff NP, Jung HY, Thiagarajan T, Yao M, Spruston N (2000) Resting and active properties of
1111 pyramidal neurons in subiculum and CA1 of rat hippocampus. J Neurophysiol.

1112 Stone ME, Fontanini A, Maffei A (2020) Synaptic integration of thalamic and limbic inputs in
1113 rodent gustatory cortex. eNeuro.

1114 Suzuki A, Josselyn SA, Frankland PW, Masushige S, Silva AJ, Kida S (2004) Memory
1115 reconsolidation and extinction have distinct temporal and biochemical signatures. Journal of
1116 Neuroscience 24:4787–4795.

1117 Turrigiano G (2011) Too many cooks? Intrinsic and synaptic homeostatic mechanisms in cortical
1118 circuit refinement. Annu Rev Neurosci 34.

1119 Ventura R, Morrone C, Puglisi-Allegra S (2007) Prefrontal/accumbal catecholamine system
1120 determines motivational salience attribution to both reward-and aversion-related stimuli.
1121 Proc Natl Acad Sci U S A 104:5181–5186.

1122 Vincis R, Chen K, Czarnecki L, Chen J, Fontanini A (2020) Dynamic Representation of Taste-
1123 Related Decisions in the Gustatory Insular Cortex of Mice. Current Biology.

1124 Vincis R, Fontanini A (2016) A gustocentric perspective to understanding primary sensory
1125 cortices. Curr Opin Neurobiol 40:118–124 Available at:
1126 http://dx.doi.org/10.1016/j.conb.2016.06.008.

1127 Wang L, Gillis-Smith S, Peng Y, Zhang J, Chen X, Salzman CD, Ryba NJP, Zuker CS (2018)
1128 The coding of valence and identity in the mammalian taste system. Nature 558:127–131
1129 Available at: http://dx.doi.org/10.1038/s41586-018-0165-4.

1130 Wozny C, Maier N, Schmitz D, Behr J (2008) Two different forms of long-term potentiation at
1131 CA1-subiculum synapses. Journal of Physiology 586.

1132 Wu C-H, Ramos R, Katz DB, Turrigiano GG (2021) Homeostatic synaptic scaling establishes the

specificity of an associative memory. Current Biology.

Wu Y, Chen C, Chen M, Qian K, Lv X, Wang H, Jian L, Yu L, Zhu M, Qiu S (2020) The anterior insular cortex unilaterally controls feeding in response to aversive visceral stimuli in mice. Nat Commun 11.

Xia F, Richards BA, Tran MM, Josselyn SA, Takehara-Nishiuchi K, Frankland PW, Bartos M, Xia F, Richards BA, Tran MM, Josselyn SA, Takehara-Nishiuchi K, Frankland PW (2017) Parvalbumin-positive interneurons mediate neocortical-hippocampal interactions that are necessary for memory consolidation. Elife 6:1–25 Available at: https://doi.org/10.7554/eLife.27868.001.

Yang SS, Li YC, Coley AA, Chamberlin LA, Yu P, Gao WJ (2018) Cell-type specific development of the hyperpolarization-activated current, Ih, in prefrontal cortical neurons. Front Synaptic Neurosci 10.

Yazaki-Sugiyama Y, Kang S, Cteau H, Fukai T, Hensch TK (2009) Bidirectional plasticity in fast-spiking GABA circuits by visual experience. Nature.

Yeomans MR (1998) Taste, palatability and the control of appetite. Proceedings of the Nutrition Society 57.

Yiannakas A, Kolatt Chandran S, Kayyal H, Gould N, Khamaisy M, Rosenblum K (2021) Parvalbumin interneuron inhibition onto anterior insula neurons projecting to the basolateral amygdala drives aversive taste memory retrieval. Current Biology 31:1–15.

Yousuf H, Ehlers VL, Sehgal M, Song C, Moyer JR (2019) Modulation of intrinsic excitability as a function of learning within the fear conditioning circuit. Neurobiol Learn Mem 167.

Zeldenrust F, Wadman WJ, Englitz B (2018) Neural coding with bursts—Current state and future perspectives.

Zhao Z, Covelo A, Mitra A, Varilh M, Wu Y, Jacky D, Cannich A, Bellocchio L, Marsicano G, Beyeler A (2022) Cannabinoids regulate an insula circuit controlling water intake. bioRxiv.

Figure legends

Graphical abstract: A model for excitability changes in IV-VI aIC-BLA neurons when the taste salience is low and highly predictive following the taste memory

- The unpredictability of future valence outcomes: Novel appetitive taste experiences /extinction of previously learned aversive taste experiences, increases the excitability (blue arrow) of aIC-BLA projecting neurons (red). This increased excitability is specific to the deep-layer aIC-BLA projecting neurons (LIV-VI).
- When the taste valence is highly predictable (familiar/aversive), excitability is reduced in LIV-VI aIC-BLA projecting neurons (red arrow).
- LIV-VI aIC-BLA neurons remain excitable facilitating the association of the taste memory trace with visceral pain when the stimulus is not adequately predictive of the outcome of the sensory experience.

Figure 1: Retrieval of appetitive and novel taste increases excitability in LIV-VI aIC-BLA projection neurons

A) Diagrammatic representation of experimental procedures. Following surgery and stereotaxic delivery of ssAAV_retro2-hSyn1-chi-mCherry-WPRE-SV40p(A) into the BLA, mice were allowed 4 weeks of recovery. Animals were subsequently assigned to treatment groups and trained to drink from pipettes (see Methods). We compared the intrinsic properties of LIV-VI aIC-BLA neurons among the Water (n=6 animals, 23 cells), Saccharin 1x (n=5 animals, 20 cells), Saccharin 1x(4h) (n=4 animals, 17 cells), Saccharin 5x (n=6 animals, 18 cells) and Quinine 1x groups (n=4 animals, 19 cells), as well as a Cage control group (n=4 animals, 19 cells) that underwent surgery

and stereotaxic delivery of ssAAV_retro2-hSyn1-chi-mCherry-WPRE-SV40p(A) at the BLA without water restriction.

B) Graph showing the water consumption prior to treatment (mean ± SD). There was no significant difference between water intakes between the groups before the treatment. One-Way ANOVA, p= 0.9766.

C) Representative traces of LIV-VI aIC-BLA projecting neurons from the six treatment groups. Scale bars 20 mV vertical and 50ms horizontal from 300 pA step.

D) The dependence of firing rate on current step magnitude in LIV-VI aIC-BLA neurons was significantly different among the treatment groups. Excitability in the Saccharin 1x was increased compared to all other groups. Two-way repeated measures ANOVA, Current x Treatment: $p<0.0001$; Cage control vs. Saccharin 1x: **$p<0.01$, ***$p<0.001$; Saccharin 1x vs. Saccharin 1x (4hr): #$p<0.05$, ##$p<0.01$, ####$p<0.0001$; Water vs. Saccharin 1x: ^$p<0.05$, ^^$p<0.01$, ^^^ $p<0.001$; Saccharin 1x vs. Quinine 1x: **$** $p<0.05$, **$$**$p<0.01$; Saccharin 1x vs. Saccharin 5x: **-** $p<0.05$; Saccharin 1x (4hr) vs. Saccharin 5x: + $p<0.05$.

E) Representative of all fAHP measurements in response to 500 ms step current injections. Scale bars 20 mV vertical and 50 ms horizontal.

F) Representative of all action potential properties were taken. Scale bars 20 mV vertical and 5 ms horizontal.

G) Measurements for all input resistance, sag ratio and membrane time constants were analyzed in response to 1 sec, -150pA step current injection. P- peak voltage, S- steady state voltage. Scale bars 5 mV vertical and 100 ms horizontal.

H) Significant differences were observed among the treatment groups in terms of fAHP. Cage control (9.191 ± 1.449 mV), Water (8.150 ± 0.8288 mV), Saccharin 1x (3.016 ± 0.9423 mV), Quinine 1x (13.58 ± 1.562 mV) Saccharin 5x (8.158 ± 1.356 mV), Saccharin 1x (4hrs) (5.989 ± 1.074 mV), One-Way ANOVA, $p<0.0001$.

I) Action potential half-width in the Saccharin 1x group (0.6005 ± 0.03260 ms) was significantly decreased compared to Saccharin 1x (4hr) (0.7765 ± 0.03641 ms), One-Way ANOVA, $p=0.0065$.

J) The membrane time constant was significantly different between the Cage Control (15.03 ± 1.376 ms) and Saccharin 1x (4hr) (26.21 ± 2.421 ms), Water (19.24 ±1.620 ms) and Saccharin 1x (4hr) (26.21 ± 2.421 ms), Saccharin 1x (14.82 ± 1.485 ms) and Saccharin 1x (4hrs) (26.21 ± 2.421 ms), Saccharin 5x (17.30 ±1.660 ms) and Saccharin 1x (4hr) (26.21 ± 2.421 ms) groups. One-Way ANOVA, $p<0.0001$.

For panels 1D, H, I and J: *$p<0.05$, **$p<0.01$, ***$p<0.001$, ****$p<0.0001$.

All data are shown as mean ± SEM.

Histological verification of viral delivery at the IC and BLA, as well as locations of whole-cell patch clamp recording electrode (see Extended Figure 1-1).

Individual IC neurons were classified as burst- and regular-spiking by post-hoc analysis of responses to rheobase current injections (see Extended Figure 1-2).

The intrinsic properties of burst spiking LIV-VI aIC-BLA projecting neurons are differentially modulated by taste valence in the context of novelty (see Extended Figures 1-3).

Figure 2: Learned aversive taste memory retrieval decreases the excitability of LIV-VI aIC-BLA projecting neurons

A) Experimental design of behavioral procedures conducted to compare the intrinsic properties of LIV-VI aIC-BLA neurons following learned aversive taste memory retrieval (CTA retrieval - n=8 animals, 27 cells), appetitive retrieval for the same tastant (Saccharin 2x - n=5 animals, 20 cells).

B) Mice showed a significantly reduced saccharin consumption following learned aversive memory retrieval (N=8) compared to appetitive retrieval mice (n=5) group. p=0.0085, Mann Whitney test.

C) Representative traces of LIV-VI aIC-BLA projecting neurons from the two treatment groups. Scale bars 20 mV vertical and 50ms horizontal from 300 pA step.

D) The excitability of LIV-VI aIC-BLA in the Saccharin 2x group was significantly enhanced compared to CTA retrieval. Two-way repeated measures ANOVA, Current x Treatment: $p<0.0001$.

E) Representative traces showing action potential measurements for both groups. Scale bar 20 mV vertical and 2ms horizontal.

F) Representative traces showing the input resistance and sag ratio measurements. Scale bar 10 mV vertical and 100ms horizontal.

G) Action potential amplitude in the CTA retrieval (56.21 ± 0.9978 mV) group was increased compared to Saccharin 2x (49.14 ± 1.568 mV), p=0.0005, Mann Whitney test.

H) Input resistance in the CTA retrieval group (136.4 ± 9.064 MΩ) was significantly decreased compared to Saccharin 2x (181.1 ± 11.7 MΩ). p=0.0036, Unpaired t test.

I) SAG ratio following CTA retrieval (13.41 ± 1.31) was significantly enhanced compared to

Saccharin 2x (7.815 ± 1.176). p=0.0037, Unpaired t test.

Data are shown as mean ± SEM. *p<0.05, **p<0.01, ***p<0.001, ****p<0.0001.

Learned aversive taste memory retrieval decreases the excitability of burst spiking LIV-VI aIC-BLA neurons (see Extended Figure 2-1).

Figure 3: Extinction of CTA enhances, whereas reinstatement decreases the excitability of LIV-VI aIC-BLA projecting neurons

A) Experimental design of behavioral procedures conducted to compare the intrinsic properties of LIV-VI aIC-BLA neurons following CTA Extinction (n=5, animals, 14 cells) and Reinstatement (n=3 animals, 15 cells).

B) The graph showing the reduced aversion following the successful extinction in both treatment groups.

C) Data showing the saccharin consumption on the test day following successful extinction and Reinstatement of CTA. CTA reinstated mice showed significantly reduced saccharin consumption compared to extinguished mice. p=0.0179, Mann Whitney test.

D) Representative traces of LIV-VI aIC-BLA projection neurons firing from the two treatment groups. Scale bars 20 mV and 50ms horizontal from 300 pA step.

E) Excitability in LIV-VI aIC-BLA neurons was significantly different among the treatment groups. Two-Way repeated measures ANOVA, Current x Treatment: p<0.0001.

F) Action potential threshold in the Reinstatement group (-29.43 ± 1.731 mV) was enhanced compared to Extinction (-36.06 ± 1.481 mV). p=0.0076, Unpaired t test.

G) The membrane time constant following Reinstatement (25.48 ± 1.58 ms) was significantly enhanced compared to Extinction (17.55 ± 2.684 ms, p=0.047). p=0.0153, Unpaired t test.

For panels 5D-F: *p<0.05, **p<0.01, ***p<0.001, ****p<0.0001.

All data are shown as mean ± SEM.

Extinction of CTA enhances the excitability of burst spiking LIV-VI aIC-BLA projecting neurons compared to CTA reinstatement (see Extended Figure 3-1).

Figure 4: Innately aversive taste is correlated with high fAHP, and prolonged conflicting experiences is correlated with an increased AP half-width in LIV-VI aIC-BLA projecting neurons

We compared the intrinsic properties of LIV-VI aIC-BLA neurons among the Saccharin 1x (n=5 animals, 20 cells), Quinine 1x (n=4 animals, 19 cells), Saccharin 2x (n=5 animals, 20 cells), CTA retrieval (n=8, 27 cells), Extinction (n=5 animals, 14 cells) and Reinstatement (n=3 animals, 15 cells) groups.

A) Groups associated with positive taste valence (Saccharin 1x, Saccharin 2x, Extinction), exhibited significantly increased excitability compared to innate or learned negative taste valence groups (Quinine 1x, CTA retrieval and Reinstatement). Two-way repeated measures ANOVA, Current x Treatment: p<0.0001; Saccharin 2x vs. CTA retrieval: *p; Saccharin 2x vs. Reinstatement: #p: Saccharin 2x vs Quinine 1x: p**$**; Saccharin 1x vs. CTA retrieval: p^; Saccharin 1x vs. Quinine 1x: p**%**; Saccharin 1x vs reinstatement: p+; Extinction vs. CTA retrieval: p**@**; Extinction vs. Reinstatement: p**&**; Extinction vs. Quinine 1x: p-.

B) fAHP was significantly enhanced in response to Quinine 1x (13.56± 1.562 mV) compared to all other groups. Significant differences were also observed between Saccharin 1x (3.016 ± 0.9423 mV), Saccharin 2x (5.223 ± 0.8217 mV), and CTA retrieval (7.97 ± 1.018 mV, p=0.0036). Extinction (4.731 ± 1.021 mV) and Reinstatement (5.932 ± 1.292 mV). One-Way ANOVA, $p<0.0001$.

C) Input resistance was significantly different between Saccharin 2x (181.1 ± 11.7 MΩ) and CTA retrieval (136.4 ± 9.064 MΩ), p= 0.0352. Conversely, input resistance in Saccharin 1X (145.8 ± 12.56), Quinine 1X (146 ± 9.094), Extinction (151.1 ± 15.63), and Reinstatement groups was similar. One-Way ANOVA, p= 0.0213.

D) SAG ratio was significantly different between Saccharin 2x (7.815 ± 1.176) and CTA retrieval (13.41 ± 1.31), p= 0.0209. Conversely, SAG ratio in Saccharin 1x (10.89 ± 1.621), Quinine 1x (12.13 ± 1.23), Extinction (12.37 ± 1.471) and Reinstatement (9.245 ± 0.884) groups was similar One-Way ANOVA, p= 0.0286.

E) Action potential amplitude in the Quinine 1x group (57.11 ± 1.376 mV), and CTA retrieval (56.21 ± 0.9978 mV), was significantly increased compared to Saccharin 2x (49.14 ± 1.568 mV, p= 0.0175, and 0.0229, respectively). Conversely, action potential attitude in the Saccharin 1x (52.03 ± 1.308 mV), Extinction (55.09 ± 2.122 mV) and Reinstatement (53.1 ± 2.906 mV) groups was similar. One-Way ANOVA, p = 0.0061.

F) Action potential half-width following Extinction (0.7386 ± 0.03145 ms) and Reinstatement (0.8187 ± 0.06929 ms) was elevated compared to Saccharin 1x (0.6005 ± 0.03260 ms), Saccharin 2x (0.5780 ± 0.02994 ms) as well as CTA retrieval (0.5959 ± 0.02080 ms, but no with Quinine 1x (0.6300 ± 0.03555 ms). One-Way ANOVA, p = 0.0002.

G) The membrane time constant in the Saccharin 1x (14.82 ± 1.485 ms) group was significantly decreased compared to Reinstatement (25.48 ± 1.58 ms, p= 0.0043) groups was. Differences between CTA retrieval (20.96 ± 1.724 ms, p=0.0189), Quinine 1x (21.55 ± 1.638 ms), Saccharin 2x (19.28 ± 1.837 ms) and Extinction (17.55 ± 2.684 ms) groups failed to reach significance. One-Way ANOVA, p = 0.0047.

Figure 5: The intrinsic properties of burst spiking LIV-VI aIC-BLA projecting neurons represent taste experience and the probability for further learning

A) Data across all intrinsic properties from BS LIV-VI aIC-BLA neurons of the Saccharin 1x, Saccharin 2x and Extinction groups were combined and assigned to the Low predictive following memory group (32 BS cells). Conversely, the intrinsic properties of BS LIV-VI aIC-BLA neurons from animals having undergone CTA retrieval, 5x Saccharin, and Reinstatement were combined and assigned to the High predictive following memory group (31 BS cells). The resultant three-dimensional scatter representation of the two groups encompassed Excitability at 350pA; AP amplitude, AP halfwidth, AP threshold; fAHP, mAHP, sAHP; IR, Rheobase, RMP, SAG ratio and τ in BS LIV-VI aIC-BLA neurons. See Extended Figure 5-1.

B) Three-dimensional representation of the contribution of individual parameters (loadings matrix) to the principal components segregating the two groups of treatments (scores matrix).

PCA variable contributions and component loadings of BS and RS LIV-VI aIC-BLA projecting neurons in Extended Figure 5-2.

Extended figures and Tables

Extended Figure 1-1: Histological verification of rAAV-mCherry virus expression and locations of whole- cell patch clamp recordings

A) A representative image showing the distribution of retrograde injections into the BLA and aIC-BLA projection neuron at aIC.

B) Locations showing the retroviral injections sites in the BLA.

C) Mean localization of BLA projecting neurons of the agranular aIC used for electrophysiological whole-cell recordings.

Extended Figure 1-2: The ratio of burst spiking and regular spiking LIV-VI aIC-BLA projecting neurons changes in relation to the uncertainty associated with taste experiences

A) Representative traces from Burst (BS) and Regular (RS) spiking LIV-VI aIC-BLA projecting neurons in response to rheobase current injections. The neurons showing doublets or triplets in response to rheobase current injection were considered BS. The neurons showing single spike in response to rheobase current injection considered RS. Scale bars 20 mV and 100 ms.

B) Pie charts showing the change in the ratio of BS vs RS LIV-VI aIC-BLA projection neurons, expressed as a percentage of the sampled population across the Saccharin 1x, Saccharin 2x, Saccharin 5x, CTA retrieval, Extinction, and Reinstatement groups.

C) Heat map summary of the change in the ratio of BS vs RS LIV-VI aIC-BLA projection neurons, expressed as a percentage of the sampled population across the six treatment groups.

Extended Figure 1-3: Appetitive novel taste alters the intrinsic properties of burst spiking LIV-VI aIC-BLA neurons

We compared the intrinsic properties of BS and RS LIV-VI aIC-BLA neurons among the Cage control (n=13 cells), Water (n= 11cells), Saccharin 1X (n=17 cells), Quinine 1x (n=9 cells), Saccharin 5x (n=10 cells) and Saccharin 1x (4hrs, n=6 cells).

A) Excitability in BS LIV-VI aIC-BLA was not significantly different among the treatment groups. Two-Way repeated measures ANOVA, Current x Treatment: $p<0.0001$, Group interaction $p= 0.0666$.

B) fAHP was significantly enhanced in Quinine 1x (13.67 ±2.681 mV) and Saccharin 5x (11.30 ±1.727 mV) BS neurons compared to Saccharin 1x BS neurons (2.870 ±1.044 mV). One-Way ANOVA, P= 0.0004.

C) Action potential amplitude was significantly different between the groups. Cage controls (56.27 ±1.147 mV), Water (54.21 ±1.572 mV), Saccharin 1x (51.64 ± 1.473 mV), Quinine 1X (58.86 ± 2.003 mV), Saccharin 5x (58.40 ± 1.812 mV), and Saccharin 1x (4hr) (46.79 ± 4.359 mV). One-Way ANOVA, P= 0.0097.

D) Action potential half-width in BS LIV-VI aIC-BLA neurons of the Saccharin 1x (4 hrs.) group (0.8850 ± 0.05943ms) was increased compared to the Saccharin 1x (1hr) group - 0.5976 ± 0.03555ms. One-Way ANOVA, P=0.0139.

E) Action potential threshold was not significantly different between the groups. Cage control (-31.83± 2.971 mV), Water (-29.27 ± 2.060 mV), Saccharin 1x (-30.73 ± 2.385 mV), Quinine 1x (-29.35 ± 3.071 mV), Saccharin 5x (-30.38 ± 2.493 mV), and Saccharin 1x (4hr) (-34.61 ± 2.174

mV). One-Way ANOVA, P= 0.7652.

F) Input resistance was similar among the different treatment groups. Cage control (118.4 ± 9.771 MΩ), Water (136.5 ± 14.40 MΩ), Saccharin 1x (146.6 ±14.22 MΩ), Quinine 1x (139.2 ± 16.86 MΩ), Saccharin 5x (156.1 ± 22.85 MΩ), and Saccharin 1x (4hr) (154.9 ± 22.41 MΩ). One-Way ANOVA, P= 0.6304.

G) SAG ratio was not significantly different between the groups. Cage control (14.91 ± 2.195), Water (8.751± 2.021), Saccharin 1x (11.67±1.790), Quinine 1x (14.15 ± 2.159), Saccharin 5x (11.92 ± 3.395), and Saccharin 1x (4hr) (14.99 ± 2.770). One-Way ANOVA, P= 0.2232.

H) Membrane time constant was significantly different among the treatment groups. Cage control (14.71±1.944 ms), Water (18.03 ± 2.309 ms), Saccharin 1x (14.27 ± 1.666 ms), Quinine 1x (23.21 ± 2.717 ms), Saccharin 5x (17.11 ± 2.296 ms), and Saccharin 1x (4hr) (26.09 ± 5.331 ms). One-Way ANOVA, P= 0.0321.

Data are shown as mean ± SEM. *p<0.05, **p<0.01.

Extended Figure 2-1: Learned aversive taste memory retrieval decreases the excitability of burst spiking LIV-VI aIC-BLA neurons

We compared the intrinsic properties of BS and RS LIV-VI aIC-BLA neurons following Saccharin 2xs (BS=13, RS=7, cells) and CTA memory retrieval (BS=12, RS=15, cells).

A) Excitability in BS LIV-VI aIC-BLA neurons was significantly reduced in the CTA retrieval group compared to Saccharin 2x. Two-Way repeated measures ANOVA, Current x Treatment: p<0.0001.

B) Input resistance in BS LIV-VI aIC-BLA neurons was significantly enhanced in the Saccharin 2x (180.3 ± 15.15 MΩ) compared to CTA retrieval (110.9 ± 12.98 MΩ). Unpaired t test, p= 0.0022.

C) Action potential amplitude in BS LIV-VI aIC-BLA neurons was significantly increased in the CTA retrieval group compared to Saccharin 2x (46.18 ± 1.666 mV), and CTA retrieval (57.87 ± 1.678 mV). Mann Whitney test, p<0.0001.

D) SAG ratio in BS LIV-VI aIC-BLA neurons was significantly decreased in the Saccharin 2x (7.017 ± 1.317) compared to CTA retrieval (16.8 ± 1.869). Mann Whitney test, p= 0.0005.

E) Representative traces of RS LIV-VI aIC-BLA neurons firing from the two treatments. Scale bars 20 mV vertical and 50ms horizontal in response to 150 pA step current.

F) Excitability in RS LIV-VI aIC-BLA neurons was similar in the CTA retrieval and Saccharin 2x. Two-Way repeated measures ANOVA, Current x Treatment: p= 0.0953.

G) Input resistance in RS LIV-VI aIC-BLA neurons was not significantly different in between the groups. Saccharin 2x (182.6 ± 19.62 MΩ), and CTA retrieval (156.7 ± 10.11 MΩ). Mann Whitney test, p >0.9999.

H) SAG ratio in RS LIV-VI aIC-BLA neurons was not significantly different between the groups. Saccharin 2x (9.297 ± 2.347), and CTA retrieval (10.71 ± 1.536). Mann Whitney test, p= 0.5815.

I) Action potential amplitude in RS LIV-VI aIC-BLA neurons was not significantly different between the groups. Saccharin 2x (54.62 ± 2.058 mV), and CTA retrieval (54.89 ± 1.13 mV). Mann Whitney test, p>0.9999.

J) AP half-width in RS LIV-VI aIC-BLA neurons was significantly reduced following CTA memory retrieval (0.5633 ± 0.01703 ms) compared to the Saccharin 2x (0.6614 ± 0.04149 ms).

Mann Whitney test, p= 0.0200.

K) Membrane time constant was similar in both treatment groups. Saccharin 2x RS (18.36 ± 2.842ms), and CTA memory retrieval RS (24.08 ± 2.023 ms). Mann Whitney test, p= 0.0777.

Data are shown as mean ± SEM. *p<0.05, **p<0.01, ***p<0.001, ****p<0.0001.

Extended Figure 3-1: Extinction of CTA enhances, excitability of burst spiking LIV-VI aIC-BLA projecting neurons

We compared the intrinsic properties of BS and RS LIV-VI aIC-BLA neurons following the Extinction (BS=11, RS=3, cells) and Reinstatement (BS=10, RS=5, cells).

A) Excitability in BS LIV-VI aIC-BLA was significantly enhanced in Extinction group comparing to Reinstatement. Two-Way repeated measures ANOVA, Current x Treatment: p<0.0001.

B) sAHP in BS LIV-VI aIC-BLA neurons was significantly enhanced in the Extinction group (-2.104 ± 0.4466 mV) compared to Reinstatement (-3.804 ± 1.339 mV) neurons. Mann Whitney test, p=0.0230.

C) Action potential threshold in BS LIV-VI aIC-BLA neurons was significantly reduced in the Extinction group (-37.41 ± 1.636 mV) compared to Reinstatement (-27.5 ± 2.195 mV). Unpaired t test, p= 0.0016.

D) Input resistance in BS LIV-VI aIC-BLA neurons was similar in the two treatment groups. Extinction (131.1 ± 13.93 MΩ) and Reinstatement BS (157.4 ± 10.56 MΩ). Mann Whitney test, p= 0.1321.

E) SAG ratio in BS LIV-VI aIC-BLA neurons was enhanced following Extinction (13.69 ± 1.541)

neurons compared to Reinstatement BS (9.124 ± 1.03). Unpaired t test, p= 0.0262.

F) Membrane time constant in BS LIV-VI aIC-BLA neurons was significantly reduced in the Extinction group (14.52 ± 2.714 ms) compared to Reinstatement (26.93 ± 1.893) neurons. Mann Whitney test, p= 0.0062.

G) Representative traces of RS LIV-VI aIC-BLA firing from two treatment groups. Scale bars 20 mV vertical and 50 ms horizontal in response to 150 pA current step.

H) Excitability of RS LIV-VI aIC-BLA neurons in both treatment groups.

I) Input resistance in RS LIV-VI aIC-BLA neurons was similar in the Extinction (224.2 ± 21.29 MΩ) and Reinstatement (221.2 ± 18.9 MΩ) groups.

J) SAG ratio in RS LIV-VI aIC-BLA neurons was not different between the Extinction (7.515 ± 2.666) and Reinstatement (9.486 ± 1.846) groups.

K) Membrane time constant in RS LIV-VI aIC-BLA neurons was not different between the Extinction (28.69 ± 2.138 ms) and Reinstatement groups (22.58 ± 2.632 ms).

Extended Figure 5-1: PCA showing Burst vs Regular spiking LIV-VI aIC-BLA neurons all range of excitability vs 350 pA only

A) PCA of BS and RS LIV-VI aIC-BLA neurons all range of excitability (50-350 pA and all other intrinsic properties measured). Sampled population across six treatment groups (Saccharin 1x, Saccharin 2x, Saccharin 5x, CTA retrieval, Extinction, Reinstatement).

B) PCA of BS and RS LIV-VI aIC-BLA neurons excitability of 350 pA only and all other intrinsic properties measured. Sampled population across six treatment groups (Saccharin 1x, Saccharin 2x, Saccharin 5x, CTA retrieval, Extinction, Reinstatement).

Extended Figure 5-2: PCA variable contributions and component loadings of burst- and regular-spiking LIV-VI aIC-BLA projecting neurons

A) Column chart demonstrating the individual and cumulative proportion of the variance accounted by principal components following PCA of BS LIV-VI aIC-BLA projecting neurons in the two groups of treatments (Saccharin 1x, Saccharin 2x, Extinction vs. CTA retrieval, 5x Saccharin, Reinstatement).

B) Table summarizing the contribution of individual variables (loadings) to the coordinate value of the principal components segregating the two groups (score).

C) Communalities table, demonstrating the amount of variance in each variable that is accounted for by the extraction of principal components. Initial communalities are estimates of the variance in each variable accounted for by all components or factors (=1.00).

Table 1: Summary of LIV-VI aIC-BLA intrinsic properties

Values are expressed in mean ± SEM. The number of cells is in parentheses. Statistical analysis was performed by One-way ANOVA Post-hoc Tukey's and Dunn's multiple comparisons. Student's t-test was performed for the comparison between two groups. RMP - resting membrane potential, fAHP, mAHP and sAHP - fast, medium, slow after hyperpolarization potentials, respectively. AP Thresh - action potential threshold, AP Amp - action potential amplitude. AP half-

1475 width - action potential half-width. Data are shown as mean ± SEM. *p<0.05, **p<0.01,
1476 ***p<0.001, ****p<0.0001, with respect to the corresponding symbols.

1477

1478 Table 2: Summary of LI-III aIC-BLA intrinsic properties

1479 Values are expressed as mean ± SEM. The number of cells is in parentheses. Statistical analysis
1480 was performed by Student's t-test. RMP - resting membrane potential, mAHP - medium after
1481 hyperpolarization potentials. AP Thresh - action potential threshold, AP Amp - action potential
1482 amplitude. AP half-width - action potential half-width.

1483

1484 Table 3: Summary of BS LIV-VI aIC-BLA intrinsic properties

1485 Values are expressed in mean ± SEM. The number of cells is in parentheses. Statistical analysis
1486 was performed by One-way ANOVA Post-hoc Tukey's and Dunn's multiple comparisons.
1487 Student's t-test was performed for the comparison between two groups. RMP - resting membrane
1488 potential, fAHP, mAHP and sAHP - fast, medium, slow after hyperpolarization potentials,
1489 respectively. AP Thresh - action potential threshold, AP Amp - action potential amplitude. AP half-
1490 width - action potential half-width.

1491

1492 Table 4: Summary of RS LIV-VI aIC-BLA intrinsic properties

1493 Values are expressed in mean ± SEM. The number of cells is in parentheses. Statistical analysis
1494 was performed by One-way ANOVA Post-hoc Tukey's and Dunn's multiple comparisons.
1495 Student's t-test was performed for the comparison of two groups. RMP - resting membrane
1496 potential, fAHP, mAHP and sAHP - fast, medium, slow after hyperpolarization potentials,

respectively. AP Thresh - action potential threshold, AP Amp - action potential amplitude. AP half-width - action potential half-width.

Table 5: Statistics Table.

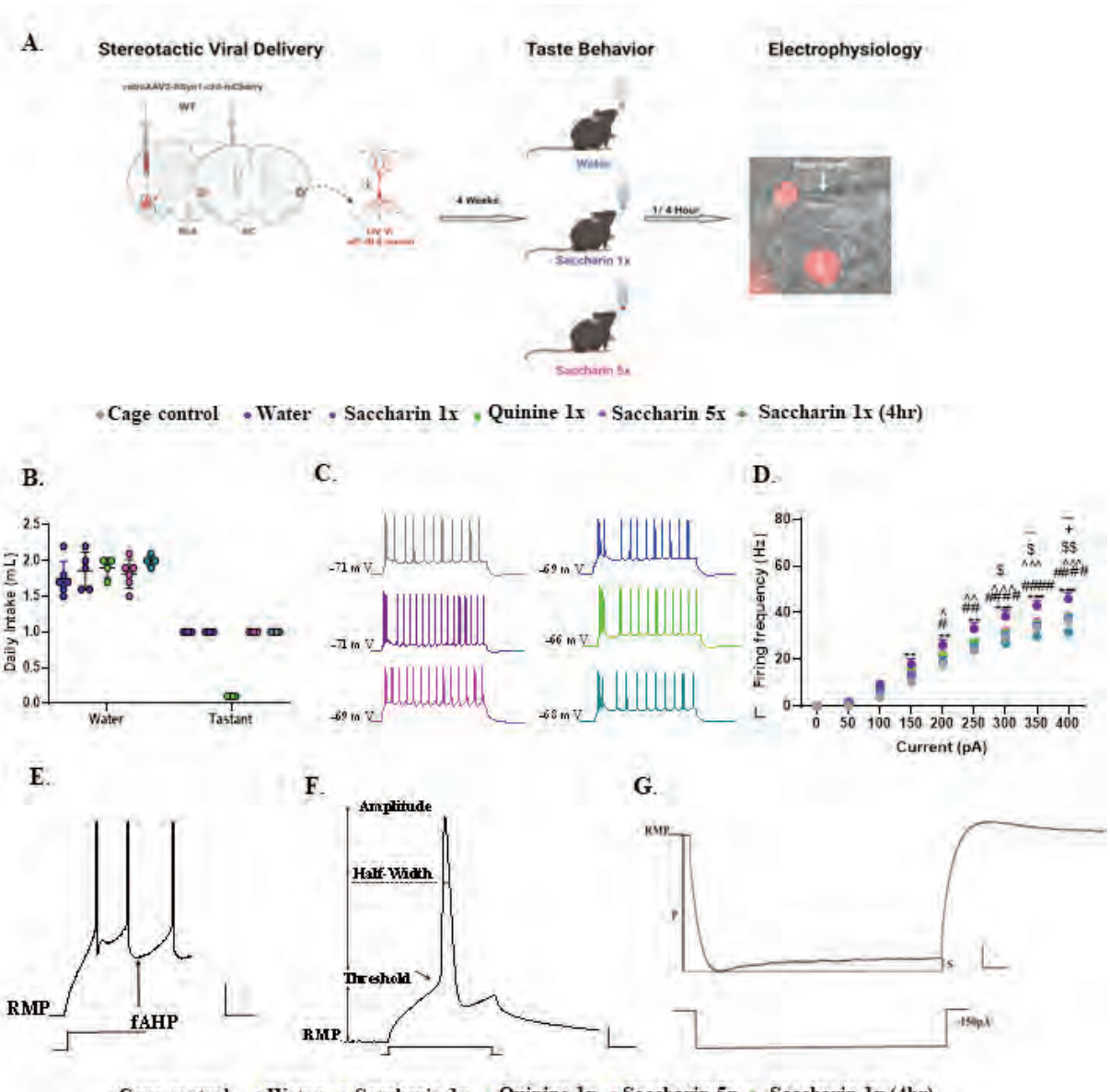

* Cage control vs. Saccharin 1x, # Saccharin 1x vs. Saccharin 1x (4hr), ^ Water vs. Saccharin 1x,

$ Saccharin 1x vs. Quinine 1x, - Saccharin 1x vs. Saccharin 5x, + Saccharin 1x (4hr) vs. Saccharin 5x.

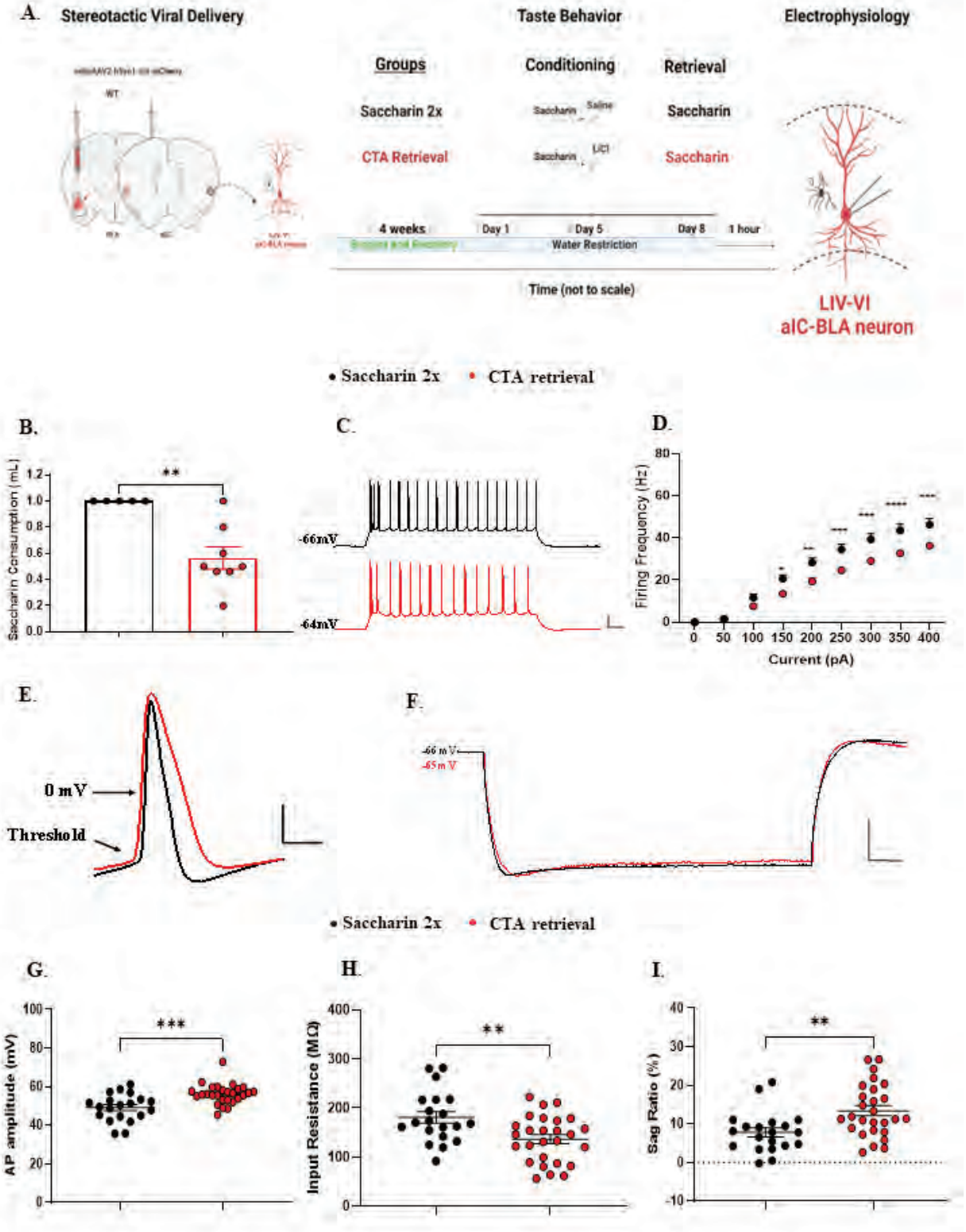

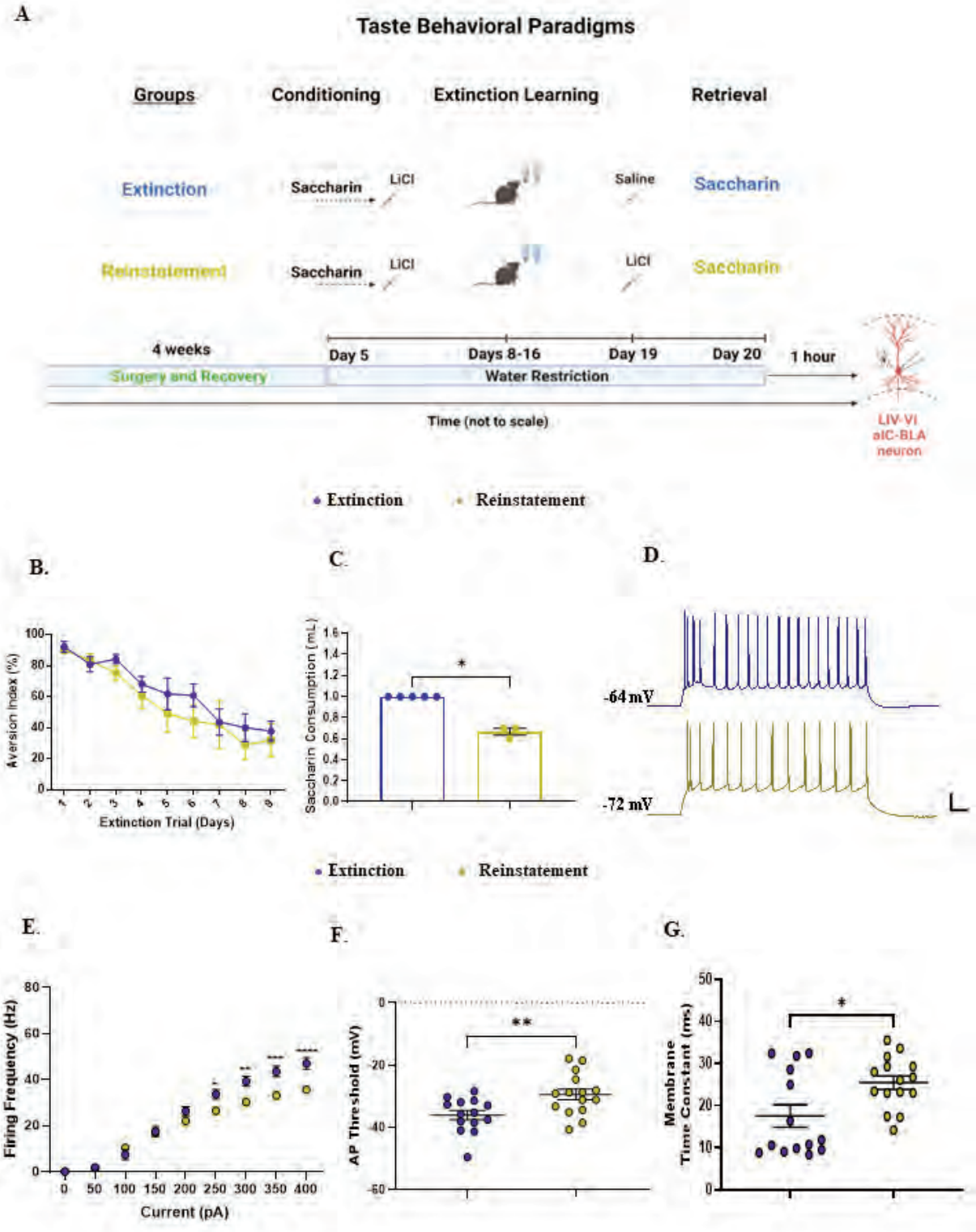

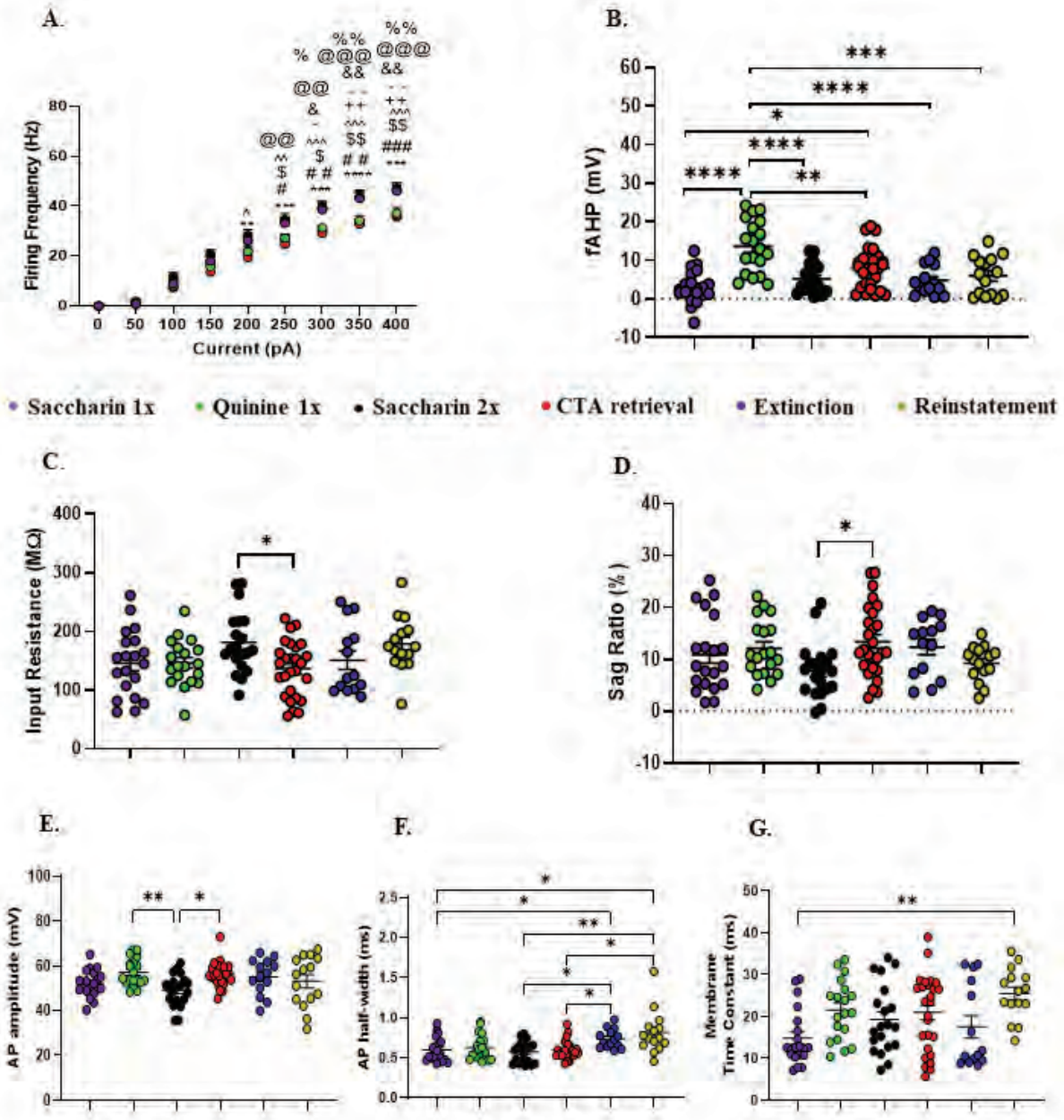

* Saccharin 2x vs. CTA retrieval, # Saccharin 2x vs. Reinstatement, $ Saccharin 2x vs Quinine, ^ Saccharin 1x vs. CTA retrieval, % Saccharin 1x vs. Quinine 1x, + Saccharin 1x vs reinstatement, @ Extinction vs. CTA retrieval, & Extinction vs. Reinstatement, - Extinction vs. Quinine 1x.

A.

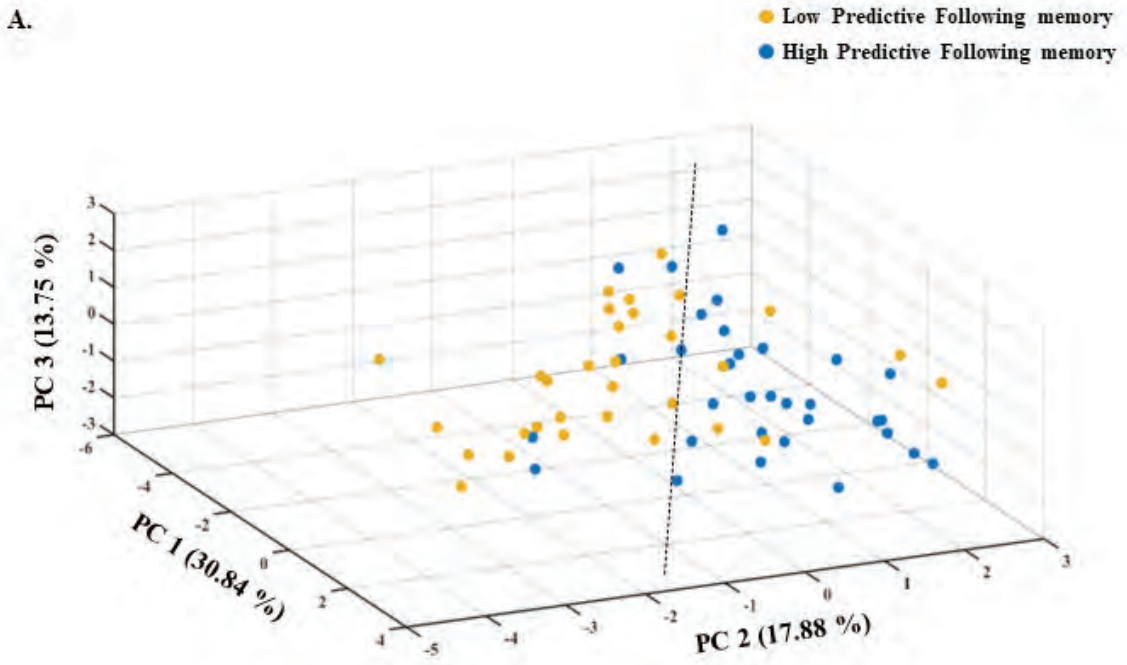

B.

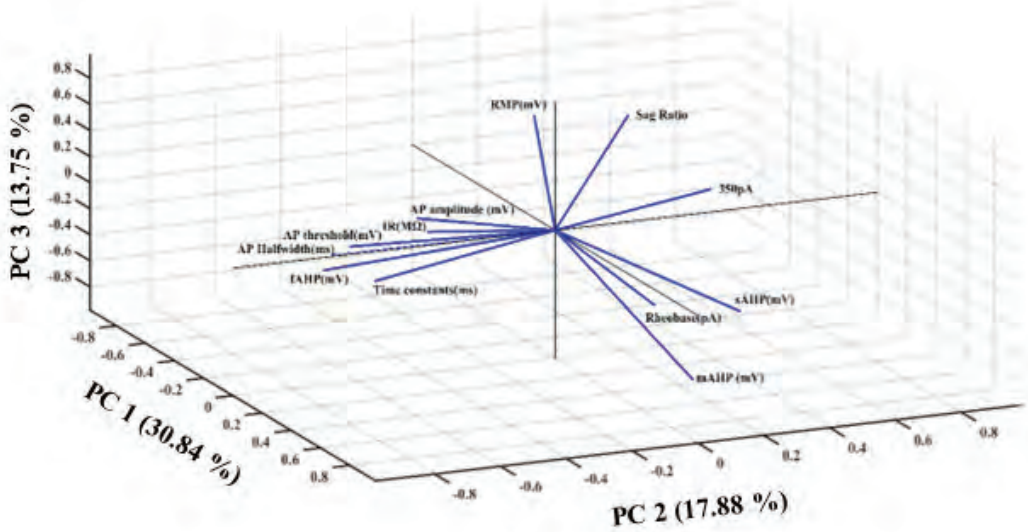

Groups	RMP (mV)	fAHP (mV)	mAHP (mV)	sAHP (mV)	Input Resistance (MΩ)	Sag ratio (%)	Time constant (ms)	AP threshold (mV)	AP Amplitude (mV)	AP half-width (ms)	Rheobase (pA)
LIV-VI aIC-BLA Cage control	-68.28 ± 0.8506 (19)	9.191 ± 1.449 (19) ** ##	-3.73 ± 0.4241 (19)	-1.881 ± 0.3376 (19)	120.7 ± 7.686 (19)	12.41 ± 1.938 (19)	15.03 ± 1.376 (19)	-30.76 ± 2.139 (19)	56.28 ± 0.8818 (19) ^^	0.6774 ± 0.03816 (19)	87.47 ± 9.127 (19)
LIV-VI aIC-BLA Water	-69.3 ± 0.9051 (23)	8.15 ± 0.8288 (23) **	-5.535 ± 0.6754 (23)	-3.277 ± 0.4603 (23)	139.1 ± 9.021(23)	8.909 ± 1.306 (23)	19.24 ± 1.62 (23)	-31.05 ± 1.30 (23)	52.43 ± 1.034 (23)	0.6243 ± 0.02021 (23)	85 ± 11.76 (23)
LIV-VI aIC-BLA Saccharin 1x	-69.21 ± 0.94 (20)	3.016 ± 0.9423 (20) ####	-4.17 ± 0.4542 (20)	-2.521 ± 0.2735 (20)	145.8 ± 12.56 (20)	10.89 ± 1.621 (20)	14.82 ± 1.485 (20) #	-30.9 ± 2.141 (20)	52.03 ± 1.308 (20)	0.6005 ± 0.0326 (20)	74.25 ± 11.39 (20)
LIV-VI aIC-BLA Quinine 1x	-67.32 ± 1.092 (19)	13.56± 1.562 (19) $$$$ ~	-5.858 ± 0.5613 (18)	-3.634 ± 0.3632 (18)	146 ± 9.094 (19)	12.13 ± 1.23 (19)	21.55 ± 1.638 (19)	-29.74 ± 1.989 (19)	57.11 ± 1.376 (19) *^^^	0.6 ± 0.03555 (19)	69.89 ± 8.932 (19)
LIV-VI aIC-BLA Saccharin 5x	-66.53 ± 1.358 (18)	8.158 ± 1.356 (18) ** ###	-3.999 ± 0.653 (18)	-2.695 ± 0.5083 (18)	144.6 ± 14.68 (18)	9.392 ± 2.127 (18)	17.3 ± 1.66 (18)	-32.66 ± 1.783 (18)	56.48 ± 1.337 (18)	0.6539 ± 0.04814 (18)	78.61 ± 10.75 (18)
LIV-VI aIC-BLA Saccharin 1x (4hr)	-69.47 ± 0.7569 (17)	5.989 ± 1.074 (17) **	-4.411 ± 0.8962 (17)	-2.631 ± 0.6949 (17)	153.9 ± 11.10 (17)	10.97 ± 1.475 (17)	26.21 ± 2.421 (17) *** $$$ % &&	-31.03 ± 1.511 (17)	52.24 ± 2.311 (17)	0.7765 ± 0.03641 (17) **	78.88 ± 9.274 (17)
LIV-VI aIC-BLA Saccharin 2x	-70.79 ± 1.242 (20)	5.223 ± 0.8217 (20) ###	-5.301 ± 0.7863 (20)	-3.351 ±0.3798 (20)	181.1 ± 11.7 (20)	7.815 ± 1.176 (20)	19.28 ± 1.837 (20)	-32.85 ± 1.447 (20)	49.14 ± 1.568 (20) ###	0.578 ± 0.02994 (20)	69.6 ± 10.71 (20)
LIV-VI aIC-BLA CTA Retrieval	-68.78 ± 0.8419 (27)	7.97 ± 1.018 (27) ##	-5.213 0.4544 (27)	-2.69 ± 0.3064 (27)	136.4 ± 9.064 (27) ^^	13.41 ± 1.31 (27) ^^	20.96 ± 1.724 (27) *	-31.61 ± 2.68 (27)	56.21 ± 0.9978 (27) ^^^	0.5959 ± 0.0208 (27)	90.44 ± 17.56 (27)
LIV-VI aIC-BLA Extinction	-65.98 ± 1.457 (14)	4.731 ± 1.021 (14)	-5.076 ± 0.6981 (14)	-2.895 ± 0.6547 (14)	151.1 ± 15.63 (14)	12.37 ± 1.471 (14)	17.55 ± 2.684 (14) ~	-36.06 ± 1.481 (14) ~	55.09 ± 2.122 (14) ^	0.7386 ± 0.03145 (14)	69.21 ± 7.454 (14)
LIV-VI aIC-BLA Reinstatement	-68.57 ± 0.936 (15)	5.932 ± 1.292 (15)	-5.673 ± 0.4288 (15)	-3.612 ±0.3033 (15)	178.7 ± 12.1 (15)	9.245 ± 0.884 (15)	25.48 ± 1.58 (15) **	-29.43 ± 1.731 (15)	53.1 ± 2.906 (15)	0.8187 ± 0.06929 (15)	67.6 ± 8.753 (15)

$Vs. Cage Control *** Vs. Saccharin 1x** **^ Vs. Saccharin 2x** **~ Vs. Reinstatement**

%Vs. Water **# Vs. Quinine 1x** **& Vs. Saccharin 5x**

Groups	RMP (mV)	mAHP (mV)	Input resistance (MΩ)	Sag ratio (%)	Time constant (ms)	AP thresh (mV)	AP Amp (mV)	AP half-width (ms)	Rheobase (pA)
LI-III aIC-BLA Water	-70.84 ± 1.09 (14)	-2.411 ± 0.6767 (14)	136.4 ± 16.85 (14)	3.172 ± 1.082 (14)	11.17 ± 1.169 (14)	-31.35 ± 1.547 (14)	56 ± 1.719 (14)	0.6557 ± 0.03222 (14)	140.7 ± 31.83 (14)
LI-III aIC-BLA Saccharin 1x	-72.27 ± 1.212 (15)	-1.752 ± 0.4953 (15)	131.6 ± 13.14 (15)	3.997 ± 0.9166 (15)	11.56 ± 1.672 (15)	-31.44 ± 1.621 (15)	56.33 ± 1.323 (15)	0.684 ± 0.02767 (15)	136.1 ± 26.44(15)
LI-III aIC-BLA Saccharin 2x	-73.44 ± 1.295 (15)	-2.165 ± 0.684 (15)	142.5 ± 13.17 (15)	5.793 ± 1.449 (15)	18.63 ± 1.9 (15)	-31.47 ± 2.511 (15)	49.76 ± 2.065 (15)	0.564 ± 0.03708 (15)	104.7 ± 25.03 (15)
LI-III aIC-BLA CTA Retrieval	-72 ± 1.117 (17)	-3.087 ± 2.914 (17)	171.1 ± 22.28 (17)	6.307 ± 1.368 (17)	18.94 ± 1.667 (17)	-34.24 ± 1.445 (17)	48.58 ± 1.472 (17)	0.5518 ± 0.02698 (17)	114.3 ± 31.57 (17)

Groups	RMP (mV)	fAHP (mV)	mAHP (mV)	sAHP (mV)	Input resistance (MΩ)	Sag ratio (%)	Time constant (ms)	AP thresh (mV)	AP Amp (mV)	AP half-width (ms)	Rheobase (pA)
BS LIV-VI aIC-BLA Cage control	-68.28 ± 0.970 5 (13)	9.192 ± 2.061 (13)	-4.194 ± 0.5072 (13)	-2.075 ± 0.4500 (13)	118.4 ± 9.771 (13)	14.91 ± 2.195 (13)	14.71±1.9 44 (13)	-31.83± 2.971 (13)	56.27 ±1.147 (13)	0.6692 ± 0.05460 (13)	74.54 ± 8.471 (13)
BS LIV-VI aIC-BLA Water	-69.00 ± 1.639 (11)	7.800 ± 1.607(11)	-4.870 ± 0.8838 (11)	-2.826 ± 0.6069 (11)	136.5 ± 14.40 (11)	8.751± 2.021 (11)	18.03 ± 2.309 (11)	-29.27 ± 2.060 (11)	54.21 ±1.572 (11)	0.6736 ± 0.03111 (11)	85.91 ±13.44 (11)
BS LIV-VI aIC-BLA Saccharin 1x	-68.80 ± 1.065 (17)	2.870 ±1.044 (17)	-4.339 ±0.5083 (17)	-2.564 ±0.3032 (17)	146.6 ±14.22 (17)	11.67±1.79 0 (17)	14.27 ± 1.666 (17)	-30.73 ± 2.385 (17)	51.64 ± 1.473 (17)	0.5976 ± 0.03555 (17)	63.65 ± 7.679 (17)
BS LIV-VI aIC-BLA Quinine 1x	-67.37 ± 1.682 (9)	13.67 ±2.681(9) ##	-6.131 ± 0.6514 (8)	-3.58 ± 0.5788 (8)	139.2 ± 16.86 (9)	14.15 ± 2.159 (9)	23.21 ± 2.717 (9)	-29.35 ± 3.071 (9)	58.86 ± 2.003 (9)	0.6378 ± 0.0491 (9)	59.56 ± 12.28 (9)
BS LIV-VI aIC-BLA Saccharin 5x	-67.20 ±1.62 4 (10)	11.30 ±1.727 (10) ##	-5.174 ±0.8427 (10)	-3.609 ± 0.7205 (10)	156.1 ± 22.85 (10)	11.92 ± 3.395 (10)	17.11 ± 2.296 (10)	-30.38 ± 2.493 (10)	58.40 ± 1.812 (10)	0.7140 ± 0.07349 (10)	76.60 ± 15.32 (10)
BS LIV-VI aIC-BLA Saccharin 1x (4hr)	-68.20 ±1.29 3 (6)	3.433 ± 0.9245(6)	-6.693 ±1.442 (6)	-3.130 ± 1.637 (6)	154.9 ± 22.41(6)	14.99 ± 2.770 (6)	26.09 ± 5.331 (6)	-34.61 ± 2.174 (6)	46.79 ± 4.359 (6)	0.8850 ± 0.05943 (6) #	60.83 ± 11.36 (6)
BS LIV-VI aIC-BLA Saccharin 2x	-71.33 ± 1.641 (13)	4.169 ± 0.9225 (13)	-5.368 ± 0.9616 (13)	-3.226 ± 0.4899 (13)	180.3 ± 15.15 (13) **	7.017 ± 1.317 (13) ***	19.77 ± 2.447 (13)	-34.20 ± 1.987 (13)	46.18 ± 1.666 (13) ***	0.5331 ± 0.03522 (13)	77.54 ± 15.69 (13)
BS LIV-VI aIC-BLA CTA Retrieval	-67.37 ± 1.21 (12)	5.473 ± 1.464 (12)	-4.633 ± 0.5831 (12)	-1.932 ± 0.4462 (12)	110.9 ± 12.98 (12)	16.8 ± 1.869 (12)	17.06 ± 2.608 (12)	-34.28 ± 1.771 (12)	57.87 ± 1.678 (12)	0.6367± 0.03961 (12)	88.75 ± 9.847 (12)
BS LIV-VI aIC-BLA Extinction	-67.36 ± 1.43 (11)	3.943 ±1.111 (11)	-4.816 ± 0.8447 (11)	-2.104 ± 0.4466 (11) ~	131.1 ± 13.93 (11)	13.69 ± 1.541 (11)	14.52 ± 2.714 (11) ~ ~	-37.41 ± 1.636 (11) ~ ~	57.3 ± 2.023 (11)	0.7155 ± 0.03674 (11)	81 ± 6.932 (11)
BS LIV-VI aIC-BLA Reinstatement	-68.88 ± 1.163 (10)	6.432 ± 1.737 (10)	-5.243 ± 0.5853 (10)	-3.804 ± 1.339 (10)	157.4 ± 10.56 (10)	9.124 ± 1.03 (10)	26.93 ± 1.893 (10)	-27.5 ± 2.195 (10)	57.36 ± 3.001 (10)	0.769 ± 0.03494 (10)	73.9 ± 12.45 (10)

*** BS LV/VI aIC-BLA Saccharin 2x vs. CTA Retrieval, *p<0.05, ** p<0.01, *** p<0.001.**

~ BS LV/VI aIC-BLA Extinction vs. Reinstatement, ~ p<0.05, ~ ~ p<0.01, ~ ~ ~ p<0.001.

 # BS LV/VI aIC-BLA Saccharin 1x vs. Quinine 1x, Saccharin 5x and Saccharin 1x (4hr),

 # p<0.05, ## p<0.01.

Groups	RMP (mV)	fAHP (mV)	mAHP (mV)	sAHP (mV)	Input resistance (MΩ)	Sag ratio (%)	Time constant (ms)	AP thresh (mV)	AP Amp (mV)	AP half-width (ms)	Rheobase (pA)
RS LIV-VI aIC-BLA Cage control	-68.29 ±1.830 (6)	9.188 ± 1.351 (6)	-2.725 ± 0.6462 (6)	-1.460 ± 0.4409 (6)	125.7 ± 13.03 (6)	6.993 ± 3.030 (6)	15.73 ± 1.333 (6)	-28.44 ± 2.166 (6)	56.30 ± 1.422 (6)	0.6950 ± 0.03170 (6)	115.5 ± 18.62 (6)
RS LIV-VI aIC-BLA Water	-69.57 ± 0.9422 (12)	8.472 ± 0.6792 (12)	-6.144 ± 1.013 (12)	-3.690 ± 0.6876 (12)	141.5 ±11.75 (12)	9.735 ± 1.400 (12)	20.35 ± 2.321 (12)	-32.67 ± 1.561 (12)	50.79 ± 1.238 (12)	0.5792 ± 0.01928 (12)	84.17 ± 19.48 (12)
RS LIV-VI aIC-BLA Saccharin 1x	-71.57 ± 1.120 (3)	3.840 ± 2.530 (3)	-3.210 ± 0.9005 (3)	-2.277 ± 0.7297 (3)	141.3 ±28.45 (3)	6.455 ± 3.099 (3)	17.95 ± 2.856 (3)	-31.86 ± 5.650 (3)	54.23 ± 2.660 (3)	0.6167 ± 0.09939 (3)	134.3 ± 58.52 (3)
RS LIV-VI aIC-BLA Quinine 1x	-67.28 ±1.505 (10)	11.63 ± 1.616 (10)	-5.639 ± 0.8918 (10)	-3.678 ± 0.4895 (10)	151.4 ± 9.055 (10)	10.31 ± 1.115 (10)	23.6 ± 1.77(10)	-30.1 ± 2.732 (10)	55.53 ± 1.845 (10)	0.6230 ± 0.0535 (10)	79.20 ± 12.73 (10)
RS LIV-VI aIC-BLA Saccharin 5x	-65.70 ± 2.378 (8)	4.235 ± 1.141 (8)	-2.530 ± 0.7960 (8)	-1.553 ±0.4915 (8)	130.1 ± 16.85 (8)	6.237 ± 1.910 (8)	17.54 ± 2.561 (8)	-35.50 ± 2.302 (8)	54.09 ± 1.734 (8)	0.5788 ± 0.05034 (8)	81.13 ±15.88 (8)
RS LIV-VI aIC-BLA Saccharin 1x (4hr)	-70.17 ± 0.9075 (11)	7.383 ± 1.439 (11)	-3.165 ± 0.9897 (11)	-2.359 ± 0.6647 (11)	153.3 ± 12.96 (11)	8.782 ± 1.389 (11)	26.28 ± 2.596 (11)	-28.43 ± 1.652 (11)	51.66 ± 3.053 (11)	0.7773 ± 0.04702 (11)	88.73 ± 12.25 (11)
RS LIV-VI aIC-BLA Saccharin 2x	-69.79 ± 1.921 (7)	7.180 ± 1.402 (7)	-5.016 ± 1.460 (7)	-3.581 ± 0.6324 (7)	182.6 ± 19.62 (7)	9.297 ± 2.347 (7)	18.36 ± 2.842 (7)	-30.36 ± 1.638 (7)	54.62 ± 2.058 (7)	0.6614 ± 0.04149 (7)	54.86 ± 8.207 (7)
RS LIV-VI aIC-BLA CTA Retrieval	-69.9 ± 1.116 (15)	9.967 ± 1.216 (15)	-5.667 ± 0.6647 (15)	-3.297 ± 0.3599(15)	156.7 ± 10.11 (15)	10.71 ± 1.536 (15)	24.08 ± 2.023 (15)	-33.9 ± 1.132 (15)	54.89 ± 1.13 (15)	0.5633 ± 0.01703 (15) *	91.8 ± 31.15 (15)

*** RS LV/VI aIC-BLA Saccharin 1x vs. CTA Retrieval, *p<0.05.**

Groups (Table 4 Cont.)	RMP (mV)	fAHP (mV)	mAHP (mV)	sAHP (mV)	Input resistance (MΩ)	Sag ratio (%)	Time constant (ms)	AP thresh (mV)	AP Amp (mV)	AP half-width (ms)	Rheobase (pA)
RS LIV-VI aIC-BLA Extinction	-60.93 ± 3.263 (3)	7.620 ± 1.907 (3)	-6.027 ± 1.062 (3)	-5.797 ± 1.997 (3)	224.2 ± 21.29 (3)	7.515 ± 2.666 (3)	28.69 ± 2.138 (3)	-31.1 ± 1.372 (3)	46.98 ± 4.432 (3)	0.8233 ± 0.02603 (3)	36.67 ± 13.33 (3)
RS LIV-VI aIC-BLA Reinstatement	-67.95 ± 1.725 (5)	4.932 ± 1.893 (5)	-6.532 ± 0.3344 (5)	-3.228 ± 0.3214 (5)	221.2 ± 18.9 (5)	9.486 ± 1.846 (5)	22.58 ± 2.632 (5)	-33.31 ± 2.035 (5)	44.58 ± 4.569 (5)	0.918 ± 0.203 (5)	55 ± 6.885 (5)

*** RS LV/VI aIC-BLA Saccharin 1x vs. CTA Retrieval, *p<0.05.**

STATISTICS TABLE		
Figure	**Statistical Test**	**Results**
FIGURE 1		

Figure 1 D	Two-way repeated measures ANOVA
	Post-hoc Tukey's multiple comparisons
	
	LIV-VI aIC-BLA neurons
	F-I curve
	
	Cage control
	Water
	Saccharin 1x
	Quinine 1x
	Saccharin 5x
	Saccharin 1x (4hr)
		ANOVA Results:
		Treatment; p=0.0057, F (5, 110) =3.491
		Current; p<0.0001, F (8, 880) =1276
		Interaction; p<0.0001, F (40, 880) =4.141
		
		Multiple Comparisons:
		
		0pA
		Cage control vs. Water
		Mean difference=0.000
		Cage control vs. Saccharin 1x
		Mean difference=0.000
		Cage control vs. Quinine 1x
		Mean difference=0.000
		Cage Control vs. Saccharin 5x
		Mean difference=0.000
		Cage Control vs. Saccharin 1x (4hr)
		Mean difference=0.000
		Water vs. Saccharin 1x
		Mean difference=0.000
		Water vs. Quinine 1x
		Mean difference=0.000
		Water vs. Saccharin 5x
		Mean difference=0.000
		Water vs. Saccharin 1x (4hr)
		Mean difference=0.000
		Saccharin 1x vs. Quinine 1x
		Mean difference=0.000
		Saccharin 1x vs. Saccharin 5x
		Mean difference=0.000
		Saccharin 1x vs. Saccharin 1x (4hr)
		Mean difference=0.000
		Quinine 1x vs. Saccharin 5x
		Mean difference=0.000
		Quinine 1x vs. Saccharin 1x (4hr)
		Mean difference=0.000
		Saccharin 5x vs. Saccharin 1x (4hr)
		Mean difference=0.000
		
		50pA
		Cage control vs. Water
		p= 0.9902, q= 0.8645, df= 990.0;
		Cage control vs. Saccharin 1x
		p= 0.9993, q= 0.5005, df= 990.0;
		Cage Control vs. Quinine 1x
		p >0.9999, q= 0.2597, df=990.00;
		Cage control vs. Saccharin 5x
		p= 0.9451, q= 1.281, df=990.00;
		Cage control vs. Saccharin 1x(4hr)
		p= 0.9922, q= 0.8240, df=990;
		Water vs. Saccharin 1x
		p=0.9999, q=0.3522, df=990
		Water vs. Quinine 1x

		p=0.9946, q=0.5927, df=990;
		Water vs. Saccharin 5x
		p=0.9984, q=0.4868, df=990;
		Water vs. Saccharin 1x (4hr)
		p>0.9999, q=0.02212, df=990;
		Saccharin 1x vs. Quinine 1x
		p>0.9999, q=0.2374, df=990;
		Saccharin 1x vs. Saccharin 5x
		p=0.9931, q=0.8029, df=990;
		Saccharin 1x vs. Saccharin 1x (4hr)
		p=0.9999, q=0.3478, df=990;
		Quinine 1x vs. Saccharin 5x
		p=0.9790, q=1.024, df=990;
		Quinine 1x vs. Saccharin 1x (4hr)
		p=0.9986, q=0.5716, df=990;
		Saccharin 5x vs. Saccharin 1x (4hr)
		p=0.9996, q=0.4320, df=990;
		
		100pA
		Cage control vs. Water
		p= 0.8652, q= 1.610, df= 990.0;
		Cage control vs. Saccharin 1x
		p= 0.2233, q= 3.159, df= 990.0;
		Cage Control vs. Quinine 1x
		p =0.4580, q= 2.563, df=990.00;
		Cage control vs. Saccharin 5x
		p= 0.6454, q= 2.163, df=990.00;
		Cage control vs. Saccharin 1x(4hr)
		p= 0.5930, q= 2.275, df=990;
		Water vs. Saccharin 1x
		p=0.8437, q=1.677, df=990
		Water vs. Quinine 1x
		p=0.9742, q=1.073, df=990;
		Water vs. Saccharin 5x
		p=0.9969, q=0.6743, df=990;
		Water vs. Saccharin 1x (4hr)
		p=0.9926, q=0.8138, df=990;
		Saccharin 1x vs. Quinine 1x
		p=0.9987, q=0.5625, df=990;
		Saccharin 1x vs. Saccharin 5x
		p=0.9867, q=0.9250, df=990;
		Saccharin 1x vs. Saccharin 1x (4hr)
		p=0.9945, q=0.7652, df=990;
		Quinine 1x vs. Saccharin 5x
		p=0.9998, q=0.3658, df=990;
		Quinine 1x vs. Saccharin 1x (4hr)
		p>0.9999, q=0.2164, df=990;
		Saccharin 5x vs. Saccharin 1x (4hr)
		p>0.9999, q=0.1422, df=990;
		
		150pA
		Cage control vs. Water
		p= 0.8024, q= 1.793, df= 990.0;
		Cage control vs. Saccharin 1x
		p= 0.0085, q= 4.836, df= 990.0;
		Cage Control vs. Quinine 1x
		p =0.1482, q= 3.431, df=990.00;
		Cage control vs. Saccharin 5x
		p= 0.2881, q= 2.970, df=990.00;
		Cage control vs. Saccharin 1x(4hr)

		p= 0.5463, q= 2.374, df=990;
		Water vs. Saccharin 1x
		p=0.1962, q=3.248, df=990
		Water vs. Quinine 1x
		p=0.8009, q=1.797, df=990;
		Water vs. Saccharin 5x
		p=0.9345, q=1.337, df=990;
		Water vs. Saccharin 1x (4hr)
		p=0.9953, q=0.7397, df=990;
		Saccharin 1x vs. Quinine 1x
		p=0.9297, q=1.361, df=990;
		Saccharin 1x vs. Saccharin 5x
		p=0.8142, q=1.762, df=990;
		Saccharin 1x vs. Saccharin 1x (4hr)
		p=0.5843, q=2.293, df=990;
		Quinine 1x vs. Saccharin 5x
		p=0.9997, q=0.4145, df=990;
		Quinine 1x vs. Saccharin 1x (4hr)
		p=0.9843, q=0. 0.9603, df=990;
		Saccharin 5x vs. Saccharin 1x (4hr)
		P=0.9989, q=0.5448, df=990;
		
		200pA
		Cage Control vs. Water
		p=0.9968, q=0.6822, df=990.0;
		Cage Control vs. Saccharin 1x
		p=0.0038, q=0.6822, df=990.0;
		Cage Control vs. Quinine 1x
		p=0.5360, q=2.396, df=990.0;
		Cage Control vs. Saccharin 5x
		p=0.5556, q=2.354, df=990.0;
		Cage Control vs. Saccharin 1x (4hr)
		p=0.9876, q=0.9108, df=990.0;
		Water vs. Saccharin 1x
		p=0.0116, q=4.708, df=990.0;
		Water vs. Quinine 1x
		p=0.7904, q=4.708, df=990.0;
		Water vs. Saccharin 5x
		p=0.8042, q=1.789, df=990.0;
		Water vs. Saccharin 1x (4hr)
		p>0.9999, q=0.2894, df=990.0;
		Saccharin 1x vs. Quinine 1x
		p=0.3853, q=2.727, df=990.0;
		Saccharin 1x vs. Saccharin 5x
		p=0.3979, q=2.698, df=990.0;
		Saccharin 1x vs. Saccharin 1x (4hr)
		p=0.0457, q=4.083, df=990.0;
		Quinine 1x vs. Saccharin 5x
		p>0.9999, q=0.008880, df=990.0;
		Quinine 1x vs. Saccharin 1x (4hr)
		p=0.9172, q=1.417, df=990.0;
		Saccharin 5x vs. Saccharin 1x (4hr)
		p=0.9233, q=1.391, df=990.0;
		
		250pA
		Cage control vs. Water
		p=0.9988, q=,0.5590 df=990.0;
		Cage control vs. Saccharin 1x
		p=0.0011, q=5.603, df=990.0;
		Cage Control vs. Quinine 1x

		p=0.7555, q=1.912, df=990.0;
		Cage Control vs. Saccharin 5x
		p=0.7478, q=1.931, df=990.0;
		Cage Control vs. Saccharin 1x (4hr)
		p>0.9999, q=0.1164, df=990.0;
		Water vs. Saccharin 1x
		p=0.0026, q=5.304, df=990.0;
		Water vs. Quinine 1x
		p=0.9113, q=1.442, df=990.0;
		Water vs. Saccharin 5x
		p=0.9051, q=1.468, df=990.0;
		Water vs. Saccharin 1x (4hr)
		p=0.9972, q=0.6633, df=990.0;
		Saccharin 1x vs. Quinine 1x
		p=0.1000, q=3.666, df=990.0;
		Saccharin 1x vs. Saccharin 5x
		p=0.1180, q=3.570, df=990.0;
		Saccharin 1x vs. Saccharin 1x (4hr)
		p=0.0013, q=5.559, df=990.0;
		Quinine 1x vs. Saccharin 5x
		p>0.9999, q=0.04456, df=990.0;
		Quinine 1x vs. Saccharin 1x (4hr)
		p=0.7292, q=1.975, df=990.0;
		Saccharin 5x vs. Saccharin 1x (4hr)
		p=0.7215, q=1.993, df=990.0;
		
		300pA
		Cage Control vs. Water
		p=0.9993, q=0.4987, df=990.0;
		Cage Control vs. Saccharin 1x
		p=0.0005, q=5.903, df=990.0;
		Cage Control vs. Quinine 1x
		p=0.9022, q=1.479, df=990.0;
		Cage Control vs. Saccharin 5x
		p=0.7419, q=1.945, df=990.0;
		Cage Control vs. Saccharin 1x (4hr)
		p=0.9641, q=1.158, df=990.0;
		Water vs. Saccharin 1x
		p=0.0009, q=5.679, df=990.0;
		Water vs. Quinine 1x
		p=0.9766, q=1.049, df=990.0;
		Water vs. Saccharin 5x
		p=0.8854, q=1.542, df=990.0;
		Water vs. Saccharin 1x (4hr)
		p=0.8386, q=1.692, df=990.0;
		Saccharin 1x vs. Quinine 1x
		p=0.0232, q=4.405, df=990.0;
		Saccharin 1x vs. Saccharin 5x
		p=0.0716, q=3.851, df=990.0;
		Saccharin 1x vs. Saccharin 1x (4hr)
		p<0.0001, q=6.905, df=990.0;
		Quinine 1x vs. Saccharin 5x
		p=.9994, q=0.4860, df=990.0;
		Quinine 1x vs. Saccharin 1x (4hr)
		p=0.4433, q=2.596, df=990.0;
		Saccharin 5x vs. Saccharin 1x (4hr)
		p=0.2645, q=3.035, df=990.0;
		
		350pA
		Cage Control vs. Water

		p=0.9973, q=0.6556, df=990.0;
		Cage Control vs. Saccharin 1x
		p=0.0003, q=6.069, df=990.0;
		Cage Control vs. Quinine 1x
		p=0.9972, q=0.6596, df=990.0;
		Cage Control vs. Saccharin 5x
		p=0.8294, q=1.719, df=990.0;
		Cage Control vs. Saccharin 1x (4hr)
		p=0.7347, q=1.962, df=990.0;
		Water vs. Saccharin 1x
		p=0.0009, q=5.694, df=990.0;
		Water vs. Quinine 1x
		p>0.9999, q=0.03478, df=990.0;
		Water vs. Saccharin 5x
		p=0.9650, q=1.151, df=990.0;
		Water vs. Saccharin 1x (4hr)
		p=0.4043, q=2.683, df=990.0;
		Saccharin 1x vs. Quinine 1x
		p=0.0020, q=5.401, df=990.0;
		Saccharin 1x vs. Saccharin 5x
		p=0.0328, q=4.244, df=990.0;
		Saccharin 1x vs. Saccharin 1x (4hr)
		p<0.0001, q=7.879, df=990.0;
		Quinine 1x vs. Saccharin 5x
		p=0.9747, q=1.068, df=990.0;
		Quinine 1x vs. Saccharin 1x (4hr)
		p=0.4400, q=2.603, df=990.0;
		Saccharin 5x vs. Saccharin 1x (4hr)
		p=0.1105, q=3.609, df=990.0;
		
		400pA
		Cage Control vs. Water
		p=0.9988, q=0.5513, df=990.0;
		Cage Control vs. Saccharin 1x
		p=0.0004, q=5.939, df=990.0;
		Cage Control vs. Quinine 1x
		p=0.9987, q=0.5623, df=990.0;
		Cage Control vs. Saccharin 5x
		p=0.9132, q=1.435, df=990.0;
		Cage Control vs. Saccharin 1x (4hr)
		p=0.3765, q=2.748, df=990.0;
		Water vs. Saccharin 1x
		p=0.0009, q=5.663, df=990.0;
		Water vs. Quinine 1x
		p>0.9999, q=0.03710, df=990.0;
		Water vs. Saccharin 5x
		p=0.9845, q=0.9564, df=990.0;
		Water vs. Saccharin 1x (4hr)
		p=0.1551, q=3.402, df=990.0;
		Saccharin 1x vs. Quinine 1x
		p=0.0021, q=5.369, df=990.0;
		Saccharin 1x vs. Saccharin 5x
		p=0.0233, q=4.403, df=990.0;
		Saccharin 1x vs. Saccharin 1x (4hr)
		p<0.0001, q=8.548, df=990.0;
		Quinine 1x vs. Saccharin 5x
		p=0.9894, q=0.8800, df=990.0;
		Quinine 1x vs. Saccharin 1x (4hr)
		p=0.1832, q=3.294, df=990.0;
		Saccharin 5x vs. Saccharin 1x (4hr)

		p=0.0435, q=4.108, df=990.0.
Figure 1 B	One -Way Anova Water consumption the before the test Water Saccharin 1x Quinine 1x Saccharin 5x Saccharin 1x (4hrs)	ANOVA results: F=0.9766 P= 0.4424 R squared, 0.1634

Figure 1H	One-way ANOVA
	
	Kruskal-Wallis test
	Post-hoc Dunn's multiple comparisons test
	
	LIV-VI aIC-BLA neurons
	fAHP
	
	Cage control
	Water
	Saccharin 1x
	Quinine 1x
	Saccharin 5x
	Saccharin 1x (4hr)
		ANOVA results:
		Kruskal-Wallis test, p<0.0001;
		Kruskal-Wallis statistic,29.91.
		Multiple Comparisons:
		
		Cage Control vs. Water
		p >0.9999, z= 0.2306;
		Cage Control vs. Saccharin 1x
		p=0.0136, z= 3.318;
		Cage Control vs. Quinine 1x
		p >0.9999, z= 1.809;
		Cage Control vs. Saccharin 5x
		p >0.9999, z= 0.4824;
		Cage Control vs. Saccharin 1x (4hr)
		p>0.9999, z= 1.648;
		Water vs. Saccharin 1x
		p= 0.0177, z= 3.243;
		Water vs. Quinine 1x
		p= 0.5054, z=2.124;
		Water vs. Saccharin 5x
		p>0.9999, z=0.2771;
		Water vs. Saccharin 1x (4hr)
		p>0.9999, z=1.497;
		Saccharin 1x vs. Quinine 1x
		p<0.0001, z=5.150;
		Saccharin 1x vs. Saccharin 5x
		p=0.0807, z=2.783;
		Saccharin 1x vs. Saccharin 1x (4hr)
		p>0.9999, z=1.554;
		Quinine 1x vs. Saccharin 5x
		p=0.3511 z=2.267;
		Quinine 1x vs. Saccharin 1x (4hr)
		p=0.0099, z=3.406;
		Saccharin 5x vs. Saccharin 1x (4hr)
		p>0.9999, z= 1.1583

Figure 1I	One-way ANOVA
	
	Kruskal-Wallis test
	Post-hoc Dunn's multiple comparisons test
	
	LIV-VI aIC-BLA neurons
	Action Potential Half-width
		ANOVA results:
		Kruskal-Wallis test, p=0.0125; Kruskal-Wallis statistic,14.54.
		Multiple Comparisons:
		
		Cage Control vs. Water
		p >0.9999, z= 0.7692;
		Cage Control vs. Saccharin 1x
		p>0.9999, z= 1.627;

	Cage control
	Water
	Saccharin 1x
	Quinine 1x
	Saccharin 5x
	Saccharin 1x (4hr)
		Cage Control vs. Quinine 1x
		p >0.9999, z=0.9868 ;
		Cage Control vs. Saccharin 5x
		p >0.9999, z= 0.6540;
		Cage Control vs. Saccharin 1x (4hr)
		P=0.8292, z= 1.917;
		Water vs. Saccharin 1x
		p >0.9999, z= 0.9244;
		Water vs. Quinine 1x
		p>0.9999, z=0.2636;
		Water vs. Saccharin 5x
		p>0.9999, z=0.07420;
		Water vs. Saccharin 1x (4hr)
		p=0.0905, z=2.746;
		Saccharin 1x vs. Quinine 1x
		p>0.9999, z=0.6271
		Saccharin 1x vs. Saccharin 5x
		p=>0.9999, z=0.9418;
		Saccharin 1x vs. Saccharin 1x (4hr)
		p=0.0065, z=3.519;
		Quinine 1x vs. Saccharin 5x
		p>0.9999z=0.3194;
		Quinine 1x vs. Saccharin 1x (4hr)
		p=0.0605, z=2.876;
		Saccharin 5x vs. Saccharin 1x (4hr)
		p= 0.1721, z= 2.528

Figure 1J	One-way ANOVA
	Post-hoc Tukey's multiple comparisons
	
	LIV-VI aIC-BLA neurons
	Membrane Time Constant
	
	Cage control
	Water
	Saccharin 1x
	Quinine 1x
	Saccharin 5x
	Saccharin 1x (4hr)
		ANOVA results:
		Treatment; p<0.0001, F (5, 110) = 6.094;
		R squared, 0.2169;
		Multiple Comparisons:
		
		Cage Control vs. Water
		p = 0.4608, q= 2.566, df=110;
		Cage Control vs. Saccharin 1x
		p >0.9999, q= 0.1233, df=110;
		Cage Control vs. Quinine 1x
		p = 0.0864, q= 3.798, df=110;
		Cage Control vs. Saccharin 5x
		p = 0.9398, q= 1.306, df=110;
		Cage Control vs. Saccharin 1x (4hr)
		p = 0.0003, q= 6.326, df=110;
		Water vs. Saccharin 1x
		p = 0.3890, q= 2.731, df=110;
		Water vs. Quinine 1x
		p = 0.9184, q= 1.408, df=110;
		Water vs. Saccharin 5x
		p = 0.9628, q= 1.163, df=110;
		Water vs. Saccharin 1x (4hr)
		p = 0.0488, q= 4.115, df=110;
		Saccharin 1x vs. Quinine 1x
		p = 0.0639, q= 3.969, df=110;
		Saccharin 1x vs. Saccharin 5x
		p = 0.9101, q= 1.443, df=110;
		Saccharin 1x vs. Saccharin 1x (4hr)
		p = 0.0002, q= 6.521, df=110;
		Quinine 1x vs. Saccharin 5x
		p = 0.5180, q= 2.440, df=110;
		Quinine 1x vs. Saccharin 1x (4hr)
		p = 0.4302, q= 2.635, df=110;

		Saccharin 5x vs. Saccharin 1x (4hr) p = 0.0081, q= 4.975, df=110;
FIGURE 2		
Figure 2B	Two-tailed Unpaired t-test Saccharin consumption on the test day Saccharin 2x CTA retrieval	t-test Results: Mann-Whitney test, p= 0.0085. Mann-Whitney U, 2.500

Figure 2D	Two-way repeated measures ANOVA
	Post-hoc Šídák's multiple comparisons test
	
	LIV-VI aIC-BLA neurons
	F-I curve
	
	Saccharin 2x
	CTA retrieval
		ANOVA Results:
		Treatment; p<0.0014, F (1, 45) =11.60
		Current; p<0.0001, F (8, 360) =483.3
		Interaction; p<0.0001, F (8, 360) =9.398
		
		Multiple Comparisons:
		0pA
		Saccharin 2x vs. CTA retrieval
		Mean difference=0.000
		50pA
		Saccharin 2x vs. CTA retrieval
		p>0.9999, t=0.1045, df=405.0;
		100pA
		Saccharin 2x vs. CTA retrieval
		p=0.5860, t=1.682, df=405.0;
		150pA
		Saccharin 2x vs. CTA retrieval
		p=0.0286, t=2.964, df=405.0;
		200pA
		Saccharin 2x vs. CTA retrieval
		p=0.0019, t=3.738, df=405.0;
		250pA
		Saccharin 2x vs. CTA retrieval
		p=0.0005, t=4.090, df=405.0;
		300pA
		Saccharin 2x vs. CTA retrieval
		p=0.0002, t=4.280, df=405.0;
		350pA
		Saccharin 2x vs. CTA retrieval
		p<0.0001, t=4.517, df=405.0;
		400pA
		Saccharin 2x vs. CTA retrieval
		p=0.0003, t=4.161, df=405.0

Figure 2G	Two-tailed Unpaired t-test LIV-VI aIC-BLA neurons Action Potential Amplitude Saccharin 2x CTA retrieval	p=0.0002 t=3.983 df=45 Difference between means=7.080±1.777 R squared, 0.2607
Figure 2H	Two-tailed Unpaired t-test LIV-VI aIC-BLA neurons Input Resistance Saccharin 2x CTA retrieval	p=0.0036 t=3.072 df=45 Difference between means= 44.75±14.57 R squared=0.1734
Figure 2I	Two-tailed Unpaired t-test	p=0.0037

	LIV-VI aIC-BLA neurons SAG Ratio Saccharin 2x CTA retrieval	t=3.060 df=45 Difference between means=5.597±1.829 R squared=0.1723
FIGURE 3		
Figure 3B	Two-way ANOVA Post-hoc Šídák's multiple comparisons test	ANOVA Results: Treatment, P=0.068, F (1, 54) = 3.466; Interaction, P=0.9697, F (8, 54) = 0.2803.
Figure 3C	Two-tailed Unpaired t-test Saccharin consumption on the test day Extinction Reinstatement	t-test Results: Mann-Whitney test, p= 0.0179; Mann-Whitney U, 0

Figure 3E	Two-way repeated measures ANOVA
	Post-hoc Šídák's multiple comparisons test
	
	LIV-VI aIC-BLA neurons
	F-I curve
		ANOVA Results:
		Treatment; p=0.0013, F (3, 72) =5.837
		Current; p<0.0001, F (1.959, 141.0) =802.5
		Interaction; p<0.0001, F (24, 567) =6.468
		
		Multiple Comparisons:
		0pA
		Extinction vs. Reinstatement
		Mean difference=0.000;
		50pA
		Extinction vs. Reinstatement
		p >0.9999, t= 0.1718, df= 243.0;
		100pA
		Extinction vs. Reinstatement
		p= 0.8899, t= 1.237, df= 243.0;
		150pA
		Extinction vs. Reinstatement
		p >0.9999, t= 0.2492, df= 243.0;
		200pA
		Extinction vs. Reinstatement
		p= 0.5553, t= 1.723, df= 243.0;
		250pA
		Extinction vs. Reinstatement
		p= 0.0341, t= 2.919, df= 243.0;
		300pA
		Extinction vs. Reinstatement
		p= 0.0030, t= 3.636, df= 243.0;
		350pA
		Extinction vs. Reinstatement
		p= 0.0003, q= 4.203, df= 243.0;
		400pA
		Extinction vs. Reinstatement
		p <0.0001, t= 4.578, df=243.0.

Figure 3F	Two-tailed Unpaired t-test LIV-VI aIC-BLA neurons Action Potential Threshold Extinction Reinstatement	<u>t-test Results:</u> p= 0.0076 t=2.887 df=27 Difference between means; 6.621 ± 2.293 R squared, 0.2359
Figure 3G	Two-tailed Unpaired t-test LIV-VI aIC-BLA neurons Membrane Time Constant Extinction Reinstatement	<u>t-test Results:</u> p= 0.0153 t=2.589 df=27 Difference between means ;7.931 ± 3.064 R squared; 0.1988
FIGURE 4		
Figure 4A	Two-way repeated measures ANOVA Post-hoc Tukey's multiple comparisons LIV-VI aIC-BLA neurons F-I Curve Saccharin 1x Quinine 1x Saccharin 2x CTA retrieval Extinction Reinstatement	<u>ANOVA results:</u> Treatment; p=0.0014, F (5, 109) =4.281 Current; p<0.0001, F (1.990, 216.9) =1218 Interaction; p<0.0001, F (40, 872) =4.978 <u>Multiple Comparisons:</u> **0pA** Saccharin 1x vs. Quinine 1x Mean difference=0.000 Saccharin 1x vs. Saccharin 2x Mean difference=0.000 Saccharin 1x vs. CTA Retrieval Mean difference=0.000 Saccharin 1x vs. Extinction Mean difference=0.000 Saccharin 1x vs. Reinstatement Mean difference=0.000 Quinine 1x vs. Saccharin 2x Mean difference=0.000 Quinine 1x vs. CTA Retrieval Mean difference=0.000 Quinine 1x vs. Extinction Mean difference=0.000 Quinine 1x vs. Reinstatement Mean difference=0.000 Saccharin 2x vs. CTA Retrieval Mean difference=0.000 Saccharin 2x vs. Extinction Mean difference=0.000 Saccharin 2x vs. Reinstatement Mean difference=0.000 CTA Retrieval vs. Extinction Mean difference=0.000 CTA Retrieval vs. Reinstatement Mean difference=0.000 Extinction vs. Reinstatement Mean difference=0.000

		50pA
		Saccharin 1x vs. Quinine 1x
		p>0.9999q=0.2195, df=981.0;
		Saccharin 1x vs. Saccharin 2x
		p=0.9993, q=0.5023, df=981.0;
		Saccharin 1x vs. CTA Retrieval
		p=0.9998, q=0.3831, df=981.0;
		Saccharin 1x vs. Extinction
		p=0.9986, q=0.5691, df=981.0;
		Saccharin 1x vs. Reinstatement
		p=0.9999q=0.3539, df=981.0;
		Quinine 1x vs. Saccharin 2x
		p=0.9960, q=0.7153, df=981.0;
		Quinine 1x vs. CTA Retrieval
		p=0.9981, q=0.6123, df=981.0;
		Quinine 1x vs. Extinction
		p=0.9945, q=0.7626, df=981.0;
		Quinine 1x vs. Reinstatement
		p=0.9988, q=0.5535, df=981.0;
		Saccharin 2x vs. CTA Retrieval
		p>0.9999, q=0.1553, df=981.0;
		Saccharin 2x vs. Extinction
		p>0.9999, q=0.1132, df=981.0;
		Saccharin 2x vs. Reinstatement
		p>0.9999, q=0.1112, df=981.0;
		CTA Retrieval vs. Extinction
		p>0.9999, q=0.2589, df=981.0;
		CTA Retrieval vs. Reinstatement
		p>0.9999, q=0.02435, df=981.0;
		Extinction vs. Reinstatement
		p>0.9999, q=0.2084, df=981.0;
		
		100pA
		Saccharin 1x vs. Quinine 1x
		p= 0.9991, q= 0.5199, df=981.0;
		Saccharin 1x vs. Saccharin 2x
		p= 0.8659, q= 1.608, df=981.0;
		Saccharin 1x vs. CTA Retrieval
		p= 0.9941, q= 0.7759, df=981.0;
		Saccharin 1x vs. Extinction
		p= 0.9933, q= 0.7975, df=981.0;
		Saccharin 1x vs. Reinstatement
		p= 0.9924, q=0.8188, df=981.0;
		Quinine 1x vs. Saccharin 2x
		p= 0.6709, q=2.107, df=981.0;
		Quinine 1x vs. CTA Retrieval
		p >0.9999, q=0.2082, df=981.0;
		Quinine 1x vs. Extinction
		p >0.9999, q=0.3161, df=981.0;
		Quinine 1x vs. Reinstatement
		p= 0.9431, q=1.292, df=981.0;
		Saccharin 2x vs. CTA Retrieval
		p= 0.4875, q=2.499, df=981.0;
		Saccharin 2x vs. Extinction
		p= 0.6016, q=2.257, df=981.0;
		Saccharin 2x vs. Reinstatement
		p= 0.9970, q=0.6698, df=981.0;
		CTA Retrieval vs. Extinction
		p >0.9999, q=0.1487, df=981.0;
		CTA Retrieval vs. Reinstatement

		p= 0.8745, q=1.579, df=981.0;
		Extinction vs. Reinstatement
		p= 0.8967, q=1.500, df=981.0
		
		150pA
		Saccharin 1x vs. Quinine 1x
		p= 0.9491, q=1.258, df=981.0;
		Saccharin 1x vs. Saccharin 2x
		p= 0.8741, q=1.258, df=981.0;
		Saccharin 1x vs. CTA Retrieval
		p= 0.3926, q=2.71, df=981.0;
		Saccharin 1x vs. Extinction
		p>0.9999, q=0.2459, df=981.0;
		Saccharin 1x vs. Reinstatement
		p= 0.9985, q=0.5798, df=981.0;
		Quinine 1x vs. Saccharin 2x
		p= 0.5798, q=2.818, df=981.0;
		Quinine 1x vs. CTA Retrieval
		p= 0.937, q=1.324, df=981.0;
		Quinine 1x vs. Extinction
		p= 0.9882, q=0.9008, df=981.0;
		Quinine 1x vs. Reinstatement
		p= 0.9983, q=0.5934, df=981.0;
		Saccharin 2x vs. CTA Retrieval
		p= 0.0233, q=4.404, df=981.0;
		Saccharin 2x vs. Extinction
		p= 0.8426, q=0.8426, df=981.0;
		Saccharin 2x vs. Reinstatement
		p= 0.6995, q=0.6995, df=981.0;
		CTA Retrieval vs. Extinction
		p= 0.6431, q=2.168, df=981.0;
		CTA Retrieval vs. Reinstatement
		p= 0.7735, q=1.868, df= 981.0;
		Extinction vs. Reinstatement
		p>0.9999, q=0.3023, df=981.0
		
		200pA
		Saccharin 1x vs. Quinine 1x
		p= 0.4777, q=2.521, df=981.0;
		Saccharin 1x vs. Saccharin 2x
		p= 0.9511, q=1.246, df=981.0;
		Saccharin 1x vs. CTA Retrieval
		p= 0.0346, q=4.219, df=981.0;
		Saccharin 1x vs. Extinction
		p>0.9999, q=0.07085, df=981.0;
		Saccharin 1x vs. Reinstatement
		p= 0.627, q=2.202, df=981.0;
		Quinine 1x vs. Saccharin 2x
		p= 0.0862, q=3.75, df=981.0;
		Quinine 1x vs. CTA Retrieval
		p= 0.907, q=1.46, df=981.0;
		Quinine 1x vs. Extinction
		p= 0.5516, q=2.363, df=981.0;
		Quinine 1x vs. Reinstatement
		p>0.9999, q=0.1599, df=981.0;
		Saccharin 2x vs. CTA Retrieval
		p= 0.0013, q=5.554, df=981.0;
		Saccharin 2x vs. Extinction
		p= 0.9756, q=1.06, df=981.0;
		Saccharin 2x vs. Reinstatement

		p= 0.1668, q=3.356, df=981.0;
		CTA Retrieval vs. Extinction
		p= 0.0712, q=3.854, df=981.0;
		CTA Retrieval vs. Reinstatement
		p= 0.8889, q=1.529, df=981.0;
		Extinction vs. Reinstatement
		p= 0.6782, q=2.091, df=981.0
		
		250pA
		Saccharin 1x vs. Quinine 1x
		p=0.1585, q= 3.389, df=981.0;
		Saccharin 1x vs. Saccharin 2x
		p=0.9907, q= 0.8555, df=981.0;
		Saccharin 1x vs. CTA Retrieval
		p=0.0038, q= 5.16, df=981.0;
		Saccharin 1x vs. Extinction
		p >0.9999, q= 0.3001, df=981.0;
		Saccharin 1x vs. Reinstatement
		p= 0.1227, q= 3.547, df=981.0;
		Quinine 1x vs. Saccharin 2x
		p= 0.0336, q= 4.233, df=981.0;
		Quinine 1x vs. CTA Retrieval
		p= 0.9074, q= 1.459, df=981.0;
		Quinine 1x vs. Extinction
		p= 0.1609, q= 3.379, df=981.0;
		Quinine 1x vs. Reinstatement
		p= 0.9998, q= 0.3641, df=981.0;
		Saccharin 2x vs. CTA Retrieval
		p= 0.0003, q= 6.078, df=981.0;
		Saccharin 2x vs. Extinction
		p= 0.9994, q= 0.4763, df=981.0;
		Saccharin 2x vs. Reinstatement
		p= 0.0268, q= 4.339, df=981.0;
		CTA Retrieval vs. Extinction
		p= 0.0066, q= 4.94, df=981.0;
		CTA Retrieval vs. Reinstatement
		p= 0.9838, q= 0.9659, df=981.0;
		Extinction vs. Reinstatement
		p= 0.1238, q= 3.541, df=981.0
		
		300pA
		Saccharin 1x vs. Quinine 1x
		p= 0.0468, q= 4.071, df=981.0;
		Saccharin 1x vs. Saccharin 2x
		p= 0.9991, q= 0.5264, df=981.0;
		Saccharin 1x vs. CTA Retrieval
		p= 0.0006, q= 5.795, df=981.0;
		Saccharin 1x vs. Extinction
		p= 0.9998, q= 0.3808, df=981.0;
		Saccharin 1x vs. Reinstatement
		p= 0.023, q= 4.41, df=981.0;
		Quinine 1x vs. Saccharin 2x
		p= 0.0153, q= 4.591, df=981.0;
		Quinine 1x vs. CTA Retrieval
		p= 0.9311, q= 1.354, df=981.0;
		Quinine 1x vs. Extinction
		p= 0.046, q= 4.08, df=981.0;
		Quinine 1x vs. Reinstatement
		p= 0.9985, q= 0.585, df=981.0;
		Saccharin 2x vs. CTA Retrieval

		p= 0.0001, q= 6.36, df=981.0;
		Saccharin 2x vs. Extinction
		p >0.9999, q= 0.09689, df=981.0;
		Saccharin 2x vs. Reinstatement
		p= 0.0073, q= 4.898, df=981.0;
		CTA Retrieval vs. Extinction
		p= 0.0011, q= 5.594, df=981.0;
		CTA Retrieval vs. Reinstatement
		p= 0.9978, q= 0.6315, df=981.0;
		Extinction vs. Reinstatement
		p= 0.0229, q= 4.411, df=981.0
		
		350pA
		Saccharin 1x vs. Quinine 1x
		p= 0.0058, q= 4.992, df=981.0;
		Saccharin 1x vs. Saccharin 2x
		p= 0.9998, q= 0.4001, df=981.0;
		Saccharin 1x vs. CTA Retrieval
		p= 0.0001, q= 6.284, df=981.0;
		Saccharin 1x vs. Extinction
		p >0.9999, q= 0.2699, df=981.0;
		Saccharin 1x vs. Reinstatement
		p= 0.0028, q= 5.272, df=981.0;
		Quinine 1x vs. Saccharin 2x
		p= 0.0021, q= 5.387, df=981.0;
		Quinine 1x vs. CTA Retrieval
		p= 0.9909, q= 0.8504, df=981.0;
		Quinine 1x vs. Extinction
		p= 0.0092, q= 4.807, df=981.0;
		Quinine 1x vs. Reinstatement
		p= 0.9985, q= 0.5836, df=981.0;
		Saccharin 2x vs. CTA Retrieval
		p <0.0001, q= 6.713, df=981.0;
		Saccharin 2x vs. Extinction
		p >0.9999, q= 0.09312, df=981.0;
		Saccharin 2x vs. Reinstatement
		p= 0.001, q= 5.642, df=981.0;
		CTA Retrieval vs. Extinction
		p= 0.0005, q= 5.914, df=981.0;
		CTA Retrieval vs. Reinstatement
		p >0.9999, q= 0.1648, df=981.0;
		Extinction vs. Reinstatement
		p= 0.0044, q= 5.099, df=981.0
		
		400pA
		Saccharin 1x vs. Quinine 1x
		p= 0.0062, q= 4.963, df=981.0;
		Saccharin 1x vs. Saccharin 2x
		p >0.9999, q= 0.24, df=981.0;
		Saccharin 1x vs. CTA Retrieval
		p= 0.0004, q= 5.925, df=981.0;
		Saccharin 1x vs. Extinction
		p= 0.9991, q= 0.5192, df=981.0;
		Saccharin 1x vs. Reinstatement
		p= 0.0014, q= 5.513, df=981.0;
		Quinine 1x vs. Saccharin 2x
		p= 0.0034, q= 5.2, df=981.0;
		Quinine 1x vs. CTA Retrieval
		p= 0.9991, q= 0.5284, df=981.0;
		Quinine 1x vs. Extinction

		p= 0.0053, q= 5.027, df=981.0;
		Quinine 1x vs. Reinstatement
		p= 0.991, q= 0.8492, df=981.0;
		Saccharin 2x vs. CTA Retrieval
		p= 0.0002, q= 6.183, df=981.0;
		Saccharin 2x vs. Extinction
		p >0.9999, q= 0.3014, df=981.0;
		Saccharin 2x vs. Reinstatement
		p= 0.0008, q= 5.736, df=981.0;
		CTA Retrieval vs. Extinction
		p= 0.0005, q= 5.857, df=981.0;
		CTA Retrieval vs. Reinstatement
		p= 0.9997, q= 0.4195, df=981.0;
		Extinction vs. Reinstatement
		p= 0.0013, q= 5.554, df=981.0

Figure 4B	One-way ANOVA
	Post-hoc Tukey's multiple comparisons
	
	LIV-VI aIC-BLA neurons
	fAHP
	
	Saccharin 1x
	Quinine 1x
	Saccharin 2x
	CTA retrieval
	Extinction
	Reinstatement
		ANOVA results:
		Treatment; p<0.0001, F (5, 109) =10.64;
		R squared, 0.3283;
		
		Multiple Comparisons:
		Saccharin 1x vs. Quinine 1x
		p<0.0001, q=9.380, df=109;
		Saccharin 1x vs. Saccharin 2x
		p= 0.7249, q= 1.985, df=109;
		Saccharin 1x vs. CTA Retrieval
		p=0.0127, q=4.774, df=109;
		Saccharin 1x vs. Extinction
		p= 0.9204, q= 1.399, df=109;
		Saccharin 1x vs. Reinstatement
		p=0.5239, q= 2.428, df=109;
		Quinine 1x vs. Saccharin 2x
		p<0.0001, q= 7.421, df=109;
		Quinine 1x vs. CTA Retrieval
		p= 0.0035, q= 5.331, df=109;
		Quinine 1x vs. Extinction
		p<0.0001, q= 7.147, df=109;
		Quinine 1x vs. Reinstatement
		p= 0.0003, q= 6.299, df=109;
		Saccharin 2x vs. CTA Retrieval
		p= 0.4251, q= 2.647, df=109;
		Saccharin 2x vs. Extinction
		p= 0.9997, q= 0.4017, df=109;
		Saccharin 2x vs. Reinstatement
		p= 0.9983, q= 0.5902, df=109;
		CTA Retrieval vs. Extinction
		p= 0.3621, q= 2.796, df=109;
		CTA Retrieval vs. Reinstatement
		p= 0.7995, q= 1.799, df=109;
		Extinction vs. Reinstatement
		p= 0.9868, q= 0.9191, df=109.

Figure 4C	One-way ANOVA
	Post-hoc Tukey's multiple comparisons
	
	LIV-VI aIC-BLA neurons
	Input Resistance
	
	Saccharin 1x
	Quinine 1x
		ANOVA results:
		Treatment; p=0.0213, F (5, 109) =2.775;
		R squared, 0.1129;
		
		Multiple Comparisons:
		Saccharin 1x vs. Quinine 1x
		p >0.9999, q= 0.03668, df=109;
		Saccharin 1x vs. Saccharin 2x
		p= 0.2331, q= 3.152, df=109;

	Saccharin 2x
	CTA retrieval
	Extinction
	Reinstatement
		Saccharin 1x vs. CTA Retrieval
		p= 0.9876, q= 0.9065, df=109;
		Saccharin 1x vs. Extinction
		p= 0.9997, q= 0.4256, df=109;
		Saccharin 1x vs. Reinstatement
		p= 0.3953, q= 2.716, df=109;
		Quinine 1x vs. Saccharin 2x
		p= 0.2582, q= 3.075, df=109;
		Quinine 1x vs. CTA Retrieval
		p= 0.9859, q= 0.9323, df=109;
		Quinine 1x vs. Extinction
		p= 0.9998, q= 0.3877, df=109;
		Quinine 1x vs. Reinstatement
		p= 0.4229, q= 2.652, df=109;
		Saccharin 2x vs. CTA Retrieval
		p= 0.0352, q= 4.286, df=109;
		Saccharin 2x vs. Extinction
		p= 0.5204, q=2.435, df=109;
		Saccharin 2x vs. Reinstatement
		p >0.9999, q=0.2024, df=109;
		CTA Retrieval vs. Extinction
		p=0.9475, q=1.262, df=109;
		CTA Retrieval vs. Reinstatement
		p=0.1001, q=3.711, df=109;
		Extinction vs. Reinstatement
		p=0.6757, q= 2.098, df=109.

Figure 4D	One-way ANOVA
	Post-hoc Tukey's multiple comparisons
	
	LIV-VI aIC-BLA neurons
	Sag ratio
	
	Saccharin 1x
	Quinine 1x
	Saccharin 2x
	CTA retrieval
	Extinction
	Reinstatement
		<u>ANOVA results:</u>
		Treatment; p=0.0286, F (5, 109) =2.610;
		R squared, 0.1069;
		
		<u>Multiple Comparisons:</u>
		Saccharin 1x vs. Quinine 1x
		p=0.9862, q= 0.9280, df=109;
		Saccharin 1x vs. Saccharin 2x
		p=0.5707, q=2.327, df=109;
		Saccharin 1x vs. CTA Retrieval
		p=0.6972, q=2.049, df=109;
		Saccharin 1x vs. Extinction
		p= 0.9794, q= 1.015, df=109;
		Saccharin 1x vs. Reinstatement
		p=0.9643, q= 1.152, df=109;
		Quinine 1x vs. Saccharin 2x
		p=0.2112, q= 3.225, df=109;
		Quinine 1x vs. CTA Retrieval
		p= 0.9784, q= 1.026, df=109;
		Quinine 1x vs. Extinction
		p>0.9999, q= 0.1598, df=109;
		Quinine 1x vs. Reinstatement
		p= 0.7184, q= 2.000, df=109;
		Saccharin 2x vs. CTA Retrieval
		p= 0.0209, q= 4.543, df=109;
		Saccharin 2x vs. Extinction
		p= 0.2415, q= 3.126, df=109;
		Saccharin 2x vs. Reinstatement
		p= 0.9805q= 1.002, df=109;
		CTA Retrieval vs. Extinction
		p= 0.9944, q= 0.7617, df=109;
		CTA Retrieval vs. Reinstatement

		p= 0.2504, q= 3.099, df=109; Extinction vs. Reinstatement p= 0.7140, q= 2.010, df=109.

Figure 4E	One-way ANOVA
	Post-hoc Tukey's multiple comparisons
	
	LIV-VI aIC-BLA neurons
	Action Potential Amplitude
	
	Saccharin 1x
	Quinine 1x
	Saccharin 2x
	CTA retrieval
	Extinction
	Reinstatement
		<u>ANOVA results:</u>
		Treatment; p=0.0054, F (5, 109) =3.526;
		R squared, 0.1392;
		
		<u>Multiple Comparisons:</u>
		Saccharin 1x vs. Quinine 1x
		p =0.2342, q= 3.149, df=109;
		Saccharin 1x vs. Saccharin 2x
		p=0.7922, q=1.818, df=109;
		Saccharin 1x vs. CTA Retrieval
		p=0.3531, q=2.818, df=109;
		Saccharin 1x vs. Extinction
		p= 0.8190, q= 1.746, df=109;
		Saccharin 1x vs. Reinstatement
		p=0.9979, q= 0.6222df=109;
		Quinine 1x vs. Saccharin 2x
		p=0.0087, q= 4.944, df=109;
		Quinine 1x vs. CTA Retrieval
		p= 0.9983, q= 0.5921, df=109;
		Quinine 1x vs. Extinction
		p=0.9662, q= 1.137, df=109;
		Quinine 1x vs. Reinstatement
		p= 0.5806, q= 2.305, df=109;
		Saccharin 2x vs. CTA Retrieval
		p= 0.0129, q= 4.768, df=109;
		Saccharin 2x vs. Extinction
		p= 0.1650, q= 3.396, df=109;
		Saccharin 2x vs. Reinstatement
		p= 0.5804, q= 2.306, df=109;
		CTA Retrieval vs. Extinction
		p= 0.9968, q= 0.6777, df=109;
		CTA Retrieval vs. Reinstatement
		p= 0.7511, q= 1.922, df=109;
		Extinction vs. Reinstatement
		p= 0.9746, q= 1.065, df=109.

Figure 4F	One-way ANOVA
	Kruskal-Wallis test
	
	Post-hoc Dunn's multiple comparisons test
	
	LIV-VI aIC-BLA neurons
	Action Potential Half-width
	
	Saccharin 1x
	Quinine 1x
	Saccharin 2x
	CTA retrieval
	Extinction
	Reinstatement
		<u>ANOVA results:</u>
		Kruskal-Wallis test; p=0.0002; Kruskal-Wallis statistic,24.03
		
		<u>Multiple Comparisons:</u>
		Saccharin 1x vs. Quinine 1x
		p >0.9999, z= 0.6106
		Saccharin 1x vs. Saccharin 2x
		p >0.9999, z= 0.2586;
		Saccharin 1x vs. CTA Retrieval
		p >0.9999, z= 0.04096;
		Saccharin 1x vs. Extinction
		p= 0.0485, z= 2.944;
		Saccharin 1x vs. Reinstatement
		p= 0.0200, z=3.208;
		Quinine 1x vs. Saccharin 2x
		p >0.9999, q=0.8658;
		Quinine 1x vs. CTA Retrieval
		p >0.9999, z=0.6129;
		Quinine 1x vs. Extinction

		p= 0.2759, z=2.358;
		Quinine 1x vs. Reinstatement
		p=0.1372, z=2.607;
		Saccharin 2x vs. CTA Retrieval
		p >0.9999, z=0.3181;
		Saccharin 2x vs. Extinction
		p=0.0222, z=3.179;
		Saccharin 2x vs. Reinstatement
		p=0.0085, z= 3.448;
		CTA Retrieval vs. Extinction
		p=0.0312, z=3.079;
		CTA Retrieval vs. Reinstatement
		p=0.0115, z=3.366;
		Extinction vs. Reinstatement
		p >0.9999, z= 0.1880.

Figure 4G	One-way ANOVA
	Post-hoc Tukey's multiple comparisons
	
	LIV-VI aIC-BLA neurons
	Membrane Time Constant
	
	Saccharin 1x
	Quinine 1x
	Saccharin 2x
	CTA retrieval
	Extinction
	Reinstatement
		<u>ANOVA results:</u>
		Treatment; p= 0.0047, F (5, 109) = 0.1419;
		R squared,0.1419;
		
		<u>Multiple Comparisons:</u>
		Saccharin 1x vs. Quinine 1x
		p= 0.0987, q= 3.720, df=109;
		Saccharin 1x vs. Saccharin 2x
		p= 0.4932, q= 2.495, df=109;
		Saccharin 1x vs. CTA Retrieval
		p= 0.1046, q= 3.685, df=109;
		Saccharin 1x vs. Extinction
		p=0.9230, q=1.388, df=109;
		Saccharin 1x vs. Reinstatement
		p= 0.0022, q=5.525, df=109;
		Quinine 1x vs. Saccharin 2x
		p=, 0.9484 q=1.257, df=109;
		Quinine 1x vs. CTA Retrieval
		p=0.9999, q=0.3489, df=109;
		Quinine 1x vs. Extinction
		p= 0.7139, q=2.010, df=109;
		Quinine 1x vs. Reinstatement
		p=0.7124, q=2.014, df=109;
		Saccharin 2x vs. CTA Retrieval
		p=0.9798, q=1.011, df=109;
		Saccharin 2x vs. Extinction
		p=0.9894, q=0.8761, df=109;
		Saccharin 2x vs. Reinstatement
		p=0.2138, q=3.216, df=109;
		CTA Retrieval vs. Extinction
		p=0.7866, q=1.833, df=109;
		CTA Retrieval vs. Reinstatement
		p=0.4978, q=2.484, df=109;
		Extinction vs. Reinstatement
		p=0.0896, q=3.777, df=109.